1993 St. Petersburg Winter School

J. Blümlein

DESY – Institut für Hochenergiephysik, O–1615 Zeuthen, FRG
January 25 – February 5 1993

Structure Functions and Parton Distributions at HERA

JB

STRUCTURE FUNCTIONS AND PARTON DISTRIBUTIONS AT HERA

(AND OTHER HE-FACILITIES)

ST. PETERSBURG
JAN 25 FEB 5 1993

DEEP INELASTIC SCATTERING – BASIC ISSUES

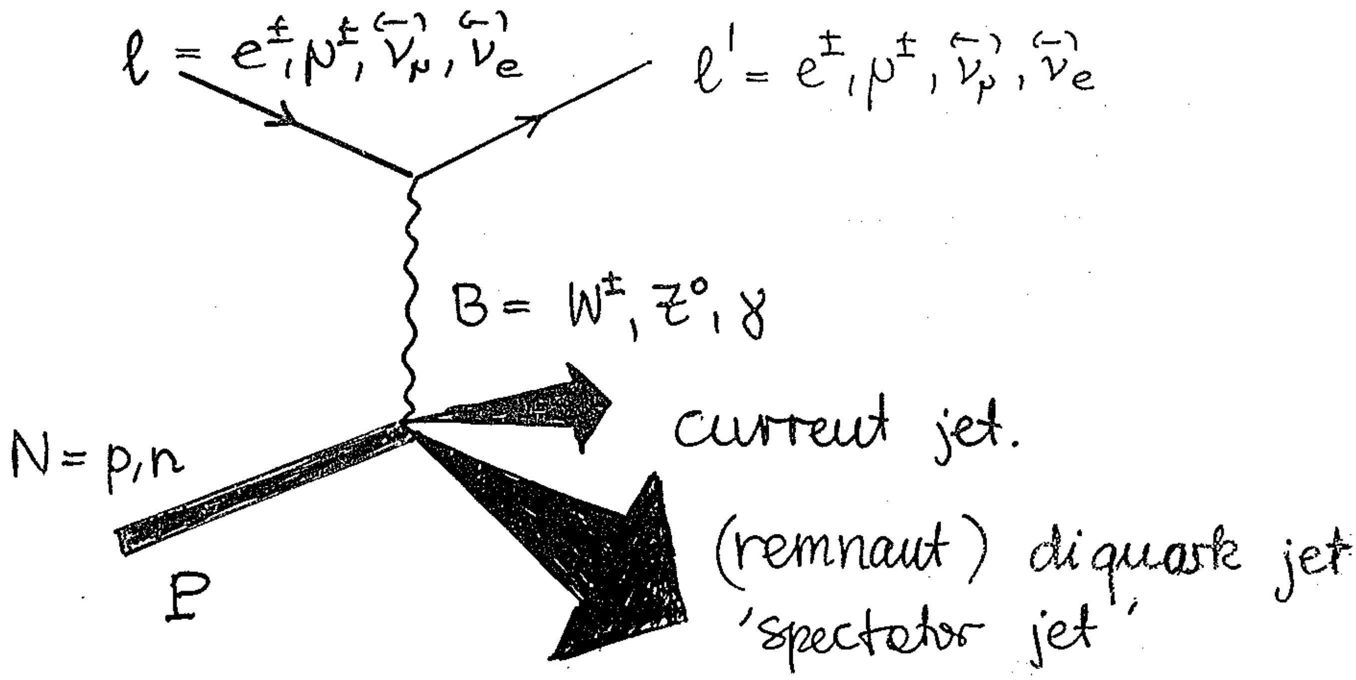

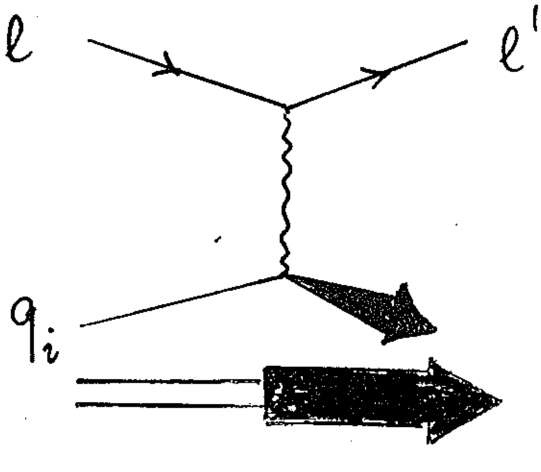

VARIABLES:

$$Q^2 = -(\ell - \ell')^2 = -(p_{q_i} - p_{q_f})^2 \geqq 0 \quad , q = \ell - \ell'$$

$$x_B \equiv x = \frac{Q^2}{2Pq} \qquad y_B \equiv y = \frac{qP}{\ell P}.$$

$$s = (P + \ell)^2.$$

THE BORN CROSS SECTIONS

CHARGED LEPTONS :

NC :

$$\frac{d^2\sigma}{dx\,dQ^2} = 2\pi\alpha^2 \frac{M_N s}{(s-M^2)^2} \frac{1}{Q^4} L^{\mu\nu}\tilde{W}_{\mu\nu}$$

$e^\pm N \to e^\pm X$ $(\mu^\pm N \to \mu^\pm X)$

pure photon exchange:

$$L_{\mu\nu} = 2\left[\ell_\mu \ell'_\nu + \ell'_\mu \ell_\nu - g_{\mu\nu}\, \ell.\ell'\right]$$

$$W_{\mu\nu} = \frac{1}{4\pi}\sum_n \langle P | J_\mu^{em\,\dagger}(0) | n\rangle \langle n | J_\nu^{em}(0) | P\rangle (2\pi)^4 \delta^{(4)}(P+q-p_n)$$

$$W_{\mu\nu} = \left(-g_{\mu\nu} + \frac{q_\mu q_\nu}{q^2}\right) W_1(x,Q^2) + \frac{1}{M^2}\left[\left(P_\mu - \frac{Pq}{q^2}q_\mu\right)\left(P_\nu - \frac{Pq}{q^2}q_\nu\right)\right. \cdot W_2(x,Q^2)$$

$$\boxed{\begin{aligned} F_2(x,Q^2) &= x\left(-g_{\mu\nu} + \frac{12x^2}{Q^2}P_\mu P_\nu\right) W^{\mu\nu} \\ F_L(x,Q^2) &= \frac{8x^3}{Q^2} P_\mu P_\nu W^{\mu\nu} \end{aligned}}$$

$(\mathcal{O}(\alpha_s))$

2 STRUCTUREFCT.

$\mathcal{O}(\alpha_s^0)$ 1 STRCT. FCT.

$$\boxed{\frac{d^2\sigma}{dx\,dQ^2} = \frac{2\pi\alpha^2}{xQ^4} Y_+ F_2(x,Q^2)}$$

$$Y_\pm = 1 \pm (1-y)^2$$

INCLUSION OF BEAM POLARIZATION

& Z EXCHANGE:

$$\boxed{\frac{d^2\sigma^\pm}{dx\,dQ^2} = \frac{2\pi\alpha^2}{x\,Q^2}\left\{Y_+\,\mathbb{F}_2^\pm(x,Q^2) + Y_-\,x\mathbb{F}_3^\pm(x,Q^2)\right\}}$$

$$\mathbb{F}_2^\pm(x,Q^2) = F_2(x,Q^2) + K_Z(Q^2)\,(-v\mp\lambda a)\,G_2(x,Q^2) + K_Z^2(Q^2)\,(v^2+a^2\pm 2\lambda v a)\,H_2(x,Q^2)$$

$$x\mathbb{F}_3^\pm(x,Q^2) = K_Z(Q^2)\,(\pm a+\lambda v)\,x G_3(x,Q^2) + K_Z^2(Q^2)\,(\mp 2va - \lambda(v^2+a^2))\,x H_3(x,Q^2)$$

5 Structurefct. (without longitud.)

+3 longitudinal Structfct.

$$K_Z(Q^2) = \frac{1}{4\sin^2\theta_W\cos^2\theta_W}\;\frac{Q^2}{Q^2+M_Z^2}$$

$$a \equiv a_e = -\frac{1}{2}$$

$$v \equiv v_e = -\frac{1}{2} + 2\sin^2\theta_W$$

$\boxed{\text{CC :}}$

$e^{\pm}(\mu^{\pm})N \to \overset{(-)}{\nu}_{e(\mu)} X$

$$\boxed{\frac{d^2\sigma^{\pm}}{dx\,dQ^2} = \frac{2\pi\alpha^2}{x\,Q^2}\,K_W^2(Q^2)\left(\frac{1\pm\lambda}{2}\right)\cdot\left\{Y_+ W_2^{\pm}(x,Q^2) \pm Y_- x W_3^{\pm}(x,Q^2)\right.}$$

$$K_W(Q^2) = \frac{Q^2}{Q^2+M_W^2}\cdot\frac{1}{4\sin^2\theta_W}$$

4 Structure fct.

+ 2 long. Structurefct.

BORN: $e^{\pm}p$ 14 Structure functions !

$e^{\pm}d$ + —— " ——

(composed out of: u, d, s, c, b

$\bar{u}, \bar{d}, \bar{s}, c=\bar{c}, b=\bar{b}$ & g

$\leq \underline{\underline{10}}$ parton densities)

NEUTRINOS :

NC

$$\frac{d^2\sigma}{dx\,dQ^2} = \frac{G_F^2 M_W^4}{4\pi \times Q^4} \cdot \frac{Q^4}{(M_Z^2+Q^2)^2} \cdot \left\{ Y_+ \hat{F}_2(x,Q^2) + Y_- \times \hat{F}_3(x,Q^2) \right.$$

NOTE, HOWEVER, THAT THE KINEMATICS IN

$$\overset{(-)}{\nu} N \longrightarrow \overset{(-)}{\nu} X$$

IS DIFFICULT TO BE DETERMINED PRECISELY IN FIXED TARGET EXPERIMENTS.

$\boxed{\text{CC}}$

$$\overset{(-)}{\nu}_{\mu(e)} N \to \mu^{\pm}(e^{\pm}) X$$

$$\boxed{\frac{d\sigma^{\nu,\bar{\nu}}}{dx\,dQ^2} = \frac{G_F^2 M_W^4}{4\pi x Q^4} \frac{Q^4}{(Q^2+M_W^2)^2} \left[Y_+ W_2^{\nu,\bar{\nu}}(x,Q^2) \pm Y_- x W_3^{\nu,\bar{\nu}}(x,Q^2) \right]}$$

$$\frac{G_F^2 M_W^4}{4\pi} = \frac{2\pi\alpha^2}{16 \sin^4\theta_W}.$$

KINEMATICS, LUMINOSITIES & EVENTRATES

CONSIDER & COMPARE

- HERA — NOW
- LEP × LHC — > 2000 AD (?)
- νN @ UNK fixed target (3 TeV p) — ? (WOULD BE INTERESTING.)

HERA: $s = 4 \cdot \overset{e}{30} \cdot \overset{p}{820}\ \mathrm{GeV}^2$

$\quad 4 \cdot 10 \cdot 300\ \mathrm{GeV}^2$

$\mathcal{L}_{yr} \simeq 100\, pb^{-1}$ (future)

$e^{\pm}p$, $e^{\pm}d$ (future possible) in

LEP × LHC: $s = 4 \cdot \overset{p}{8000} \cdot \overset{e}{100}\ \mathrm{GeV}^2$ or $= 4 \cdot \overset{p}{2000} \cdot \overset{e}{50}$ GeV

$\mathcal{L}_{\text{'typical' yr}} = 100\, pb^{-1}$ or $= 1\, fb^{-1}$

$e^{\pm}p$, $e^{\pm}d$

$\overset{(-)}{\nu}$ UNK 3 TeV: $\langle E_\nu \rangle = 400 \ldots 700$ GeV

depending on the magnetic system

$\Phi_\nu = 2.5 \cdot 10^{-3} \ldots 10^{-4}\ m^{-2}\ p^{-1}$

10^{14} p per 120 sec ('cycle period')

K3

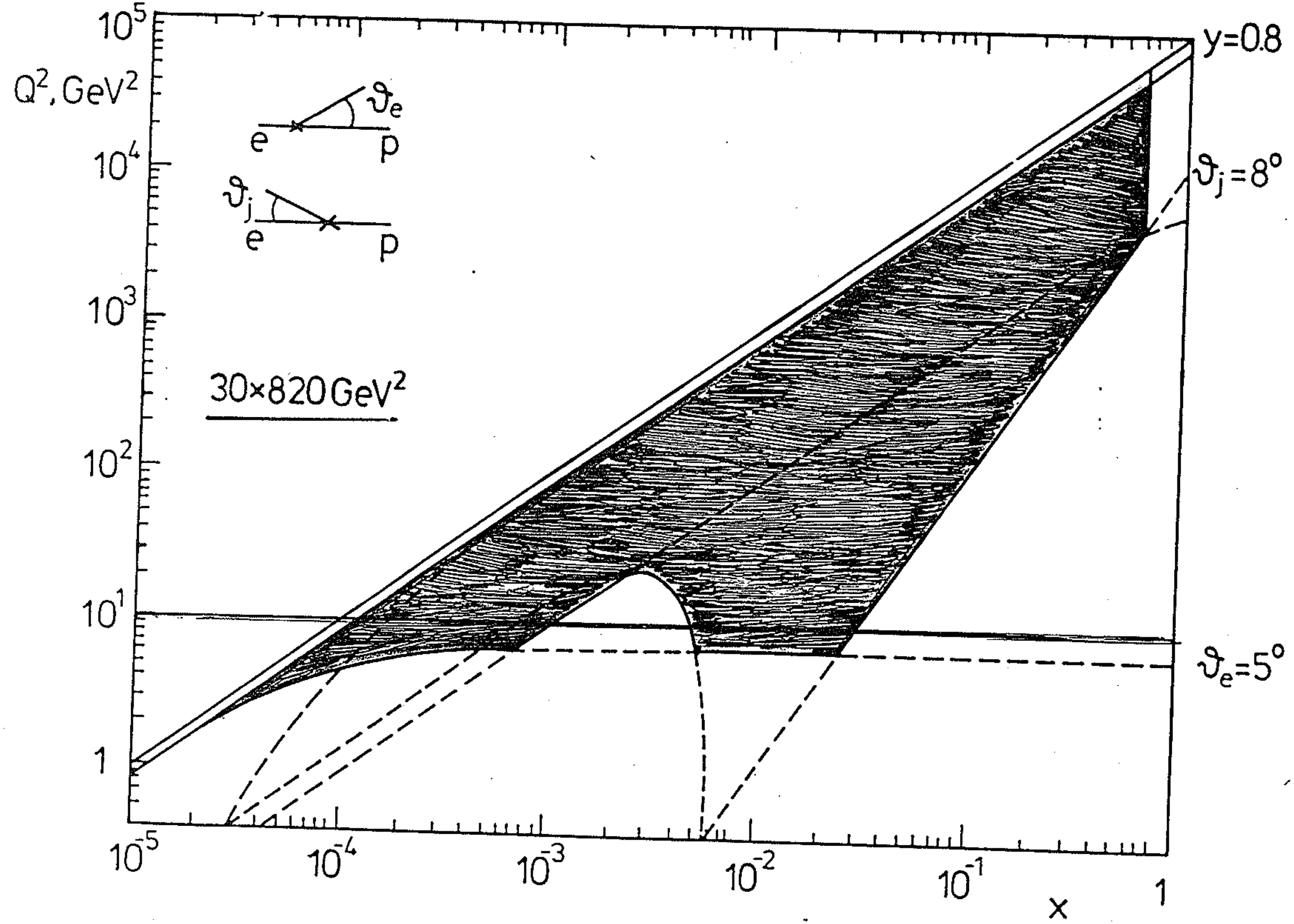

Q^2, GeV^2
10^5
10^4
10^3
10^2
10^1
1
ϑ_e
e
p
ϑ_j
e
p
30×820 GeV^2
y=0.8
$\vartheta_j=8°$
$\vartheta_e=5°$
10^{-5}
10^{-4}
10^{-3}
10^{-2}
10^{-1}
1
x

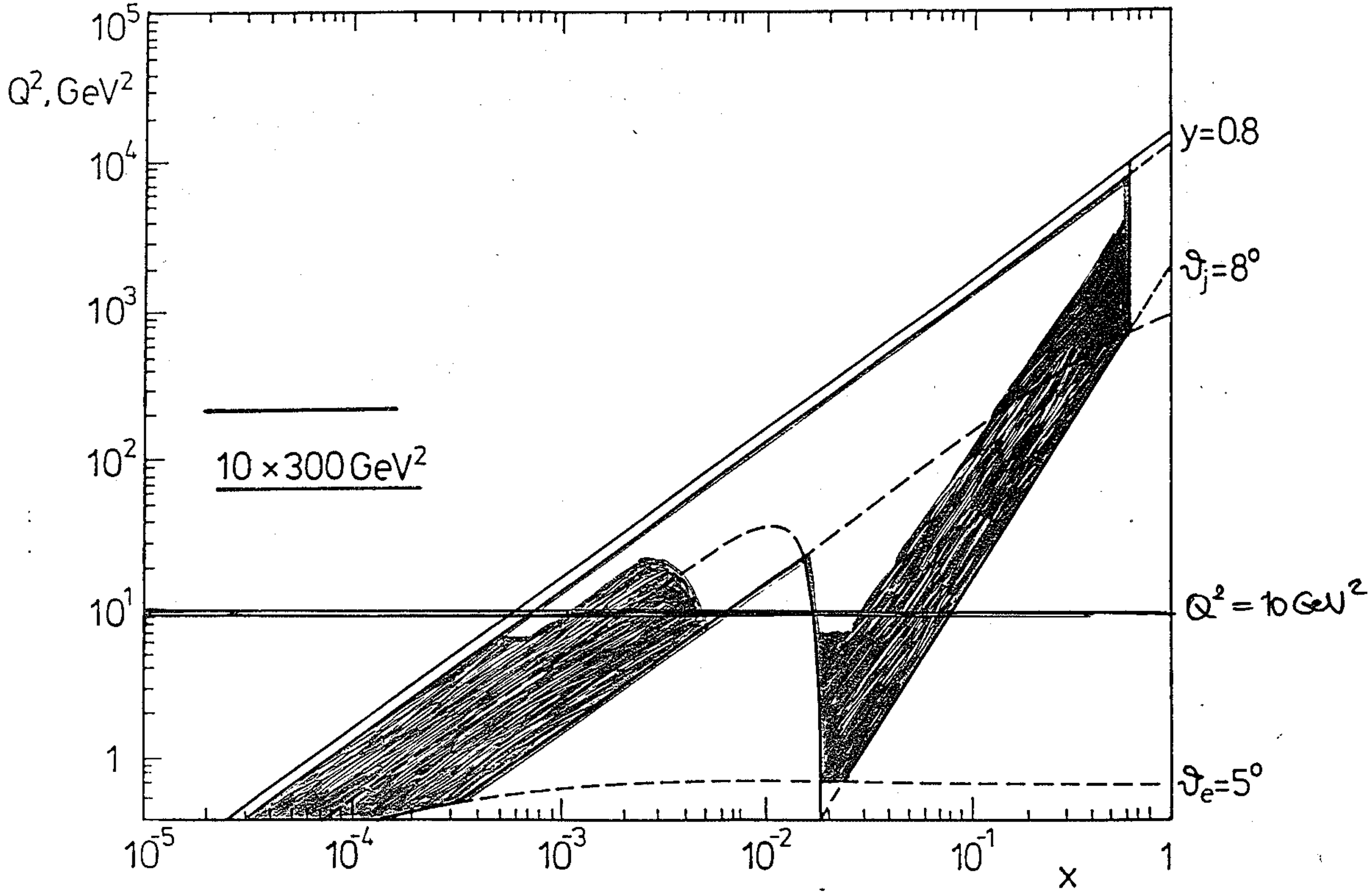

Q^2, GeV^2
10^5
10^4
10^3
10^2
10^1
1
10^{-5}
10^{-4}
10^{-3}
10^{-2}
10^{-1}
1
x
$10 \times 300\,\mathrm{GeV}^2$
y=0.8
$\vartheta_j=8°$
$Q^2 = 10\,\mathrm{GeV}^2$
$\vartheta_e=5°$

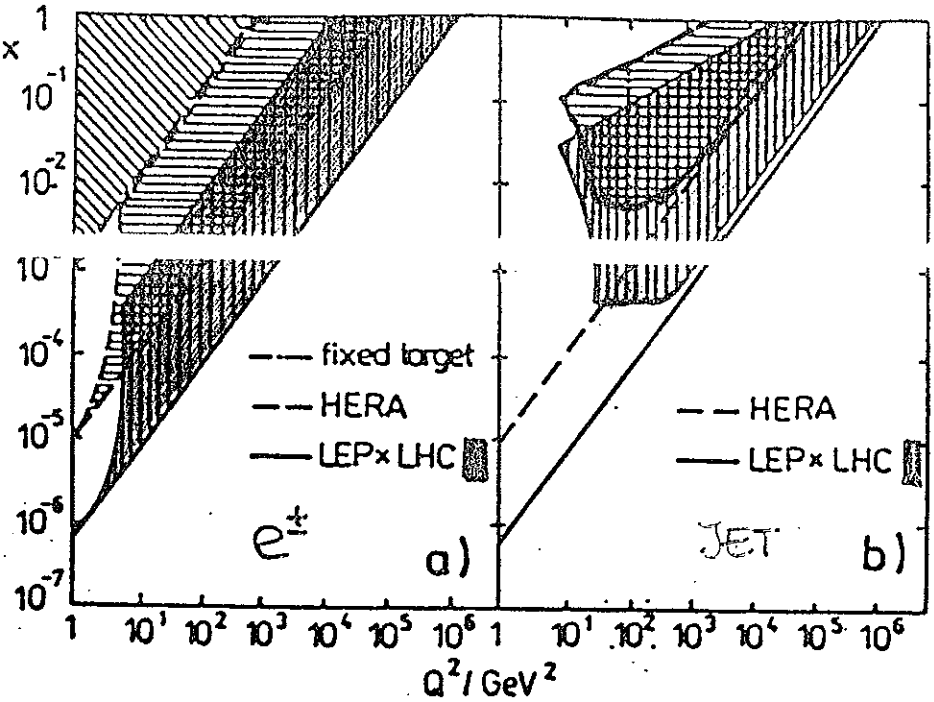

LHC⊗LEP

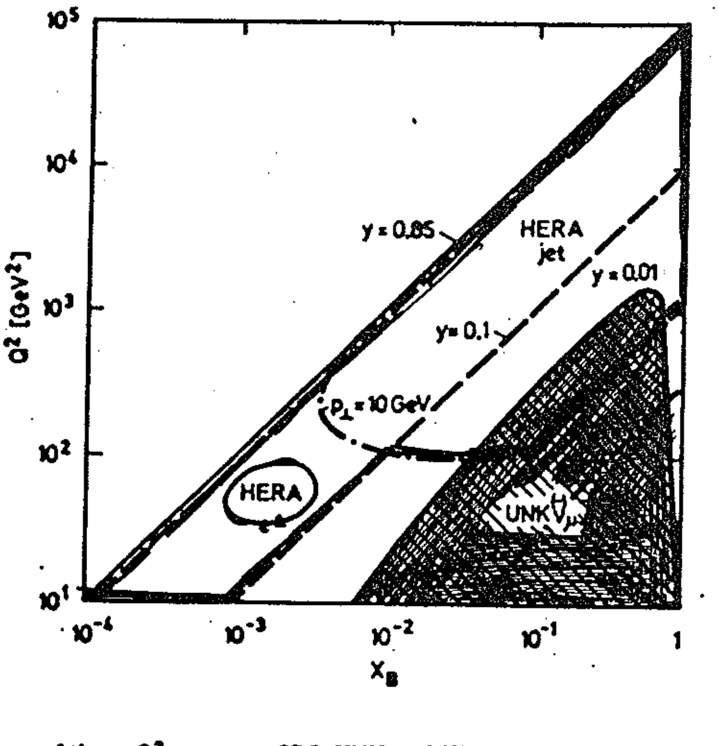

UNK
ν FACILITY

***Fig.* 7. Comparison of the x–Q^2 ranges at SPS, UNK and HERA. Below the ———— -line: SPS range; shaded area: UNK range; the dashed line bounds the range accessible by the e-measurement, the dash-dotted line the range for the jet measurement at HERA for $s = 10^5$ GeV^2**

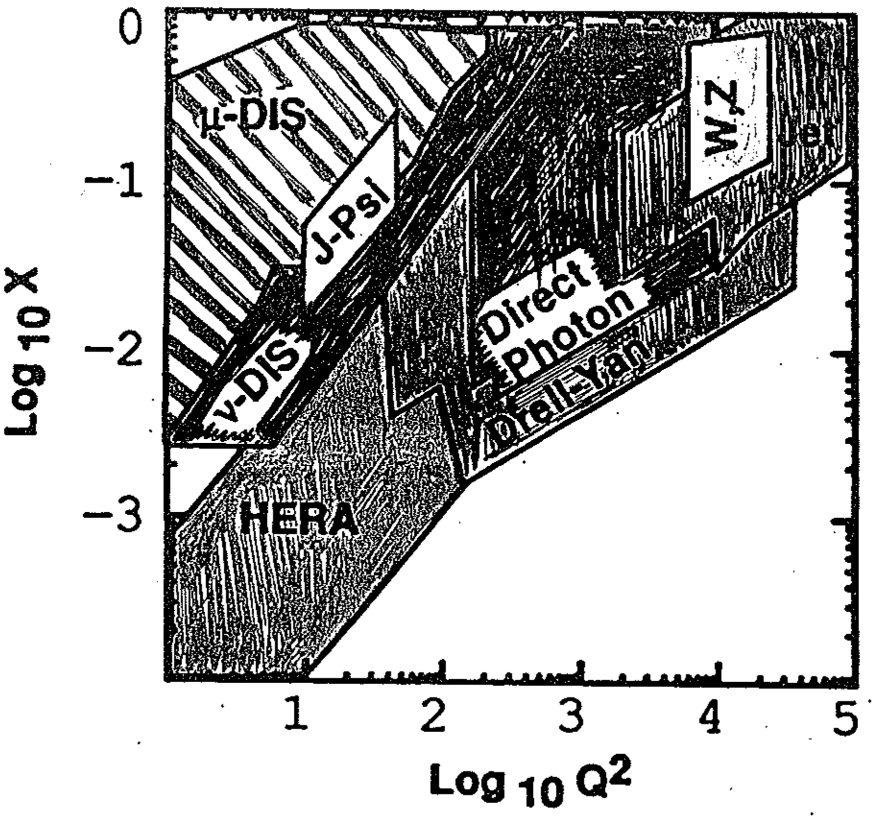

Figure 10: Summary of the $\{x, Q^2\}$ region explored.

SCHULER, OLNESS
BLÜMLEIN, TUNG
1991

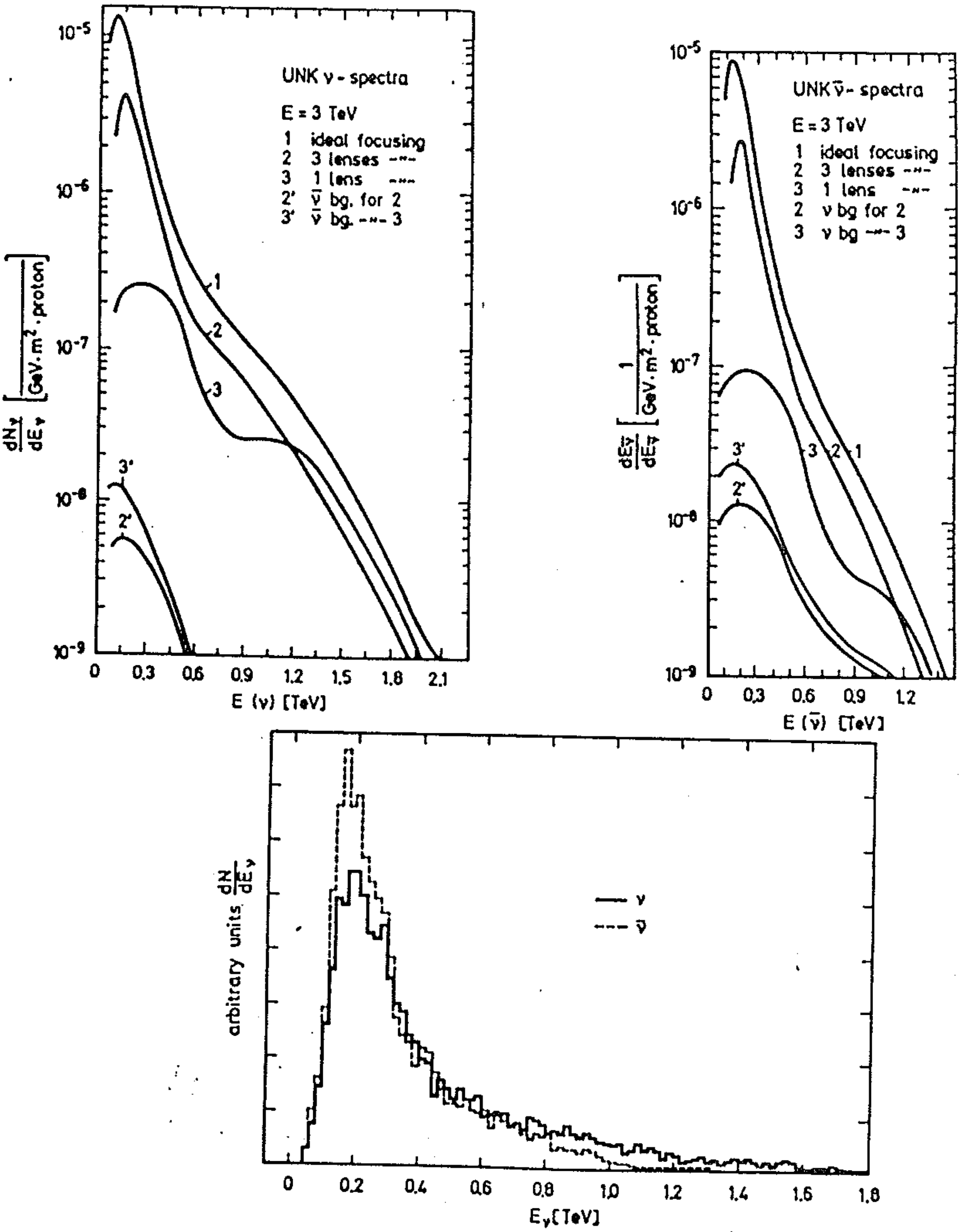

Fig. 2. **Distributions of the neutrino energy for the ideal focussed WBB's, Fig. 1 (*p*-target)**

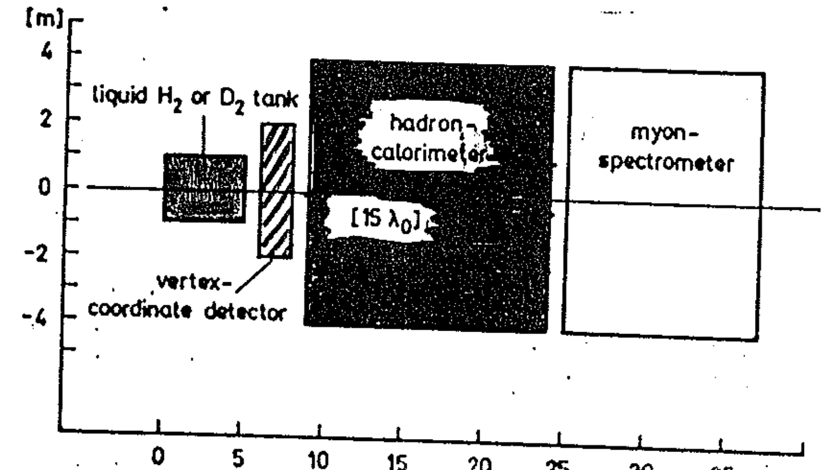

K8

EVENTRATES

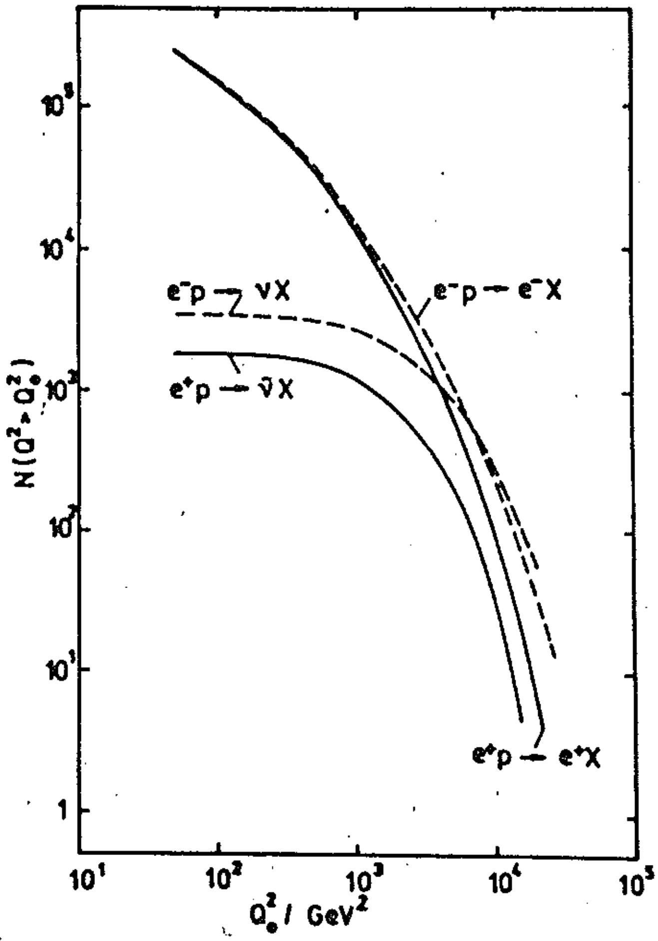

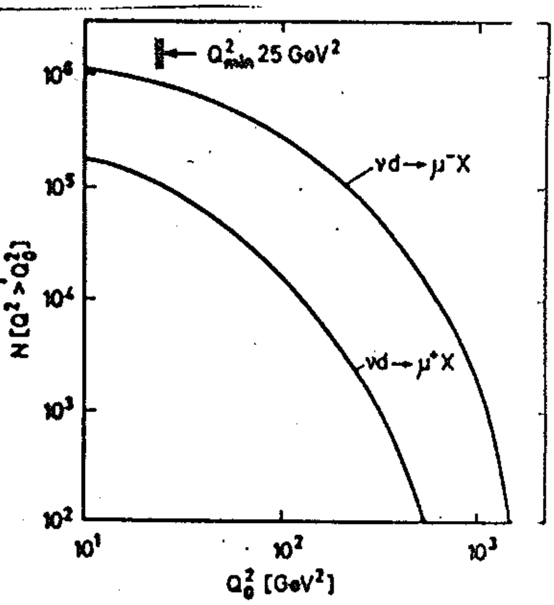

p/d FACILITY
IN UNK $\overset{(-)}{\nu}$ BEAM.

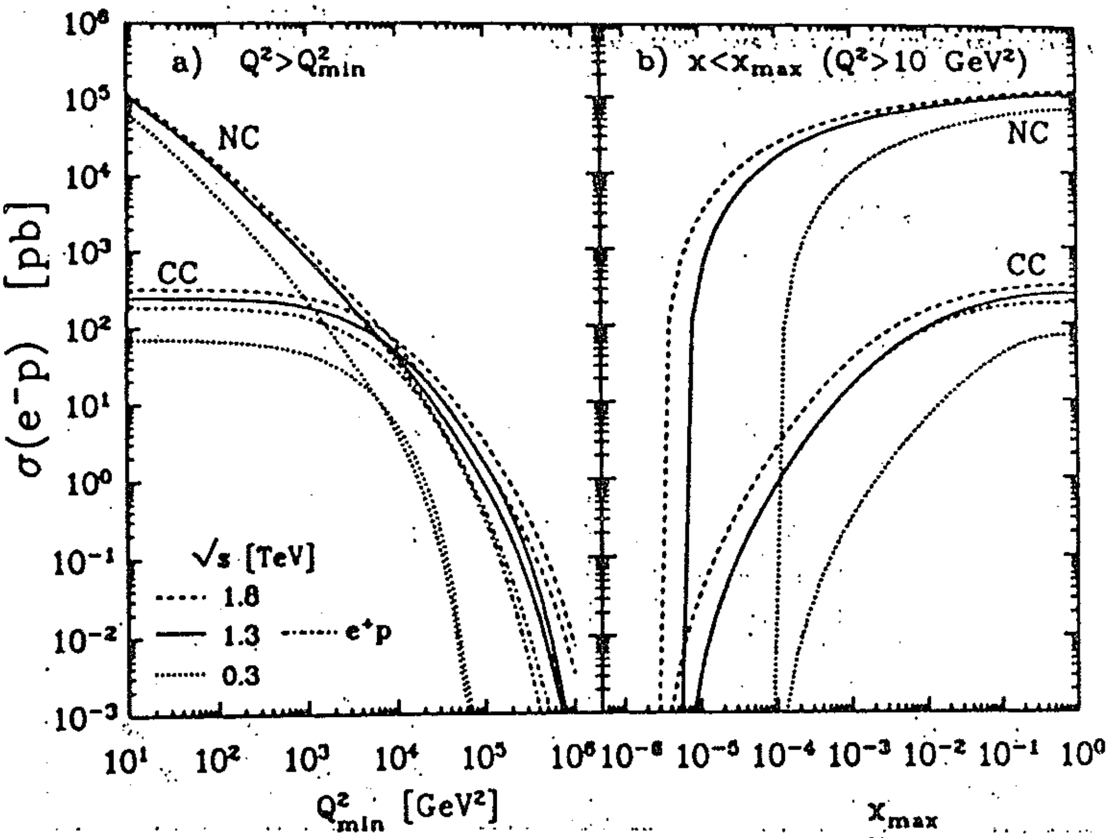

Figure 2: *Integrated DIS cross-sections versus (a) a lower cut-off in Q^2 and (b) an upper cut-off in x. Charged and neutral current interactions are compared for different e^-p*

QED RADIATIVE CORRECTIONS

- LARGE CONTRIBUTIONS
- DEPENDING ON THE CHOICE OF OUTER VARIABLES

$\longrightarrow$ DOMINATING : $\left(\frac{\alpha}{2\pi} \ln \frac{Q^2}{m_e^2}\right)$ & $\left[\left(\frac{\alpha}{2\pi} \ln \frac{Q^2}{m_e^2}\right)^2\right]$ terms

A PEDAGOGICAL VIEW (WHICH FULLY SUFFICES)

LEADING LOGS.

RECEIPT :

- ANALYZE ALL DIAGRAMS $O(\alpha^3, \alpha^4, \dots)$ FOR COLLINEAR SITUATIONS OF MASSLESS PARTICLES.
- WRITE FOR THE COLLINEAR TRANSITION THE ACCORDING SPLITTING FUNCTION (e.g. BREMSSTRAHLUNG etc.)
- NORMALIZE THE AMPLITUDES TO CONSERVE PROBABILITY, e.g.

$$e \to e \quad , \quad P_{ee}(x) = \delta(1-x) + P_{ee}^{(1)}(x)\frac{\alpha}{2\pi} + \dots$$

$$\int^1 dx \; P_{ee}(x) = 1 .$$

DIAGRAMS: NC: $ep \to eX$

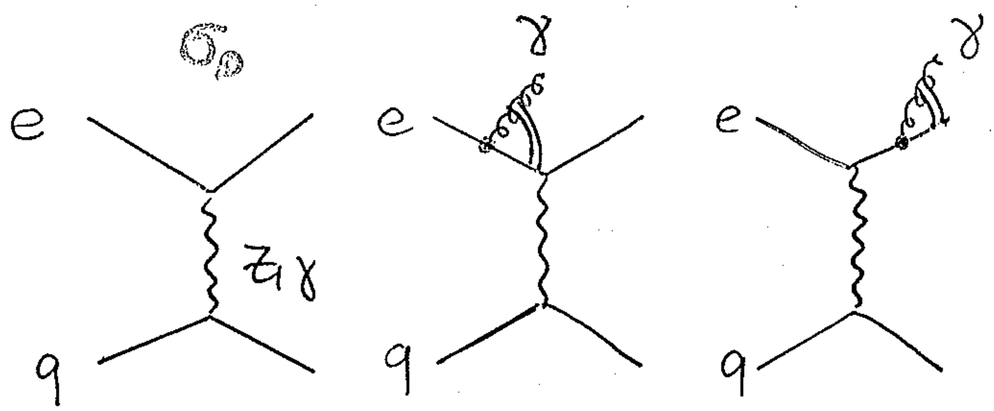

INITIAL STATE LEPTON

FINAL STATE LEPTON

RADIATION

(ISL) (FSL)

∢ COL... ANGLE

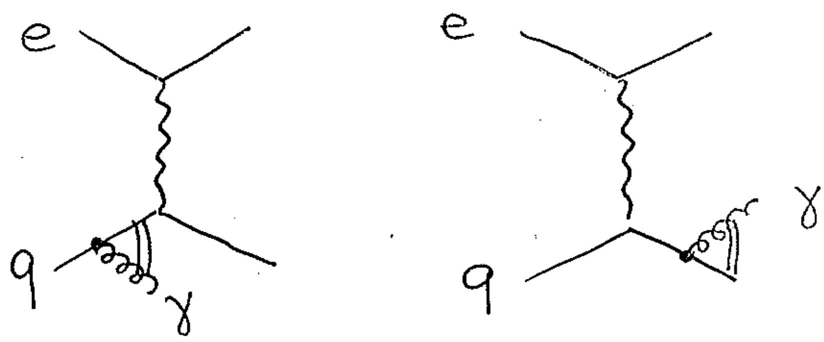

(ISQ) (FSQ)

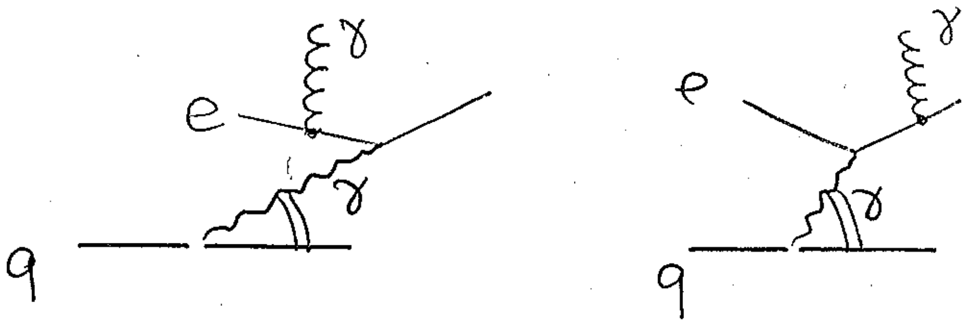

COMPTON

SIMILAR: $O(\alpha^2)$: THERE ALSO

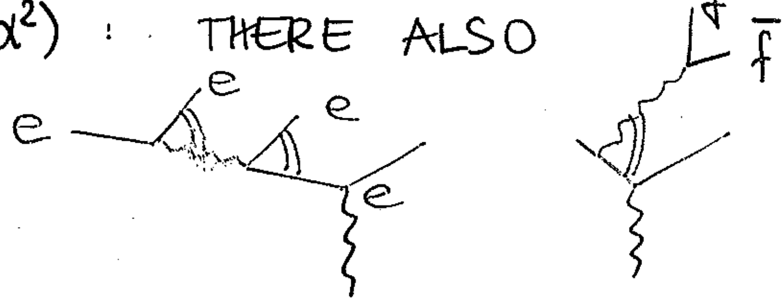

$\boxed{\text{BREMSSTRAHLUNG}}$ $\mathcal{O}\left(\frac{\alpha}{2\pi}L\right)$

$$\boxed{\frac{d\sigma_e}{dx\,dy} = \frac{\alpha}{2\pi}\ln\left(\frac{Q^2}{m_e^2}\right)\int_0^1 dz\,\frac{1+z^2}{1-z}\left\{\theta(z-z_0)\left.\frac{d^2\sigma_0}{dx\,dy}\right|_{\hat{x},\hat{y}}\mathbb{J} - \frac{d^2\sigma_0}{dx\,dy}\right\}}$$

$$\mathbb{J} = \begin{vmatrix} \frac{\partial \hat{x}}{\partial x} & \frac{\partial \hat{y}}{\partial y} \\ \frac{\partial \hat{x}}{\partial y} & \frac{\partial \hat{y}}{\partial x} \end{vmatrix}$$

INITIAL $\quad \hat{y} = \frac{z+y-1}{z} \quad \hat{Q}^2 = Q^2 z \quad \hat{S} = Sz \quad \hat{x}(z_0) = 1$

FINAL STATE RADIATION $\quad \hat{y} = \frac{z+y-1}{z} \quad \hat{Q}^2 = Q^2/z \quad \hat{S} = Sz \quad \hat{x}(z_0) = 1$

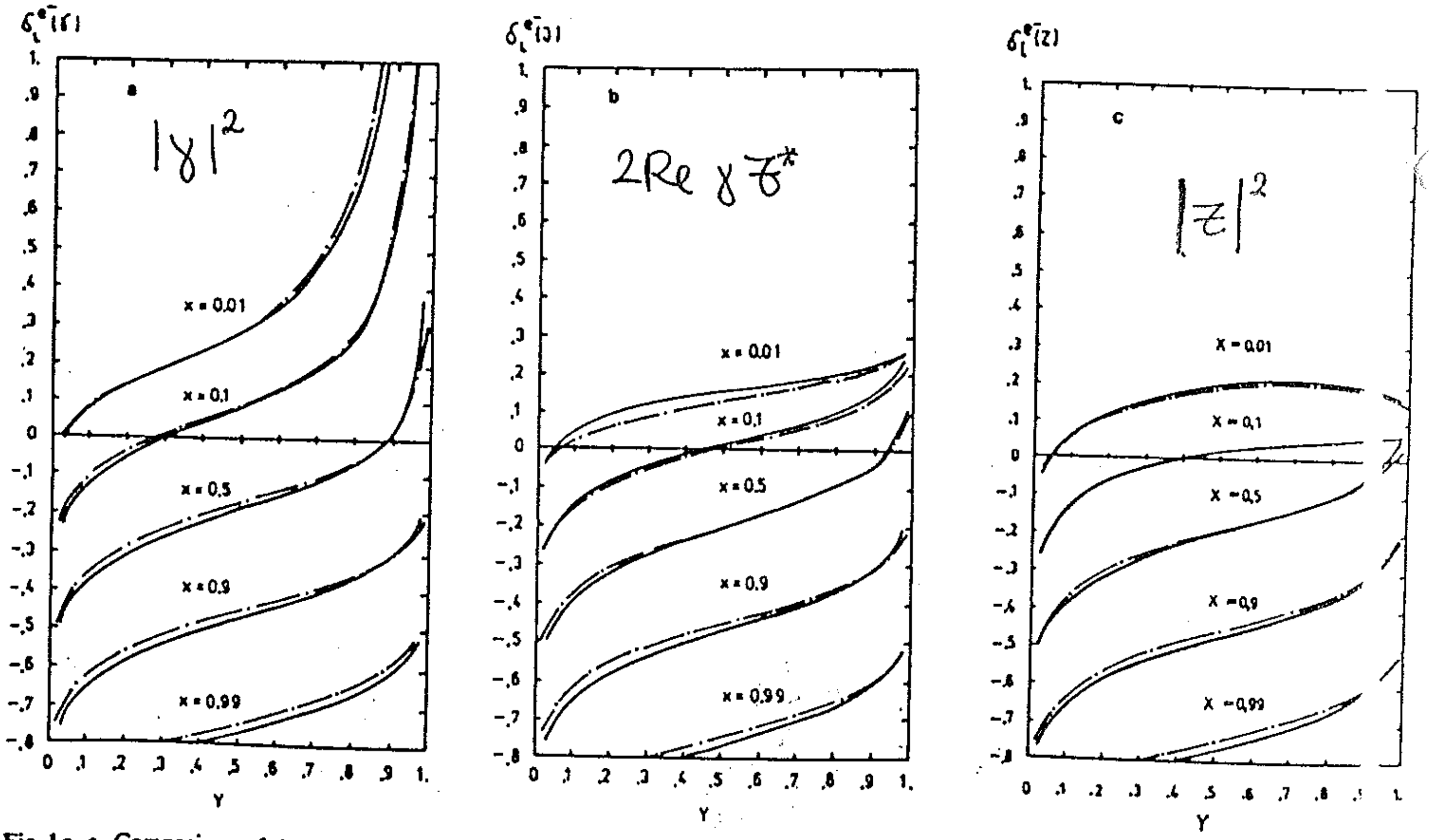

Fig. 1a–c. Comparison of the neutral current leading log radiative corrections (full lines) with the results of [5b] (dashed lines) for lepton bremsstrahlung at $\sqrt{s} = 314$ GeV for $e^- p$ scattering. The ratios $\delta_{NC}^{e}(i)$ denote the contribution $O(\alpha)$ for **a** γ-exchange, **b** $\gamma - Z$ interference, **c** Z-exchange normalized to the corresponding term in the Born cross section (1). For a direct comparison with [5] we used (5) $\sim \ln(S/M_p^2)$ in **a**

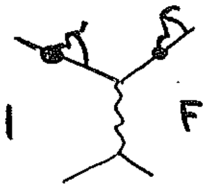

D

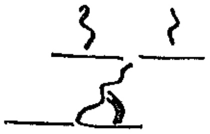

C

DEPENDENCE ON THE CHOICE OF PARAMETRIZATION

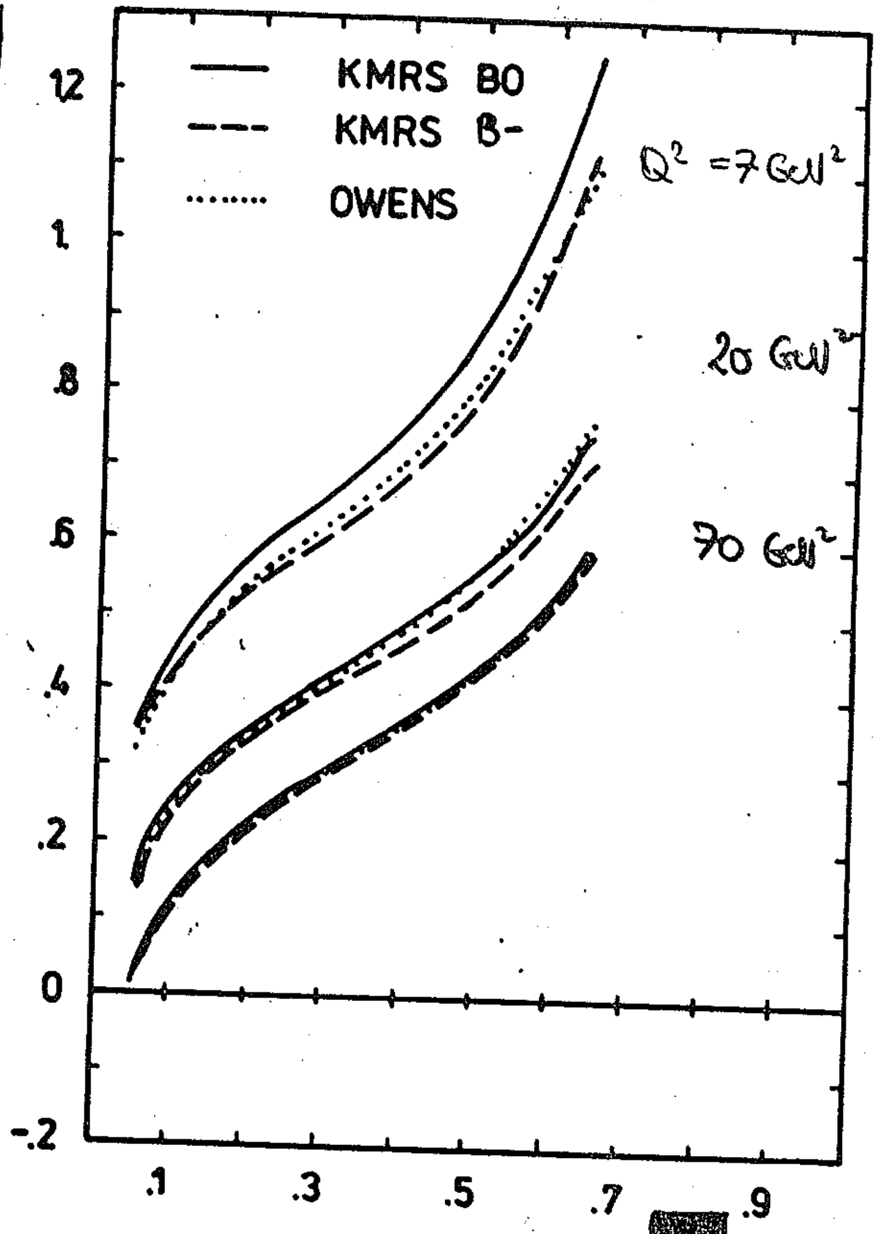

JB

cf. also RC WG DESY 91

$$\frac{d^2\sigma^{e^-p}}{dy\,dQ^2} = \frac{d^2\sigma_0^{e^-p}}{dy\,dQ^2}\left(1+\delta^{e^-p}(y,Q^2)\right)$$

$O(\alpha)$ QED.

RS

THE COMPTON PEAK

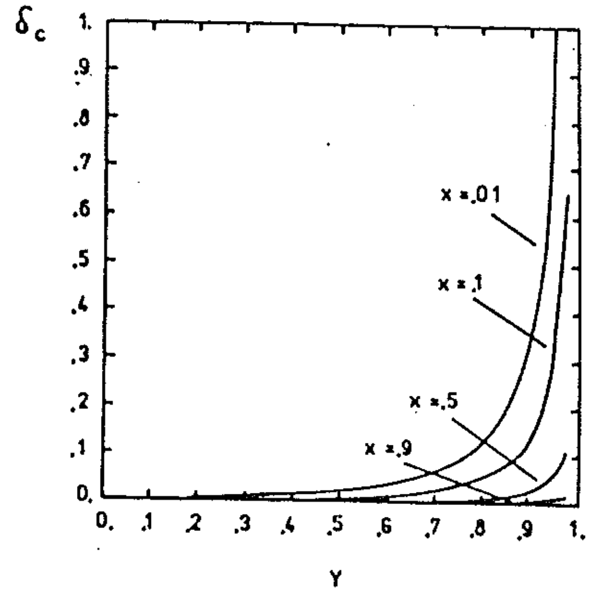

Fig. 2. $\delta_C = d^2\sigma^C/dx\,dy / d^2\sigma_0(\gamma)/dx\,dy$ due to $\gamma^* e \to \gamma e$ scattering as a function of x and y (10). The logarithmic term in (5) is $\sim \ln(Q^2/\Lambda^2)$ with $\Lambda = 200$ MeV

$$\frac{d^2\sigma^C}{dx\,dy} = \frac{\alpha^3}{Sx}\sum_f \ln\left(\frac{Q^2}{\Lambda^2}\right)\int_x^1 \frac{dz}{z^3}\, z\left[q_f(x,Q^2)+\bar{q}_f(x,Q^2)\right]\frac{z^2+(x-z)^2}{x(1-y)} \cdot Y_+$$

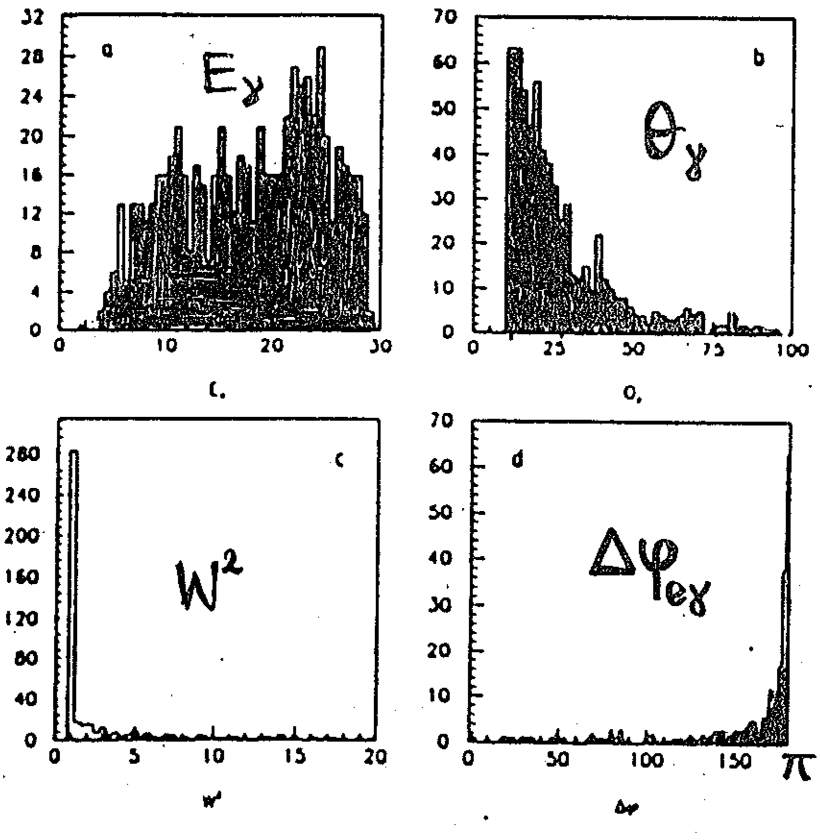

Figure 2: Distribution of the Compton events versus the en-

R6

CC
HERA

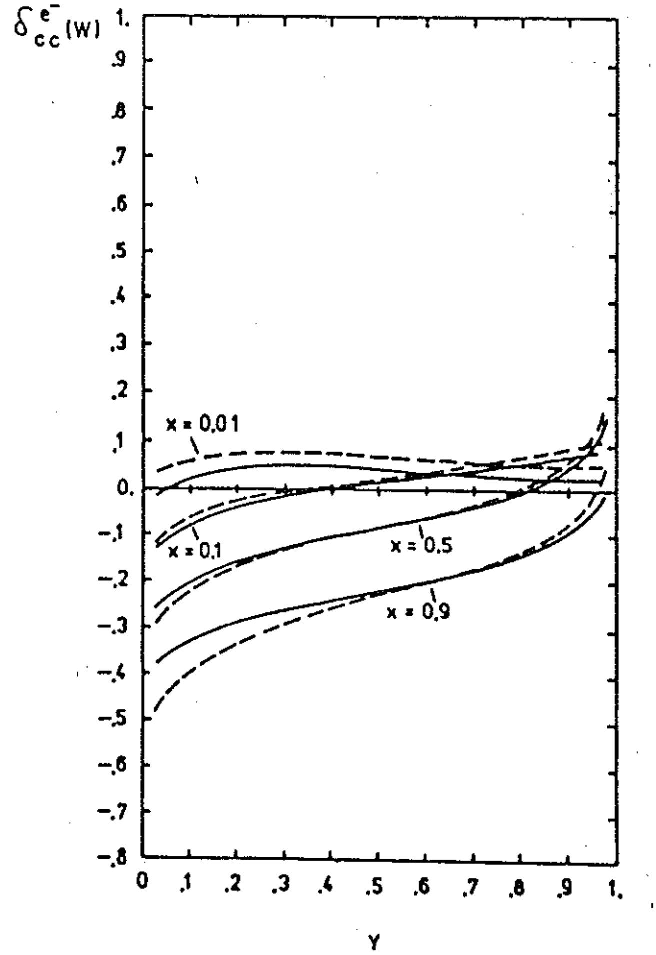

Fig. 3. Comparison of the charged current leading log radiative corrections (full lines) with the results of [6] (dashed lines) due to lepton bremsstrahlung for e^-p scattering. $\delta^{e^-}_{CC}(W)$ denotes the contribution $O(\alpha)$ normalized to the Born cross section (4)

LEP x LHC

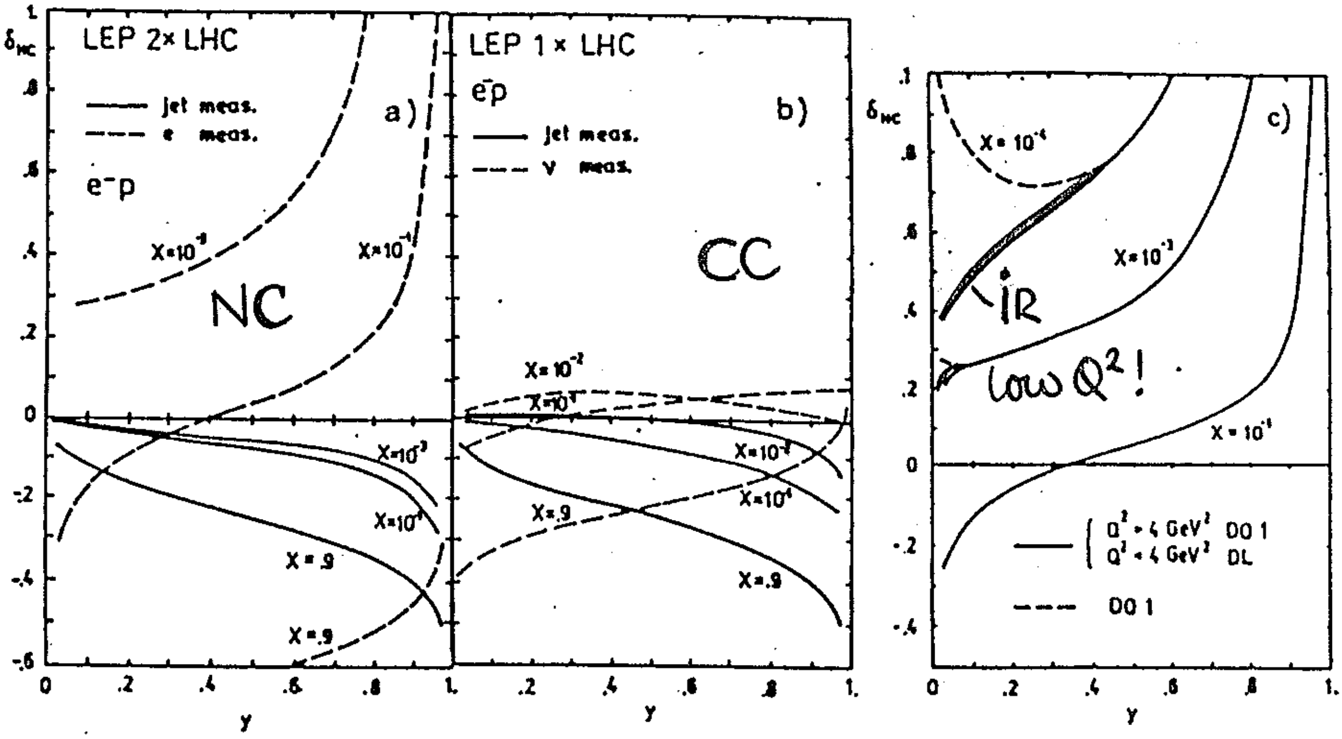

Figure 1: Comparison of the RCs to e^-p using the lepton or jet measurement: a) neutral current; b) charged current; c) Effect of the non-perturbative behaviour of quark distributions at low Q^2 (full line). The dashed line illustrates the extrapolation using the distributions [7].

JET – MEASUREMENT

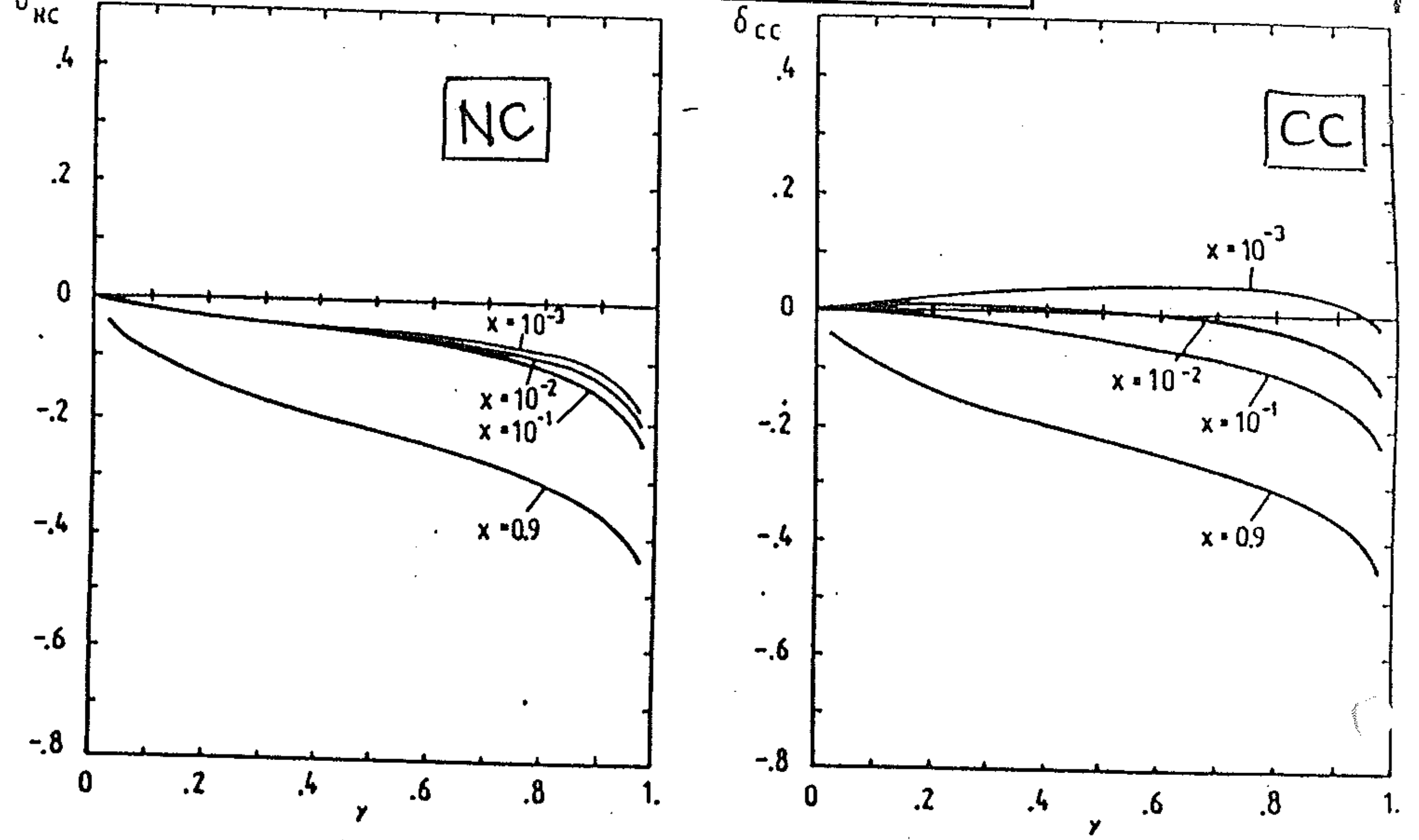

Figure 2: $\mathcal{O}(\alpha)$ leading log QED corrections to deep inelastic scattering using jet measurement at $\sqrt{s} = 314$ GeV in dependence of x and y. a) neutral current scattering; b) charged current scattering.

JET MEASUREMENT:

MIXED VARIABLES

IS:

$\hat{y} = y/z$, $\hat{s} = s z$

$\hat{Q}^2 = Q^2 \dfrac{1-y}{1-y/z}$

$\hat{x}(z_0) = 1$

FS: KLN !

$\delta_{FS} = 0$

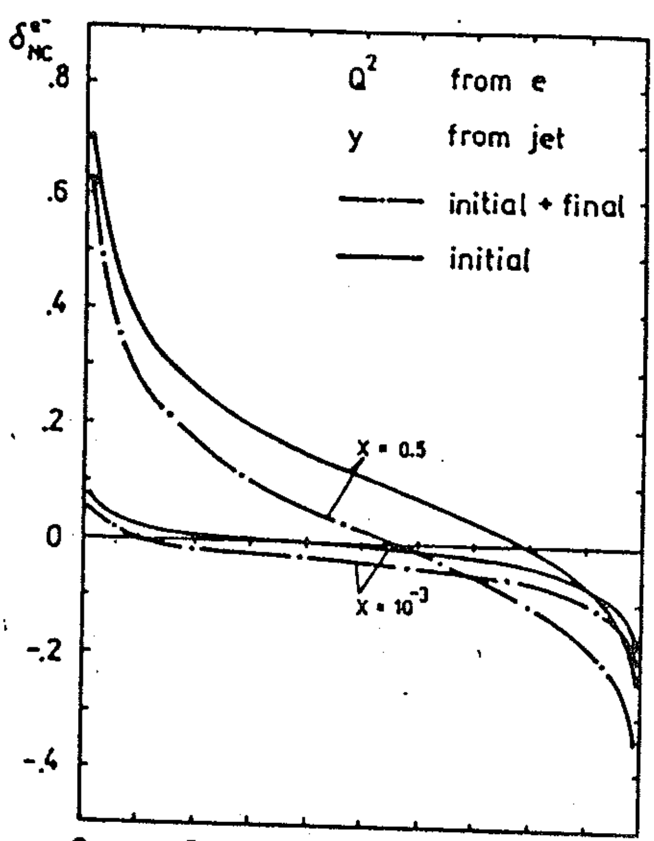

MIXED VARIABLES:

IS:

$\hat{y} = y/z$, $\hat{s} = s z$

$\hat{Q}^2 = Q^2 \cancel{z}$, $z_0 = y$

FS:

$\hat{y} = y$, $\hat{s} = s$, $\hat{Q}^2 = Q^2/z$

$z_0 = x$

BREMSSTRAHLUNG OFF QUARKS:

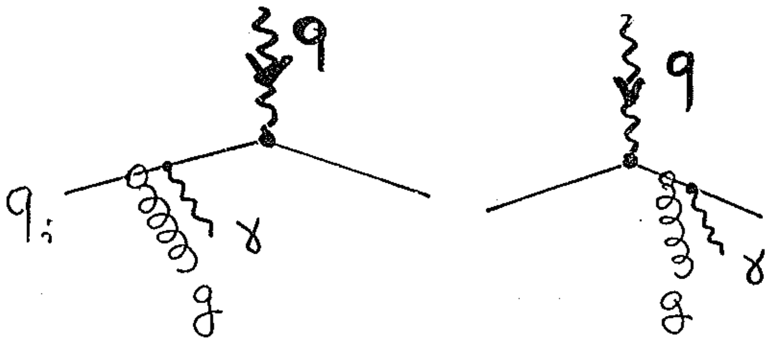

KLN $\rightarrow$ $\equiv 0$

g: P_{qq} - evolution of q_i in INITIAL OR FINAL STATE!

SOLVE AP - EQU.: WITH:

$$\boxed{P_{ff}(z) \rightarrow \left(1+\frac{3\alpha}{4\alpha_s}\right) P_{ff}(z)}$$

$\geq O(\%)$ CORRECTION TO SCALING VIOLATIONS OF STRUCTURE FUNCTIONS.

K9

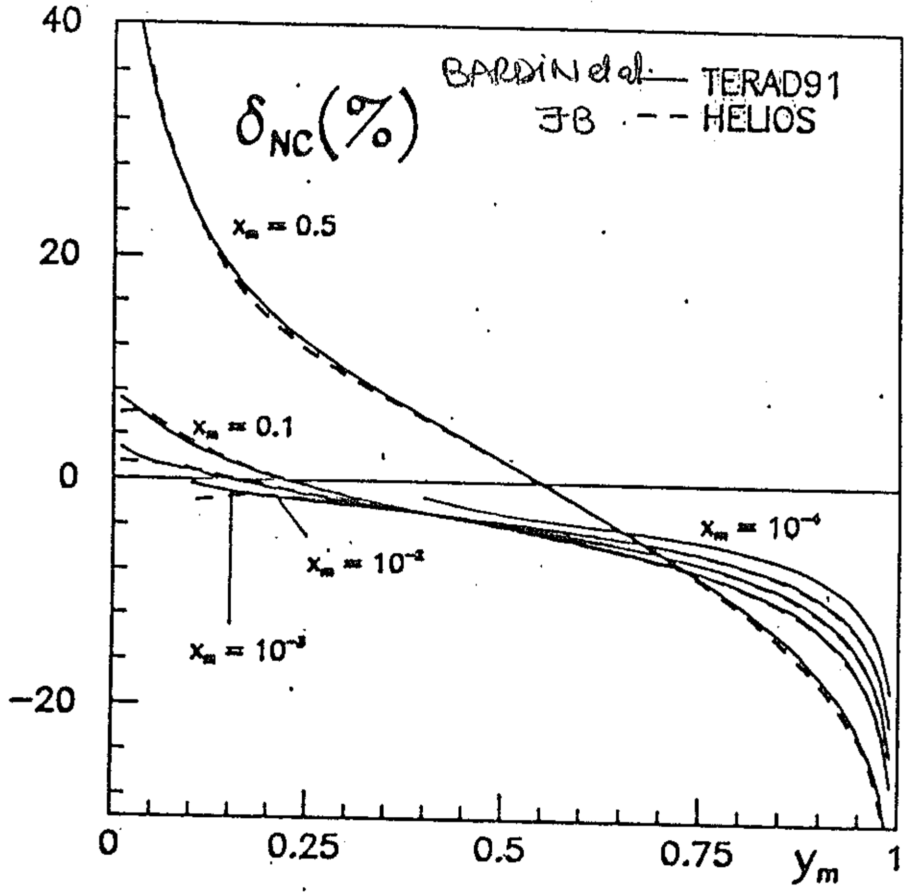

AGREEMENT:
LLA
VS. FULL
CALCULATION

Figure 7: *QED leptonic corrections to $d^2\sigma/dx_m dy_m$ in per cent. Full lines are complete $O(\alpha)$ results from TERAD91, the dashed lines represent results from the leading logarithmic approximation obtained from HELIOS.*

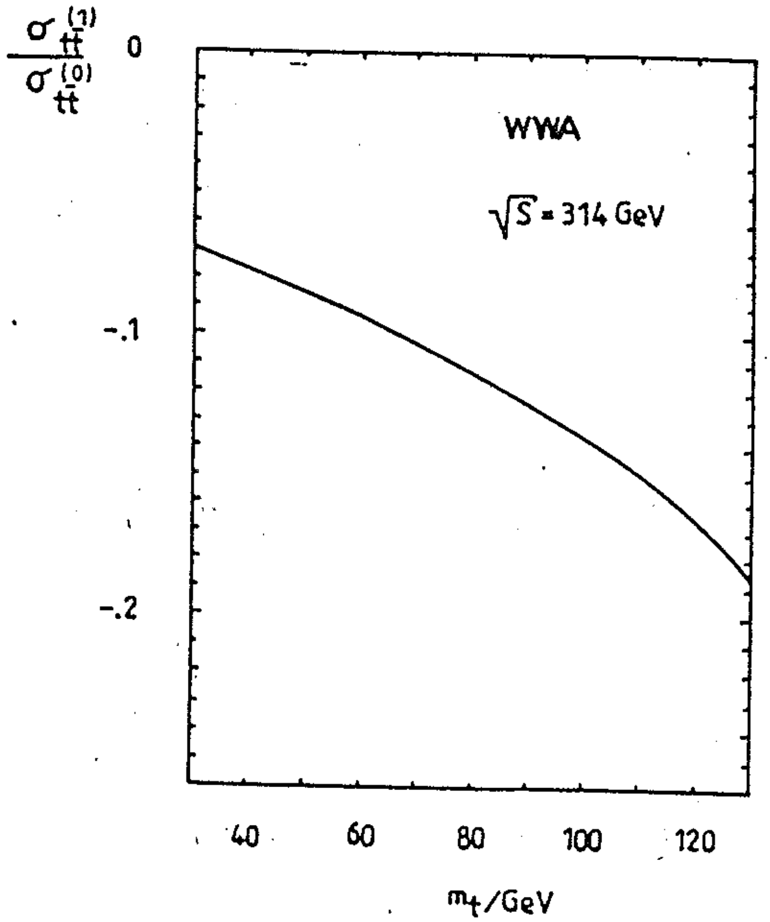

$\delta_{t\bar{t}}$ vs. m_t
HERA

WAYS TO EXTRACT STRUCTURE FUNCTIONS

CHARGED LEPTON – N DIS

NC

$$\sigma^{\pm}_{NC} = \frac{d\sigma^{\pm}_{NC}}{dx\,dQ^2} \quad , \quad \sigma^{\pm}_{CC} = \frac{d\sigma^{\pm}_{CC}}{dx\,dQ^2}$$

$F_2(x, Q^2)$:

$$\sigma^{\pm}_{NC} \quad (K_Z(Q^2) \ll 1)$$

i.e. $\dfrac{Q^2}{Q^2+M_Z^2} \lll 1$, $Q^2 \ll M_Z^2$

$(Q^2 \lesssim 700\ \mathrm{GeV}^2)$.

$$\boxed{F_2(x, Q^2) = \frac{x\,Q^4}{2\pi\alpha^2}\,\frac{1}{Y_+}\cdot\sigma^{\pm}_{NC}(x, Q^2)}$$

APPROACHING EVEN HIGHER Q^2:

$$\mathbb{B}_+(\lambda) = \frac{1}{2}\left[\sigma^{+}_{NC}(\lambda) + \sigma^{-}_{NC}(-\lambda)\right]\frac{1}{Y_+} = F_2 + \overbrace{(-v+\lambda a)}^{=0;\ v/a=\lambda\approx 0.} G_2 K_Z$$

$$+ (v^2+a^2-2va\lambda)\,H_2\,K_Z^2$$

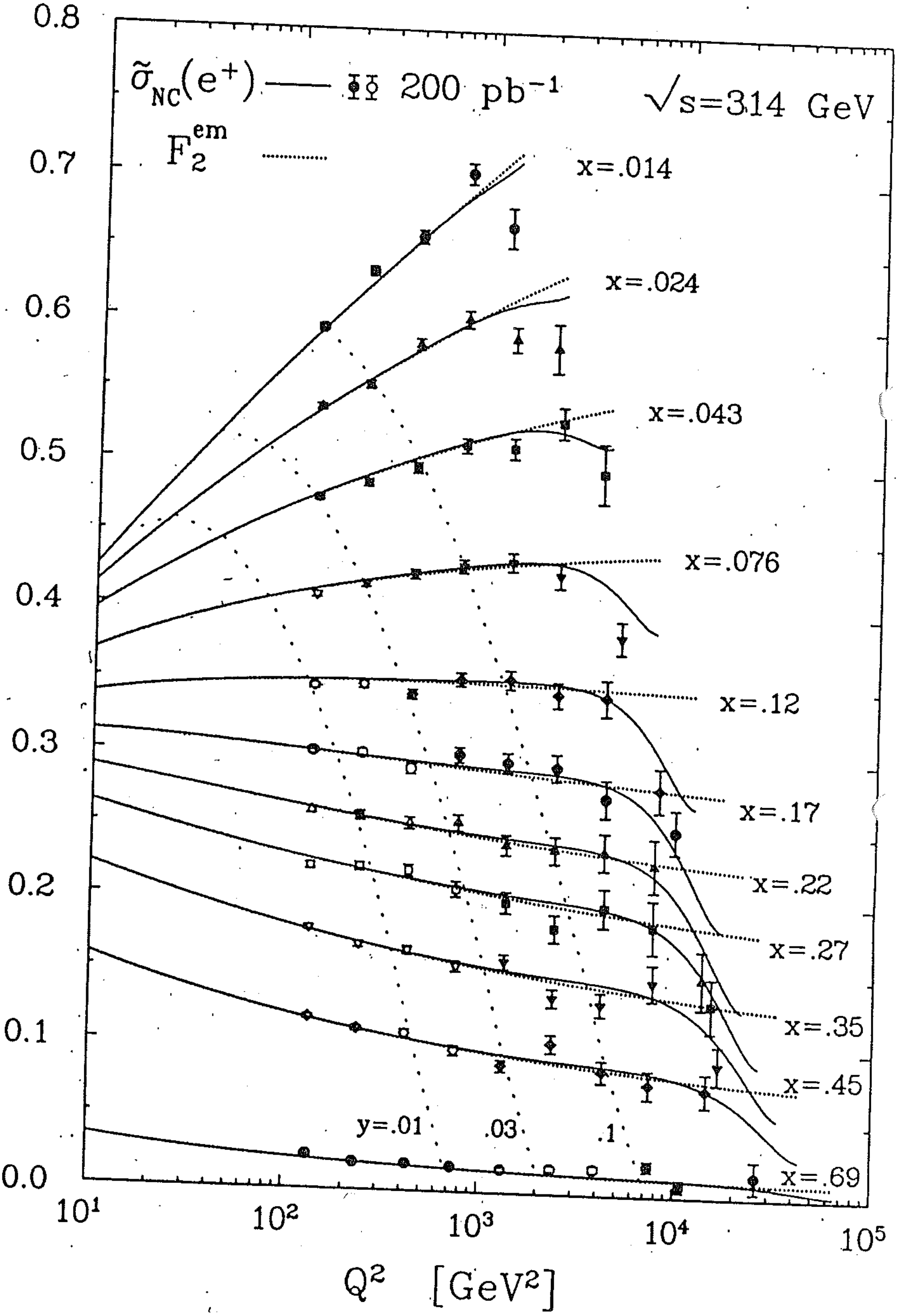

0.8
0.7
0.6
0.5
0.4
0.3
0.2
0.1
0.0
$\tilde{\sigma}_{NC}(e^+)$ —— 200 pb^{-1}
F_2^{em}
$\sqrt{s}$=314 GeV
x=.014
x=.024
x=.043
x=.076
x=.12
x=.17
x=.22
x=.27
x=.35
x=.45
x=.69
y=.01
.03
.1
10^1
10^2
10^3
10^4
10^5
Q^2 [GeV^2]

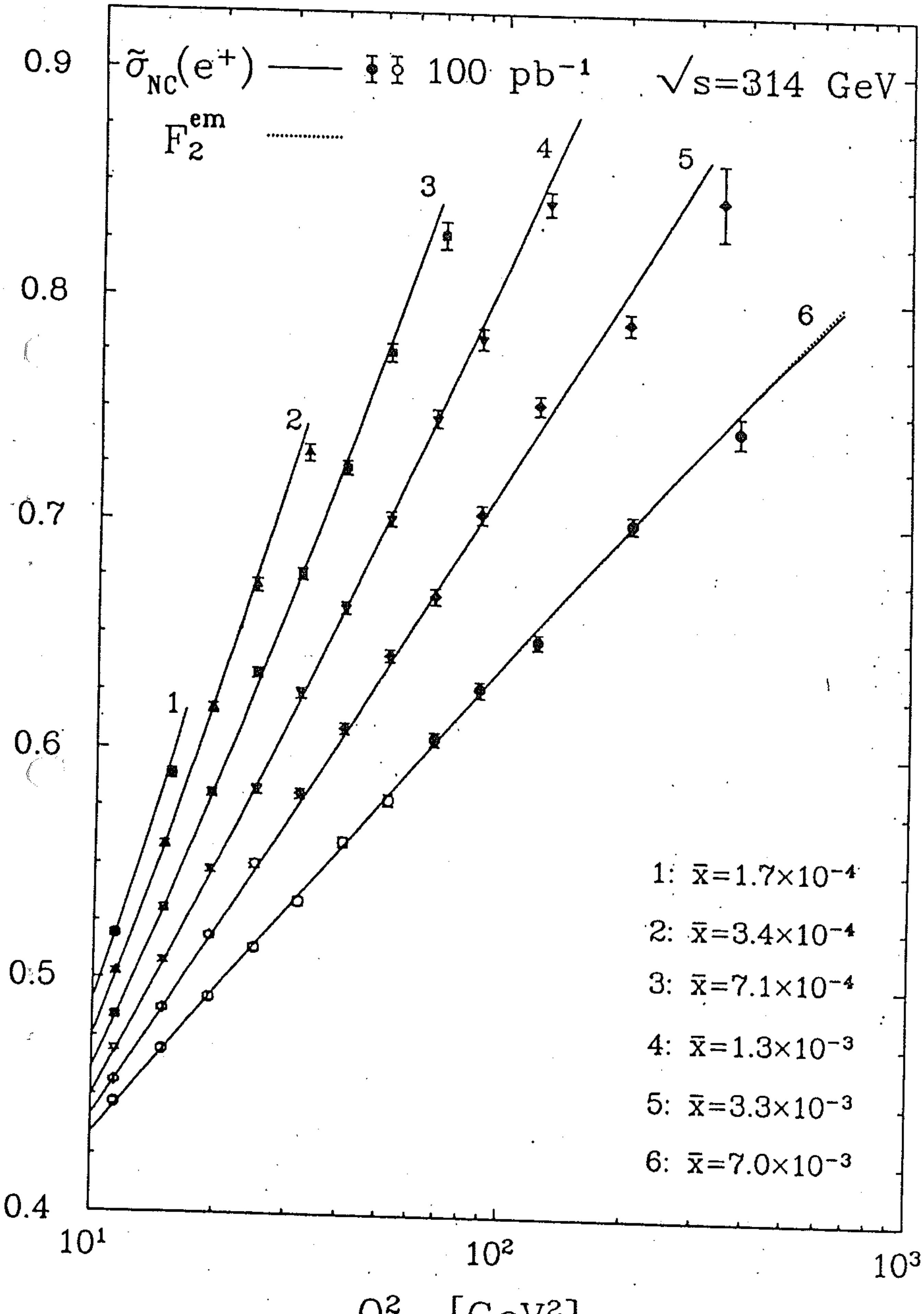

0.9
0.8
0.7
0.6
0.5
0.4
$\tilde{\sigma}_{NC}(e^+)$
100 pb^{-1}
$\sqrt{s}$=314 GeV
F_2^{em}
1
2
3
4
5
6
1: $\bar{x}=1.7\times10^{-4}$
2: $\bar{x}=3.4\times10^{-4}$
3: $\bar{x}=7.1\times10^{-4}$
4: $\bar{x}=1.3\times10^{-3}$
5: $\bar{x}=3.3\times10^{-3}$
6: $\bar{x}=7.0\times10^{-3}$
10^1
10^2
10^3

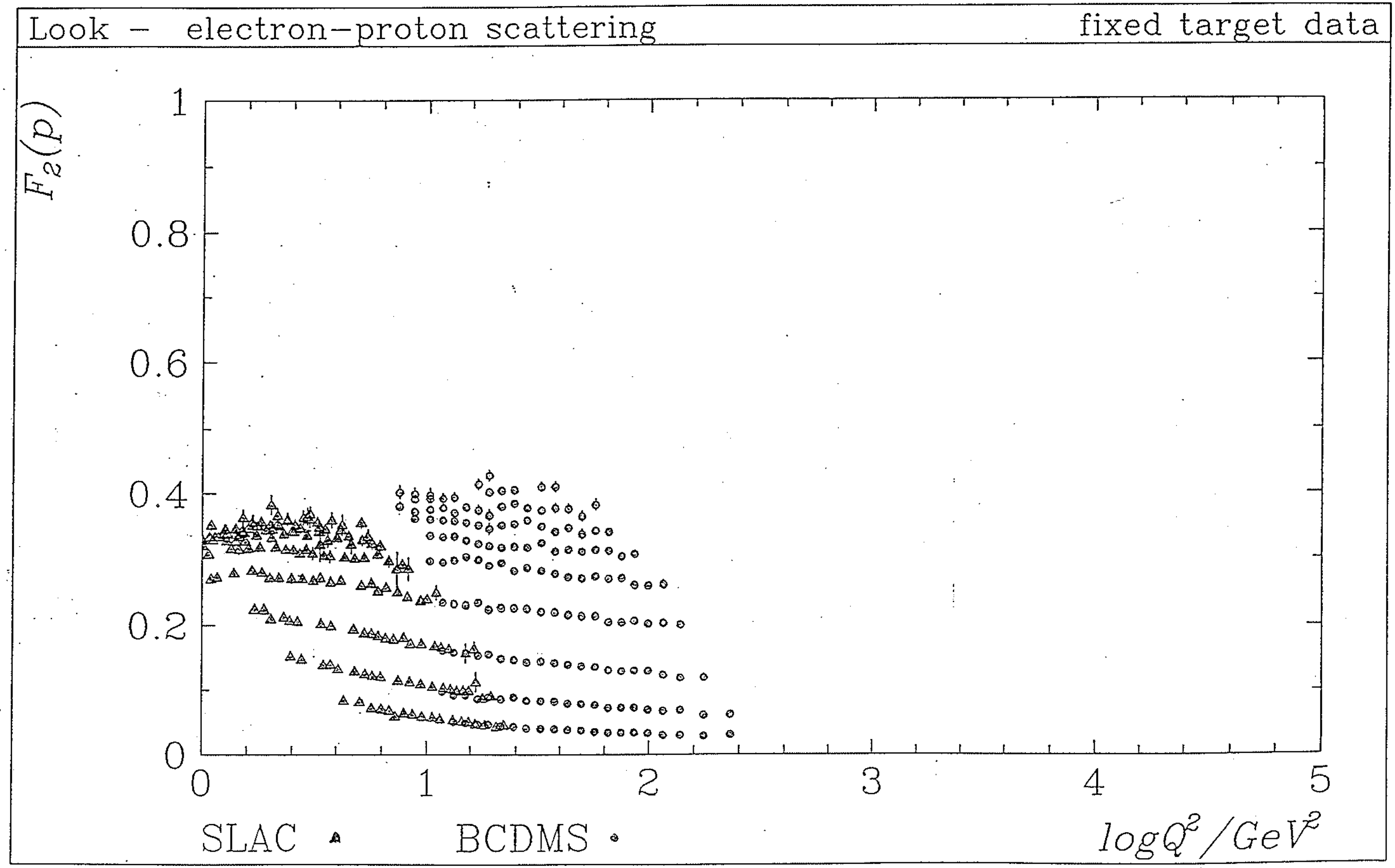
Look - electron-proton scattering
fixed target data
$F_2(p)$
1
0.8
0.6
0.4
0.2
0
0
1
2
3
4
5
SLAC
BCDMS
$log Q^2/GeV^2$

$x > .07$ $x > .07$

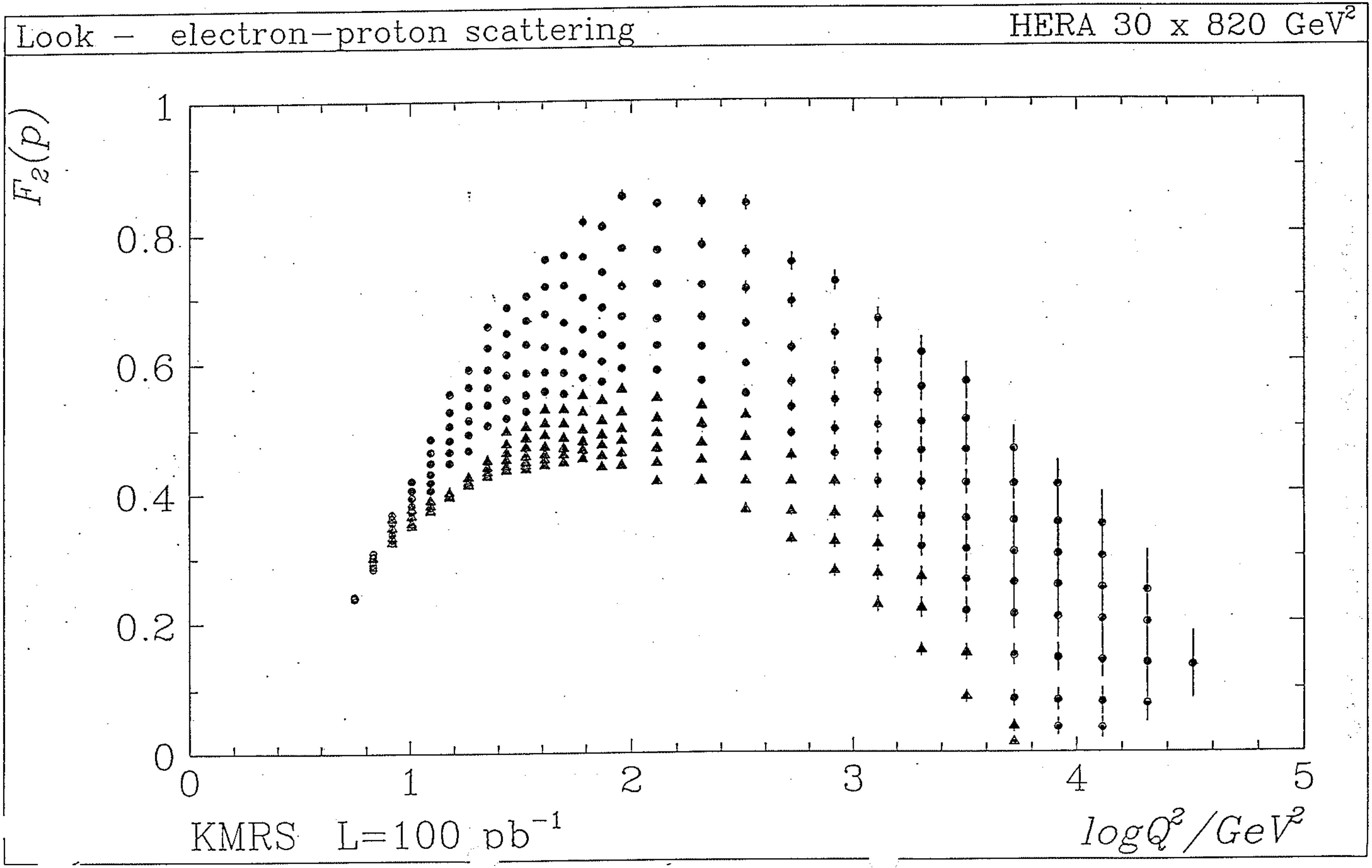

Look - electron-proton scattering
HERA 30 x 820 GeV^2
$F_2(p)$
0
0.2
0.4
0.6
0.8
1
0
1
2
3
4
5
KMRS L=100 pb^{-1}
$log Q^2/GeV^2$

BLÜMLEIN, KLEIN

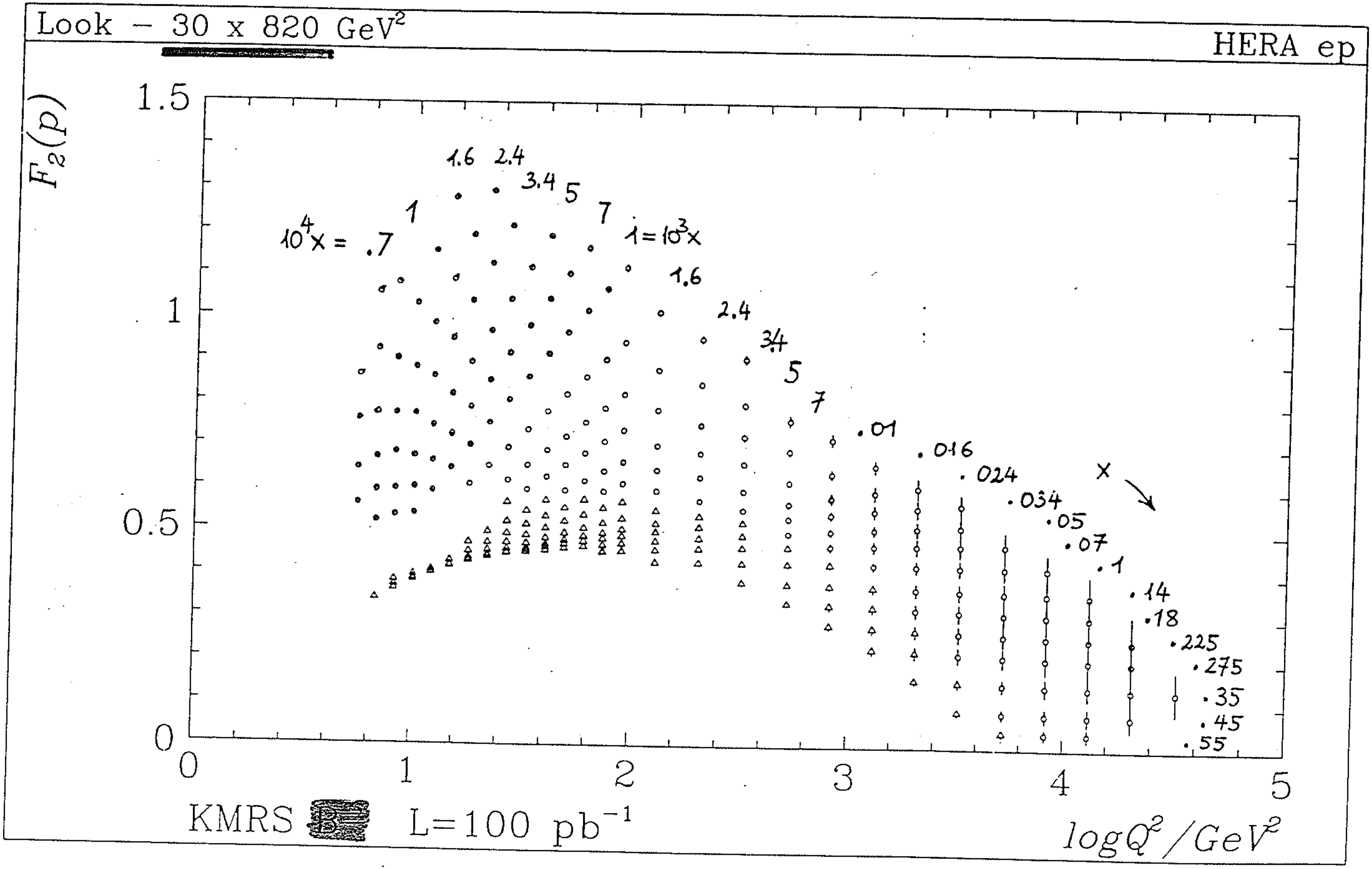

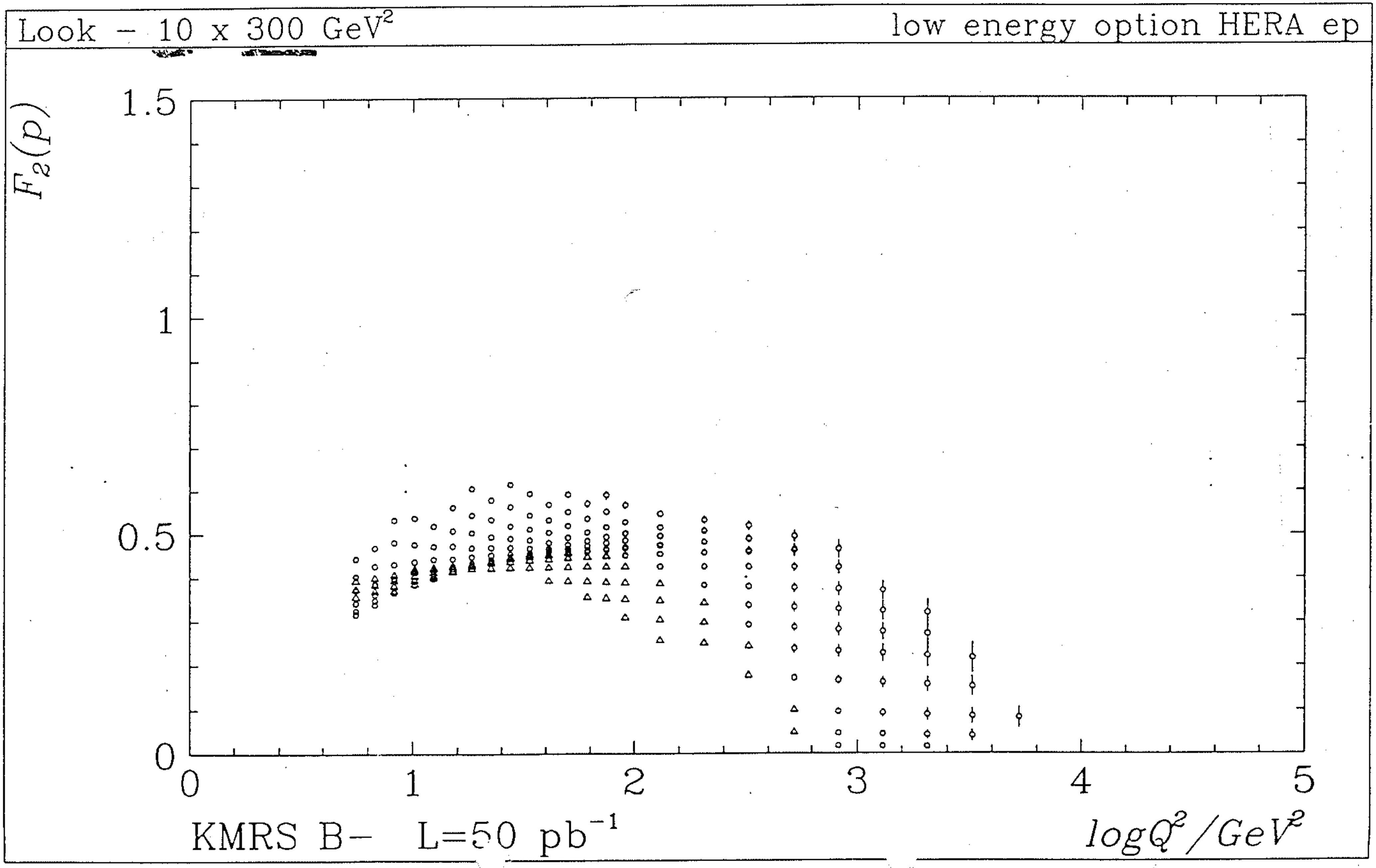

Look – 10 x 300 GeV²
low energy option HERA ep
F₂(p)
1.5
1
0.5
0
0
1
2
3
4
5
KMRS B– L=50 pb⁻¹
logQ²/GeV²

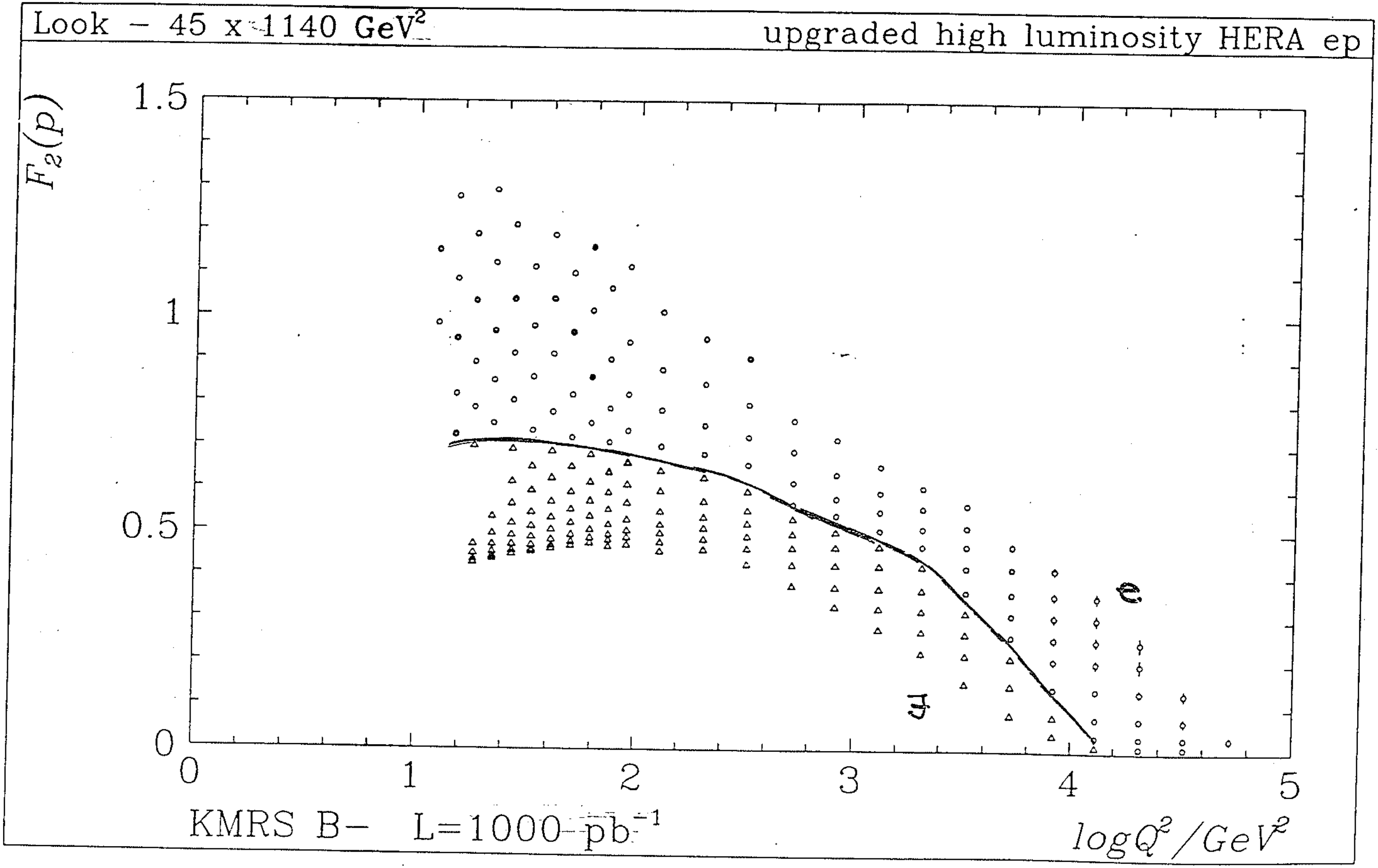

Look – 45 x 1140 GeV^2
upgraded high luminosity HERA ep
$F_2(p)$
1.5
1
0.5
0
0
1
2
3
4
5
KMRS B– L=1000 pb^{-1}
$log Q^2/GeV^2$

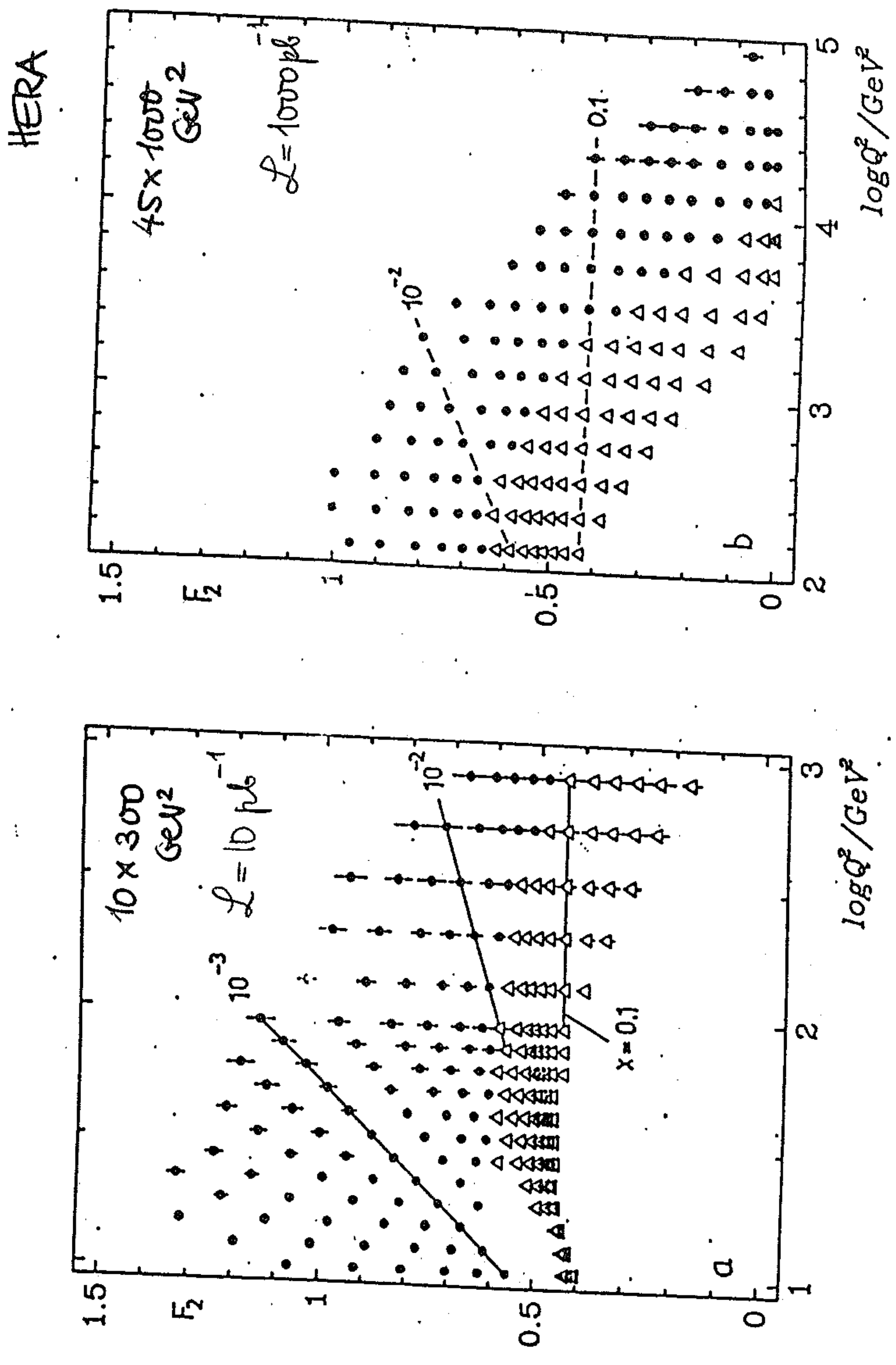

Figure 2: Expected HERA measurement of $F_2(x, Q^2)$ at lower Q^2 for a luminosity of 10 pb^{-1} at 10 × 300 (a) and at higher Q^2 for 1000 pb^{-1} at 45 × 1140 GeV^2 (b). Only statistical errors are shown. The solid points are obtainable with electron detection only ($y \geq 0.1$). The HERA data where simulated using the parametrization B^- of KMRS. The x values above $x = 0.1$ are 0.14, 0.18, 0.22, 0.27, 0.35, 0.45, 0.55, 0.65. Below they are $(0.16, 0.24, 0.34, 0.5, 0.7) \cdot 10^{-n}, n = 1, 2, 3, 4$.

Z-EXCHANGE!

LEP x LHC

$\mathcal{L} = 1000\ pb^{-1}$

$\mathcal{L} = 100\ pb^{-1}$

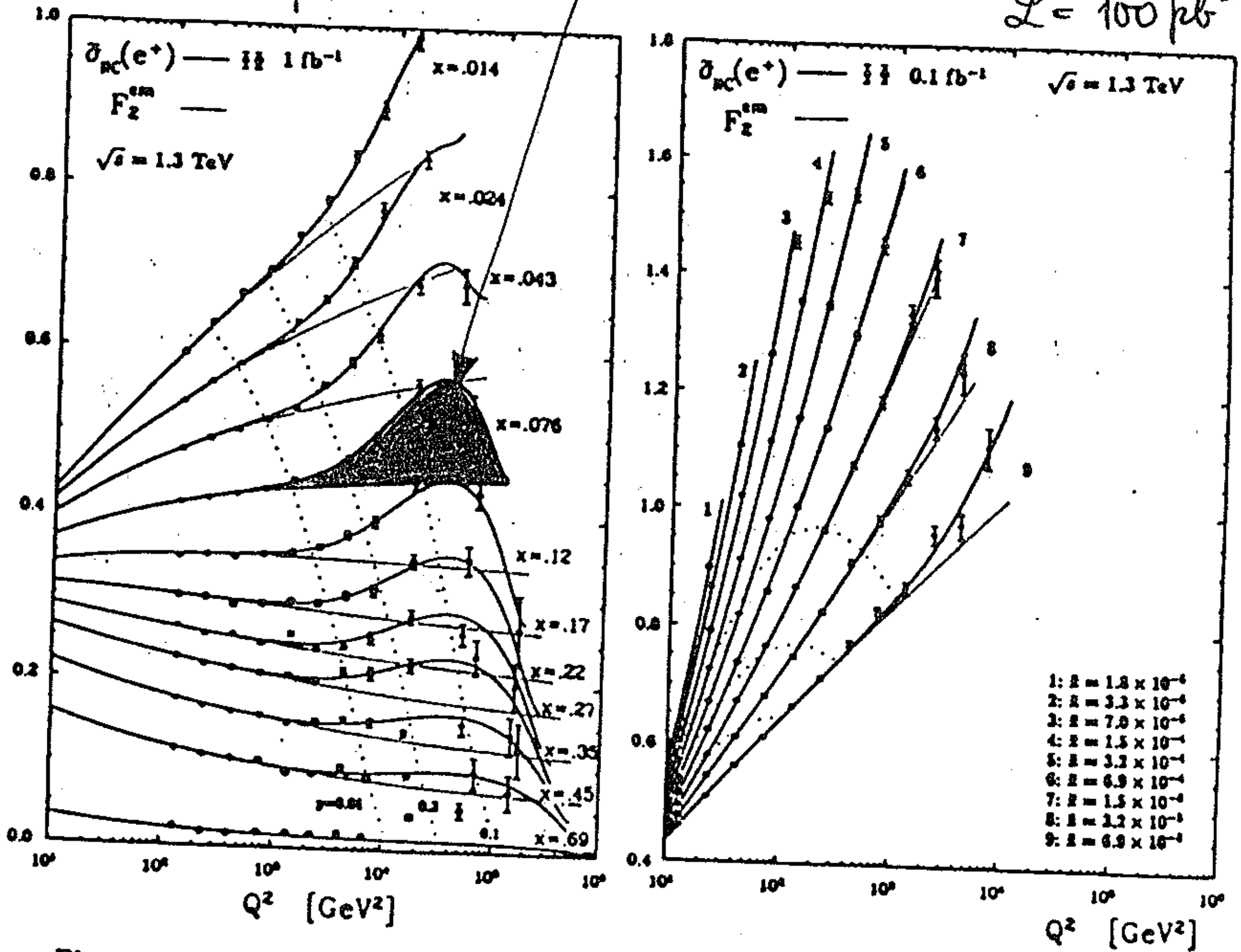

Figure 6: *Q^2 dependence of the scaled differential NC e^+p cross-section at LEP+LHC for (a) $x > 10^{-2}$ and (b) $10^{-5} < x < 10^{-2}$. The full curves correspond to $\tilde{\sigma}_{NC}(e^+)$, also represented by the MC data, while the dotted curves represent F_2^{em}, i.e. pure photon exchange, and show the pure QCD scaling violations. The full (open) MC data symbols are with (without) the restriction to the experimentally acceptable phase space region shown in Fig. 5.*

$xG_3(x,Q^2)$: PROJECT OUT THE γZ- INTERFERENCE TERM.

$$\mathbb{B}_-(\lambda) = \frac{1}{2}\frac{1}{Y_-(a-\lambda v)}\frac{1}{k_Z(Q^2)}\left[\sigma^+(-\lambda) - \sigma^-(+\lambda)\right]$$

$$= xG_3(x,Q^2) + k_Z(-2va + \lambda(v^2+a^2)) \times H_3$$

$\longrightarrow$ MEASUREMENT AT HIGH Q^2!

LEP1 × LHC $\mathcal{L} = 1000\,pb^{-1}$
LEP2 × LHC $\mathcal{L} = 100\,pb^{-1}$

HERA.

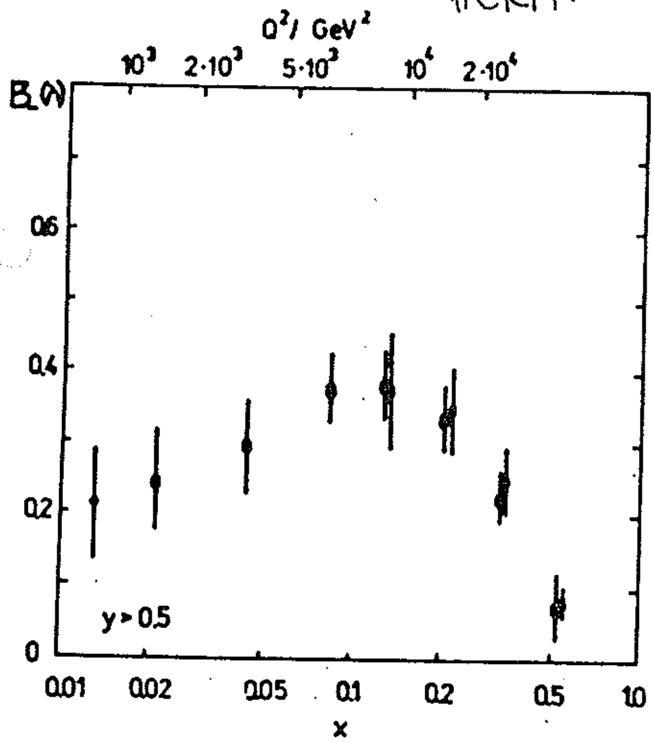

LEP × LHC

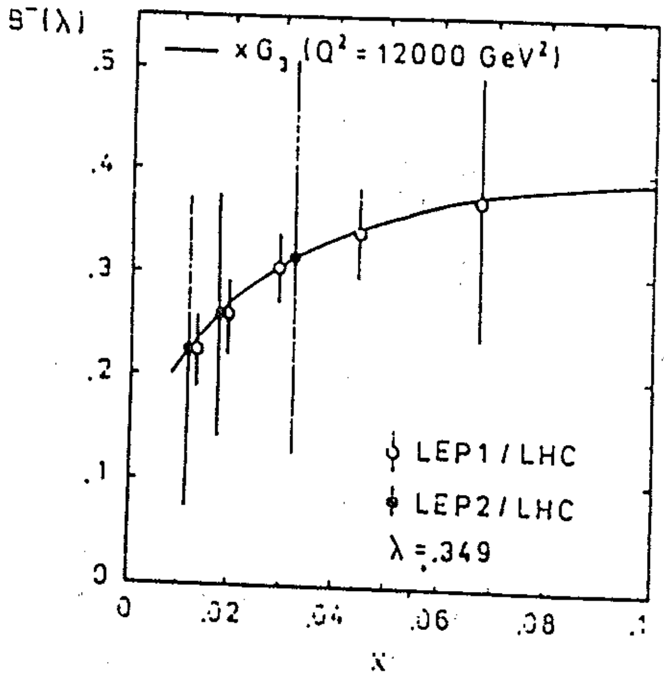

DEUTERON STRUCTURE FUNCTIONS

$e^{\pm}(\mu^{\pm})d$

NC : cf. $e^{\pm}p$

CC :

$$W_2^{eN} = \frac{1}{Y_+ K_W^2}\left[\frac{\sigma_{cc}^+}{1+\lambda_+} + \frac{\sigma_{cc}^-}{1+\lambda_-}\right]$$

$$xW_3^{eN} = \frac{1}{Y_- K_W^2}\left[\frac{\sigma_{cc}^+}{1+\lambda_+} - \frac{\sigma_{cc}^-}{1-\lambda_-}\right]$$

e^+ & e^- requir. $\mathcal{L}$-splitting.

$\overset{(-)}{\nu}_\mu(\overset{(-)}{\nu}_e)d$

NC: cf. $\overset{(-)}{\nu}p$ $\longmapsto$ very difficult to measure in 2-dimensions (x, Q^2).

CC:

$$W_2^d = \frac{2\pi x}{G_F^2 Y_+}\frac{(M_W^2+Q^2)^2}{M_W^4}\left\{\sigma^{\nu d} + \sigma^{\bar\nu d}\right\} - \frac{2xY_-}{Y_+}(s+b-c)$$

$$xW_3^d = \frac{2\pi x}{G_F^2 Y_-}\frac{(M_W^2+Q^2)^2}{M_W^4}\left\{\sigma^{\nu d} - \sigma^{\bar\nu d}\right\}$$

$\boxed{x\,G_3(x,Q^2)}$

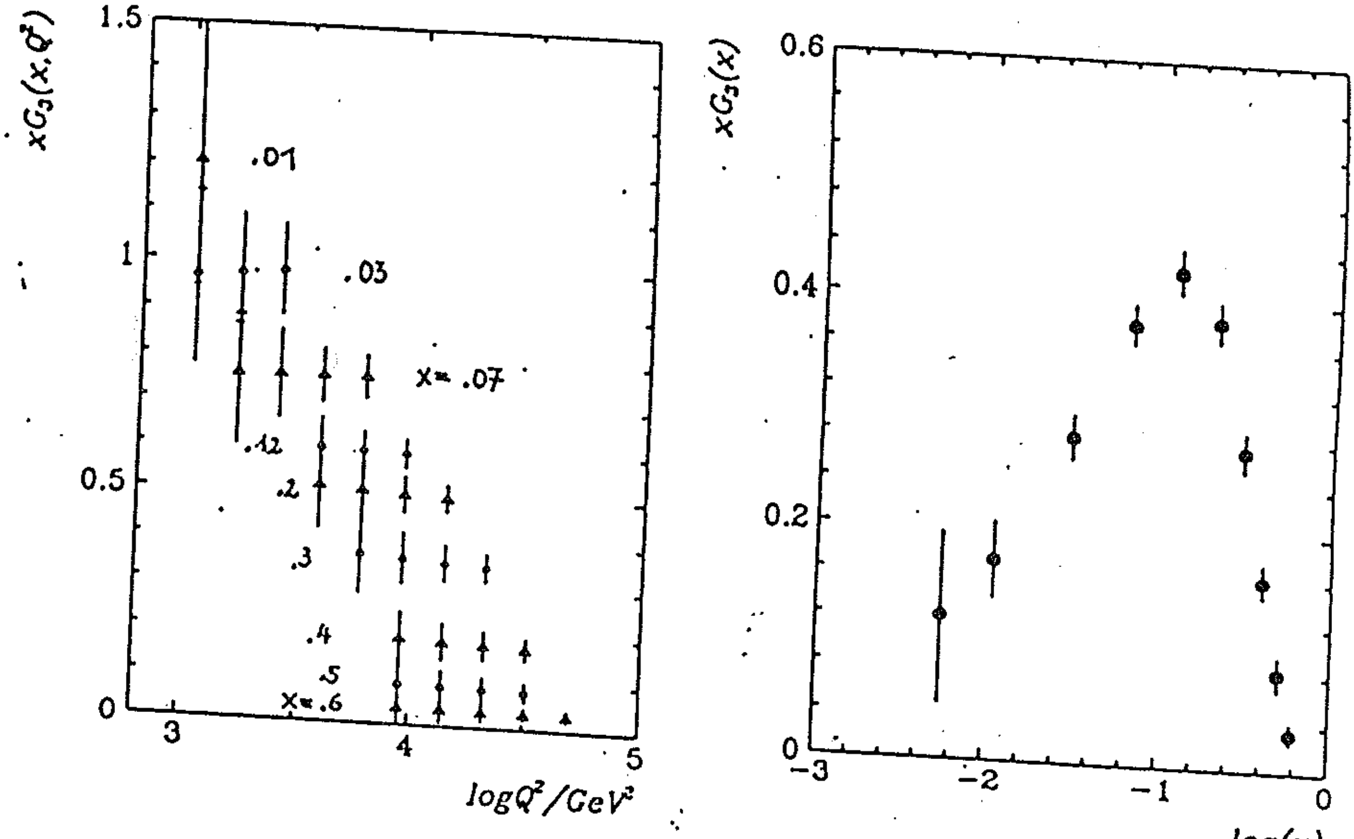

Figure 3: Statistical precision for a measurement of $xG_3(x,Q^2)$ (a) and of $xG_3(x)$ averaged over Q^2 in the accessible kinematical range (b) for $\mathcal{L} = 1\ fb^{-1}$

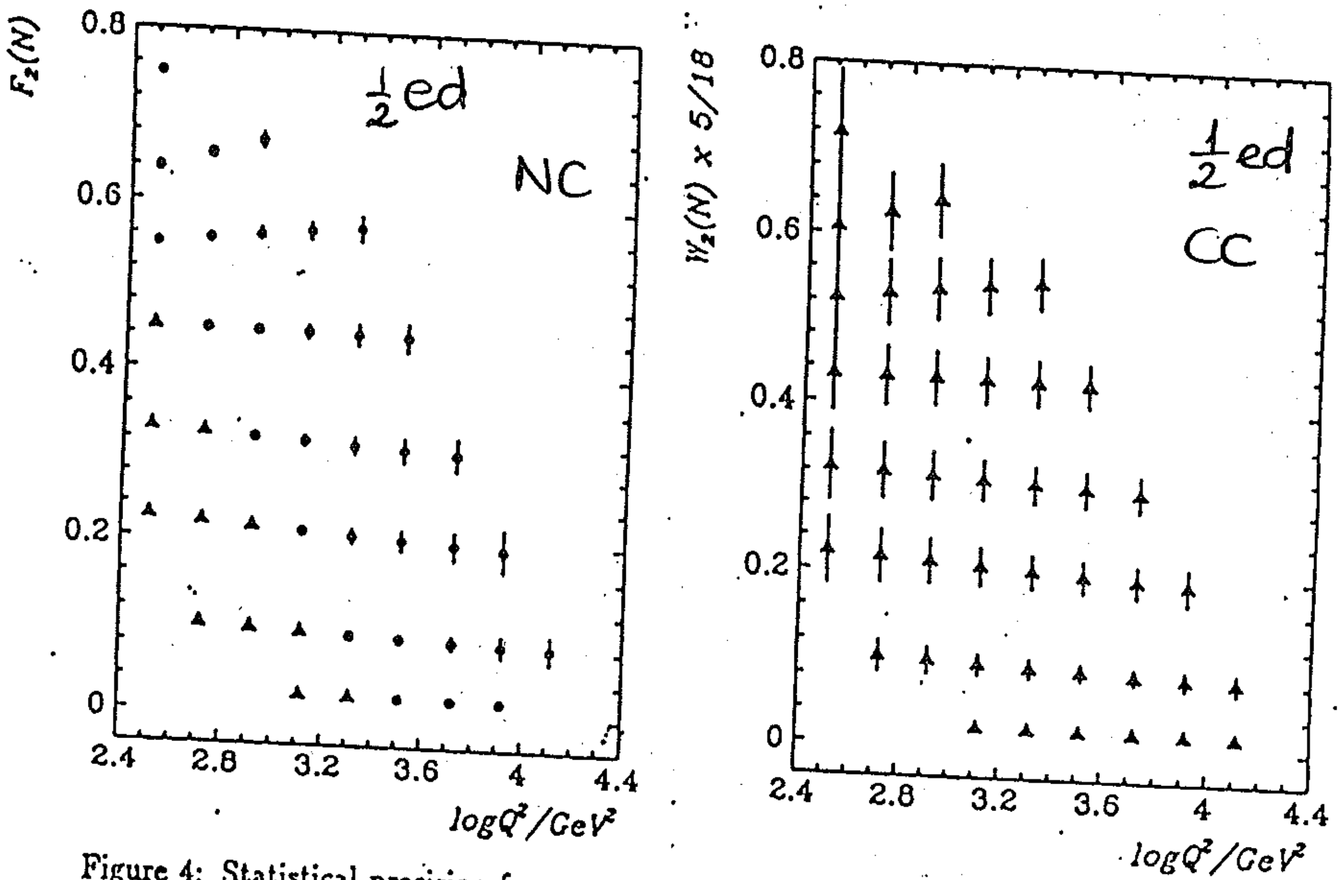

Figure 4: Statistical precision for a measurement with deuterons of F_2^{eN} and W_2^{eN}, for $\mathcal{L} = 100\ pb^{-1}$.

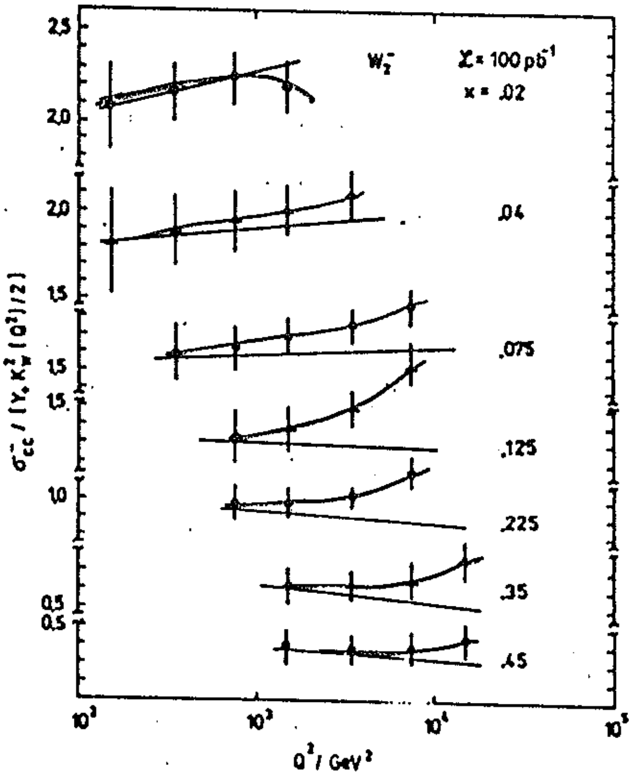

W_2^-, CC, ep
$100 pb^{-1}$

$\sigma_{CC}^{e^-p} / [Y_+ k_W^2/2]$

$(Y_-) \times W_3 \lesssim W_2$

treat as correction

$W_2^d = \frac{1}{2}[W_2^{\nu d} + W_2^{\bar{\nu} d}]$ $\overset{(-)}{\nu} d$ $x W_3^d = \frac{1}{2}[x W_3^{\nu d} + x W_3^{\bar{\nu} d}]$

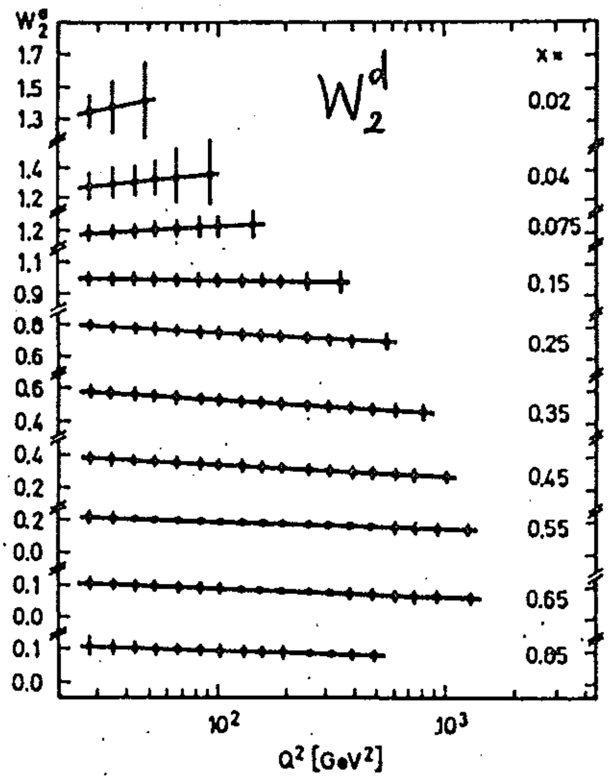

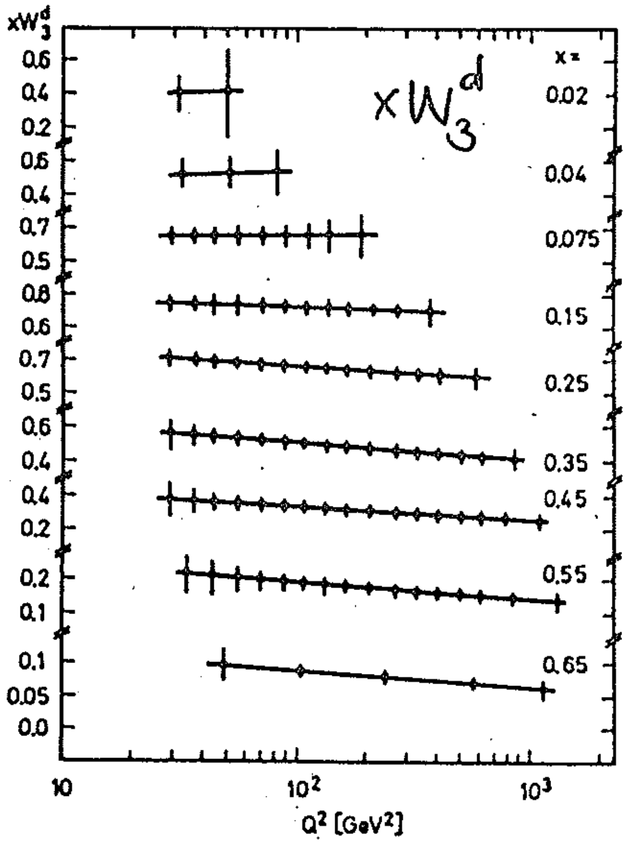

Fig. 9. **Statistical preparation of W_2 in $\overset{(-)}{\nu}$-WBB's, Eq. (5.2)**

UNK – WBB

LEP1×LHC

$e^{\pm}d$

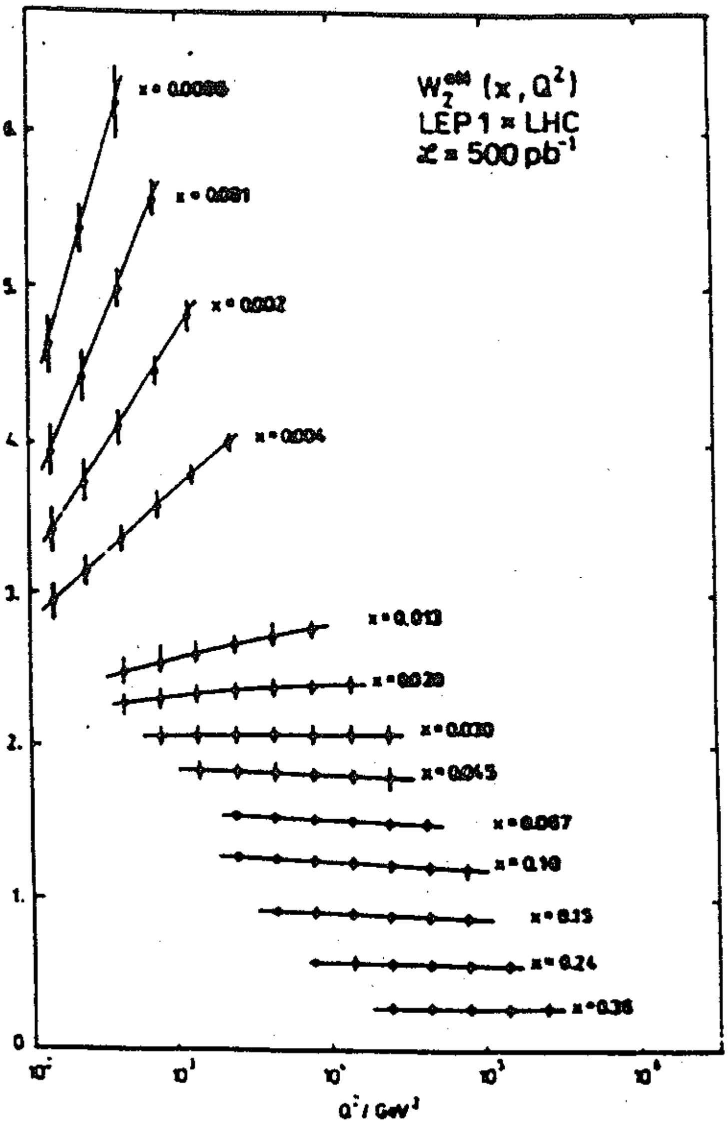

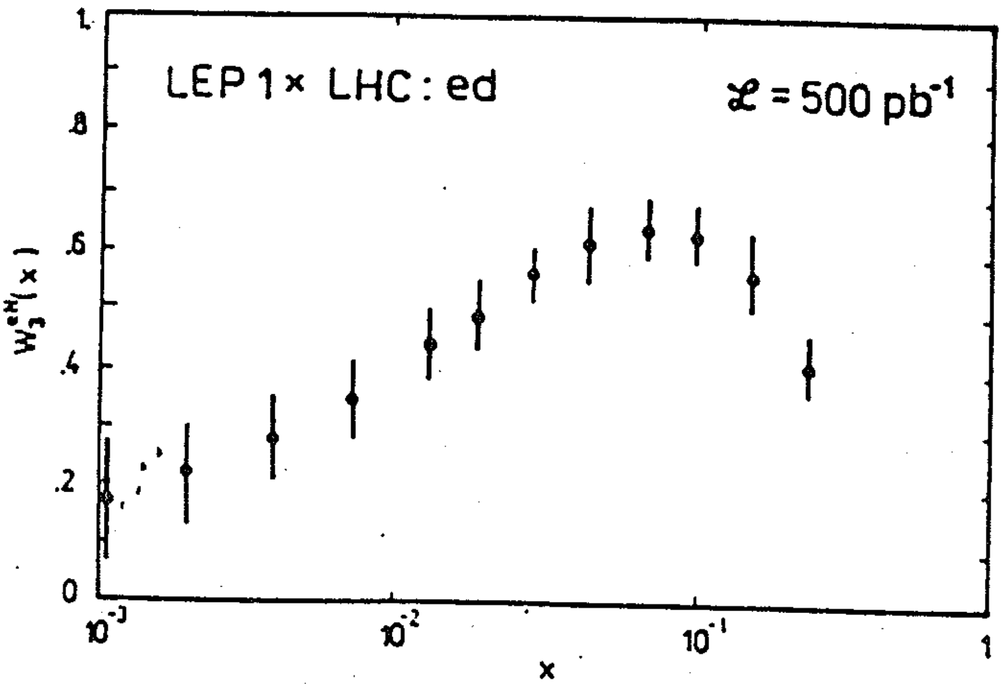

PARTON MODEL AND FLAVOUR CONTENTS OF STRUCTURE FUNCTIONS

CHARGED LEPTON (BORN) STRUCTURE FCT.:

P

$$F_2(x,Q^2) = x\sum_q e_q^2\left[q(x,Q^2)+\bar{q}(x,Q^2)\right]$$

$$G_2(x,Q^2) = x\sum_q 2e_q v_q\left[q(x,Q^2)+\bar{q}(x,Q^2)\right]$$

$$H_2(x,Q^2) = x\sum_q (v_q^2+a_q^2)\left[q(x,Q^2)+\bar{q}(x,Q^2)\right]$$

$$xG_3(x,Q^2) = 2x\sum_q e_q a_q\left[q(x,Q^2)-\bar{q}(x,Q^2)\right]$$

$$xH_3(x,Q^2) = 2x\sum_q v_q a_q\left[q(x,Q^2)-\bar{q}(x,Q^2)\right]$$

$$W_2^+(x,Q^2) = 2x\sum_i\left[d_i(x,Q^2)+\bar{u}_i(x,Q^2)\right]$$

$$W_2^-(x,Q^2) = 2x\sum_i\left[u_i(x,Q^2)+\bar{d}_i(x,Q^2)\right]$$

$$xW_3^+(x,Q^2) = 2x\sum_i\left[u_i(x,Q^2)-\bar{d}_i(x,Q^2)\right]$$

$$xW_3^-(x,Q^2) = 2x\sum_i\left[d_i(x,Q^2)-\bar{u}_i(x,Q^2)\right]$$

$$\overset{(-)}{u}_i = (\overset{(-)}{u}, \overset{(-)}{c}, \overset{(-)}{t})$$

$$\overset{(-)}{d}_i = (\overset{(-)}{d}, \overset{(-)}{s}, \overset{(-)}{b})$$

NEUTRINO (BORN) STRUCTURE FCT.:

P

$$
\boxed{
\begin{aligned}
F_2^{\nu}(x,Q^2) &= 2x\left[a_{21}\sum_i (u_i+\bar{u}_i) + a_{22}\sum_i (d_i+\bar{d}_i)\right] \\
&\equiv F_2^{\bar{\nu}}(x,Q^2) \\
xF_3^{\nu}(x,Q^2) &= 2x\left[a_{31}\sum_i (u_i-\bar{u}_i) + a_{32}\sum_i (d_i-\bar{d}_i)\right] \\
&\equiv -\,xF_3^{\bar{\nu}}(x,Q^2).
\end{aligned}
}
$$

$$
\begin{aligned}
a_{21} &= \frac{1}{4} - e_u \sin^2\theta_W + 2e_u^2 \sin^4\theta_W \\
a_{22} &= \frac{1}{4} + e_d \sin^2\theta_W + 2e_d^2 \sin^4\theta_W \\
a_{31} &= \frac{1}{4} - e_u \sin^2\theta_W \\
a_{32} &= \frac{1}{4} + e_d \sin^2\theta_W
\end{aligned}
$$

$$
\boxed{
\begin{aligned}
W_2^{\nu}(x,Q^2) &= 2x\sum_i (d_i+\bar{u}_i) \\
xW_3^{\nu}(x,Q^2) &= 2x\sum_i (d_i-\bar{u}_i) \\
W_2^{\bar{\nu}}(x,Q^2) &= 2x\sum_i (u_i+\bar{d}_i) \\
xW_3^{\nu}(x,Q^2) &= 2x\sum_i (u_i-\bar{d}_i)
\end{aligned}
}
$$

DEUTERONS & ISOSCALAR NUCLEI

d's at colliders: $s \to s/2$!

quark contents:

$$\boxed{\overset{(-)}{u}_1, \overset{(-)}{d}_1 \equiv \overset{(-)}{u}, \overset{(-)}{d} \to \frac{1}{2}\overset{(\longrightarrow)}{(u+d)}}$$

⟶ previous formulae modify accordingly.

EXAMPLES:

$e^{\pm}d$

$$F_2^{ed} = \frac{5}{18}x(u_v+d_v) + \frac{10}{9}xu_s + \frac{2}{9}xs + \frac{8}{9}xc + \frac{2}{9}xb$$

$$xG_3^{ed} = \frac{1}{2}x(u_v+d_v) = \frac{1}{2}V$$

$$W_2^{e^{\pm}d} = x(u_v+d_v) + 4xu_s + 2xs + 2xc + 2xb \equiv \Sigma$$

$$xW_3^{e^{\pm}d} = x(u_v+d_v) \pm 2x\underline{(s-c)}$$

$$W_2^{\overset{(-)}{\nu} d} = \sum_i x \left[q_i(x, Q^2) + \bar{q}_i(x, Q^2) \right] \equiv \Sigma$$

$$\frac{1}{2}\left[x W_3^{\nu d} + x W_3^{\bar{\nu} d} \right] \underset{Df}{=} x W_3^d = x(u_v + d_v) \equiv V$$

WAYS TO UNFOLD PARTON DENSITIES

$\boxed{e^{\pm}p}$ 4 CROSS SECTIONS $\sigma_{NC}^{\pm}$, $\sigma_{CC}^{\pm}$ $\hookrightarrow$ 4 COMBINATIONS OF PARTON DENSITIES

LINEAR MAPPING: $\overset{(-)}{U} = \sum_i x \overset{(-)}{u}_i$; $\overset{(-)}{D} = \sum_i x \overset{(-)}{d}_i$

$$\boxed{\begin{pmatrix} U \\ \overline{U} \\ D \\ \overline{D} \end{pmatrix} = (A_{ij}) \begin{pmatrix} \sigma_{NC}^{-} \\ \sigma_{NC}^{+} \\ \sigma_{CC}^{-} \\ \sigma_{CC}^{+} \end{pmatrix}}$$

$$\det_4 A_{ij} \sim \left\{ \kappa_Z(Q^2) \left[1 - (1-y)^4 \right] \right\}^{-1}$$

(A_{ij}) becomes singular both for: $Q^2 \ll M_Z^2$
(degenerate) $y \ll 1$

CONSIDER e.g. (WITH ASSUMPTIONS ON SEA-QUARKS)

$$\boxed{\begin{pmatrix} x u_v \\ x d_v \\ x s \end{pmatrix} = (B_{ij}) \begin{pmatrix} \sigma_{NC}^{-} \\ \sigma_{NC}^{+} \\ \sigma_{CC}^{-} \end{pmatrix}}$$

P6

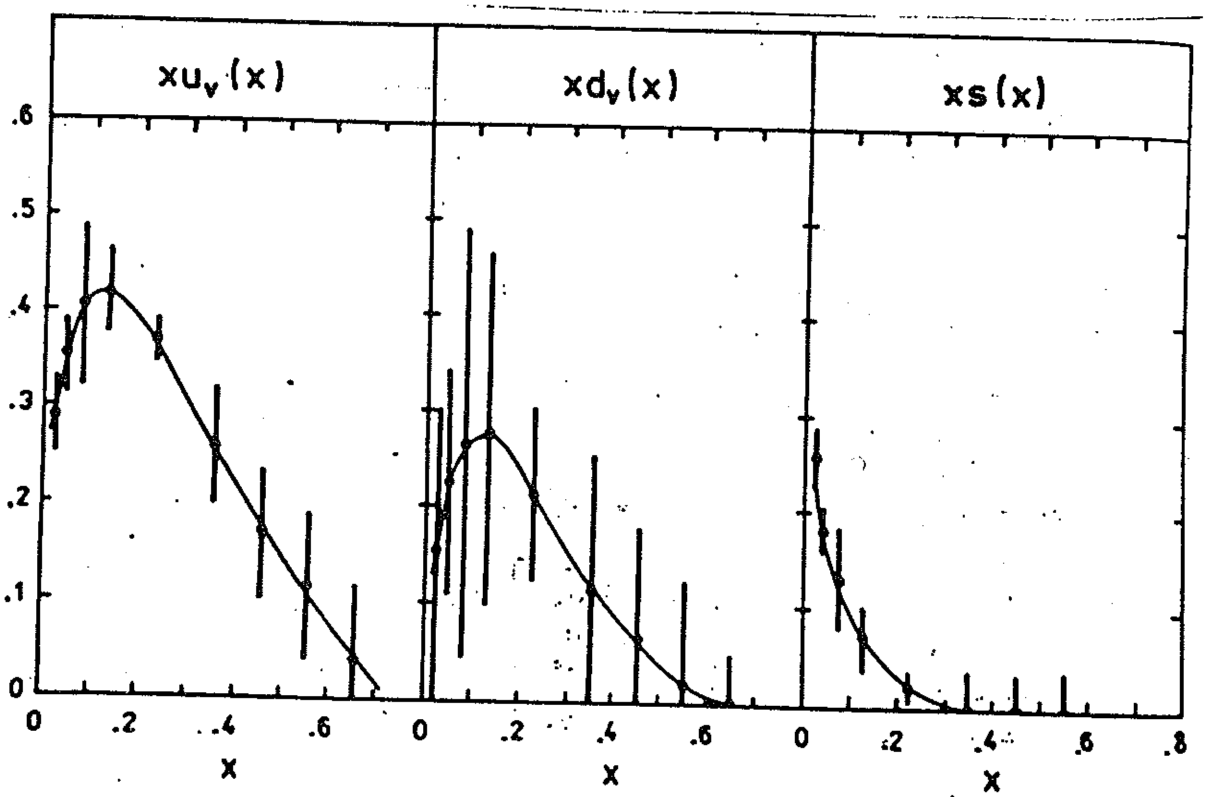

$\mathcal{L} = 100\,pb^{-1}$ / per beam

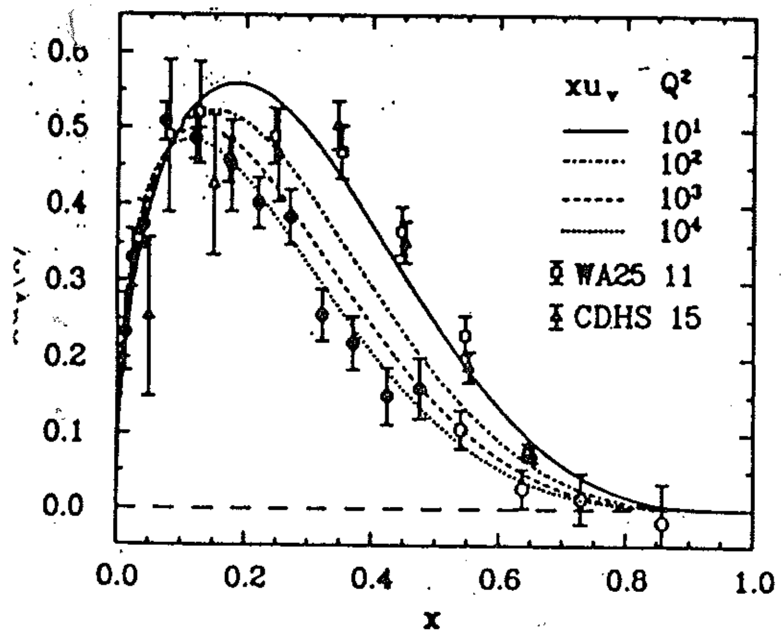

Ingelman / Rückl

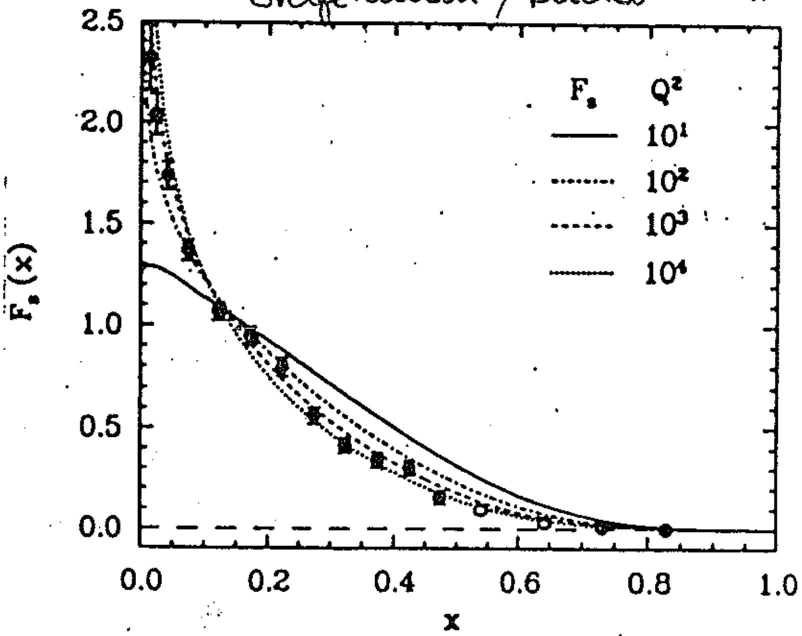

$\sum \mathcal{L} = 400\,pb^{-1}$

APPROXIMATE REPRESENTATIONS

VALENCE RANGE

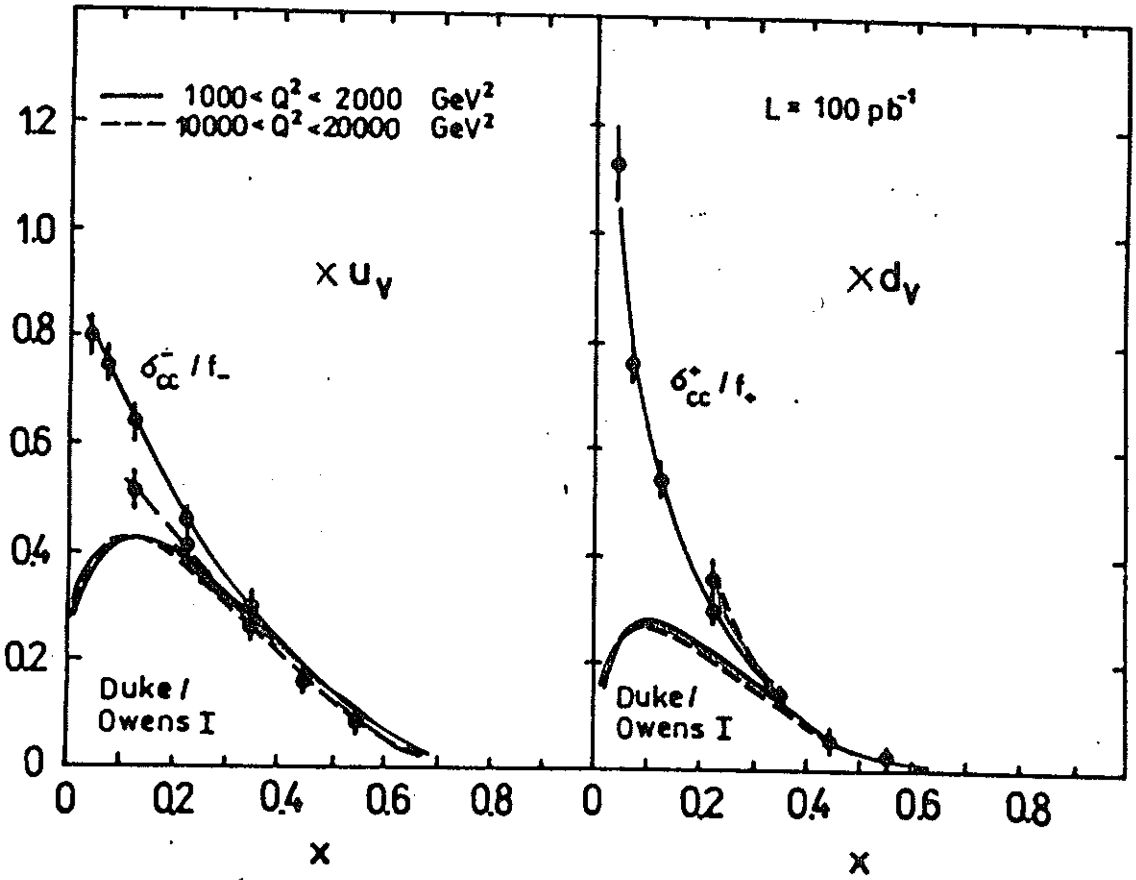

$$f_\pm = \frac{1}{2}\left(Y_+ \mp Y_-\right) K_W^2$$

$\mathcal{L} = 100\,pb^{-1}$

$e^{\pm}p$ & $e^{\pm}d$

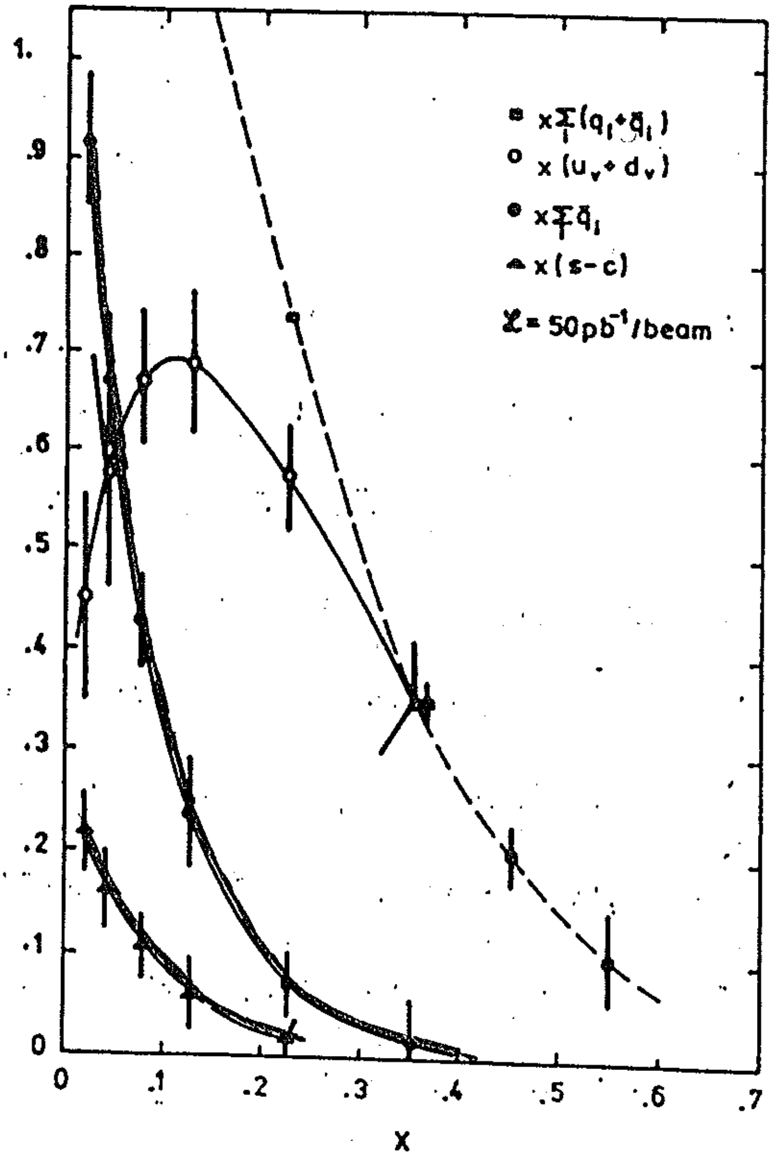

$$\bar{Q} = \frac{1}{2}\left(W_2^{eN} - x W_3^{eN}\right)$$

$$x(s-c) = \frac{5}{18} W_2^{eN} - F_2^{eN} \quad , \quad b \approx 0$$

$\mathcal{L} = 50\,pb^{-1}/\text{beam}$

$$\nu\text{'s}: \quad x(u_v - d_v) = \frac{4\pi x}{G_F^2} \frac{(M_W^2 + Q^2)^2}{M_W^4} \frac{1}{Y_+ + Y_-} \left[\frac{1}{2} \sigma^{\nu d} - \sigma^{\nu p} \right]$$

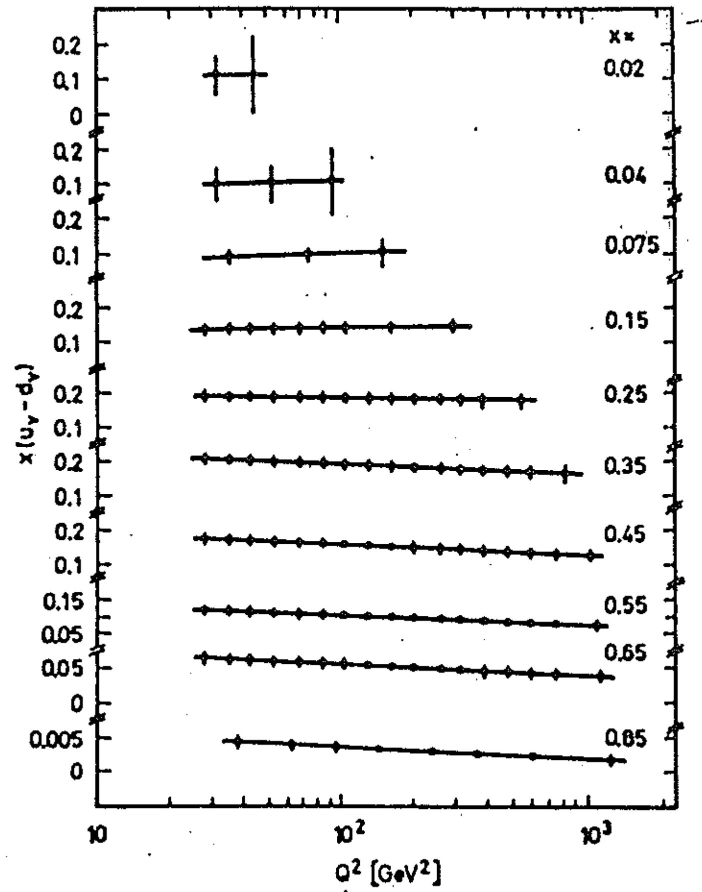

$x(u_v - d_v)$

Fig. 12. **Statistical precision of a measurement of $x(u_\nu - d_\nu)$ using Eq. (7.1)**

$$\sum_i x\bar{q}_i = \frac{\bar{Q}}{2} = \frac{2\pi x}{G_F^2} \frac{(M_W^2 + Q^2)^2}{M_W^4} \left[\sigma^{\bar{\nu} d} - \sigma^{\nu d} (1-y)^2 \right] \frac{1}{Y_+ Y_-} - \frac{x(s+b-c)}{Y_+}$$

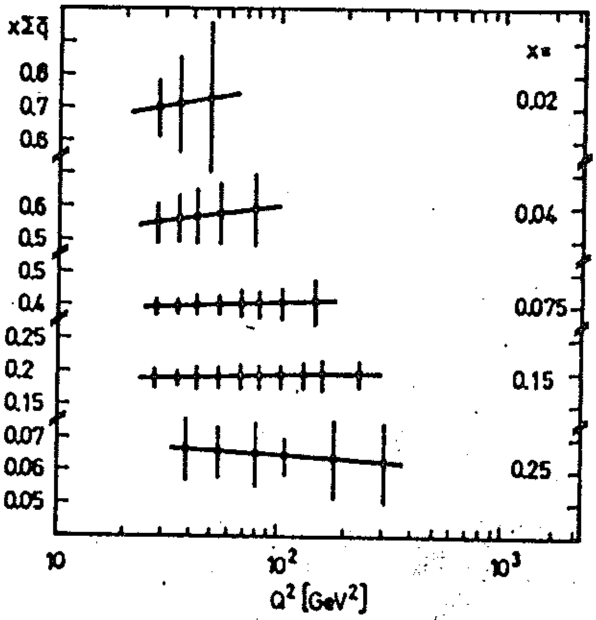

$\sum_i x\bar{q}_i$

Fig. 15. **Statistical precision of a measurement of the antiquark distribution Eq. (7.3)**

HEAVY FLAVOURS

c, b, t

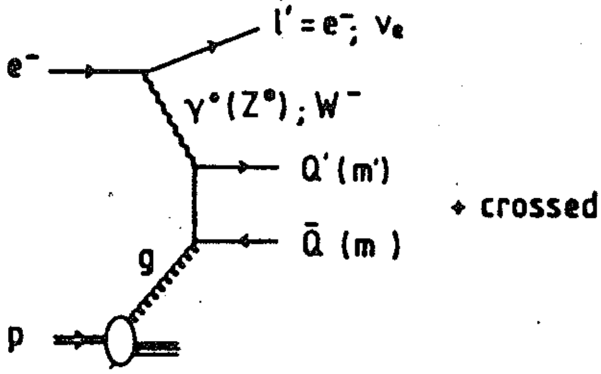

Fig. 1

GLÜCK, REYA, GODBOLE

NC

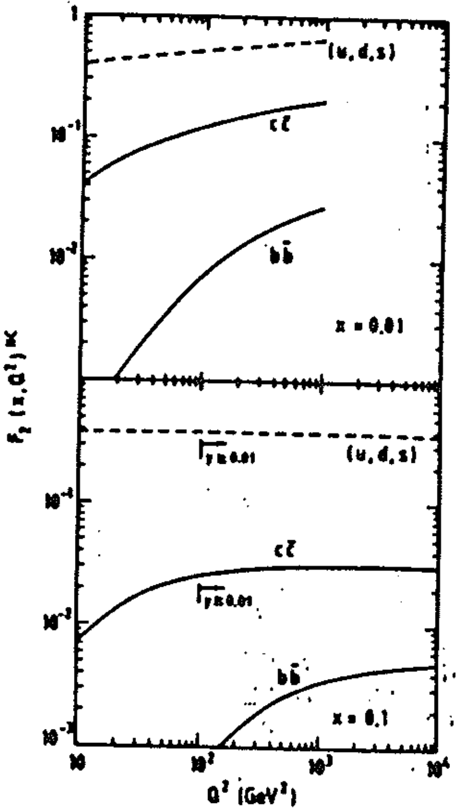

Fig. 2

CC

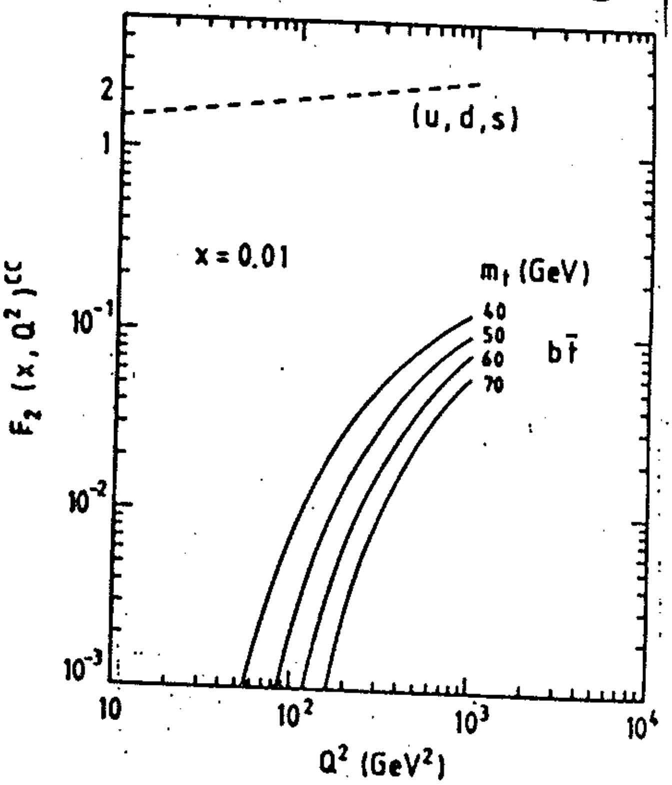

Fig. 3a

PARAMETRIZATIONS OF PARTON DISTRIBUTIONS

$x u_v$ STIRLING

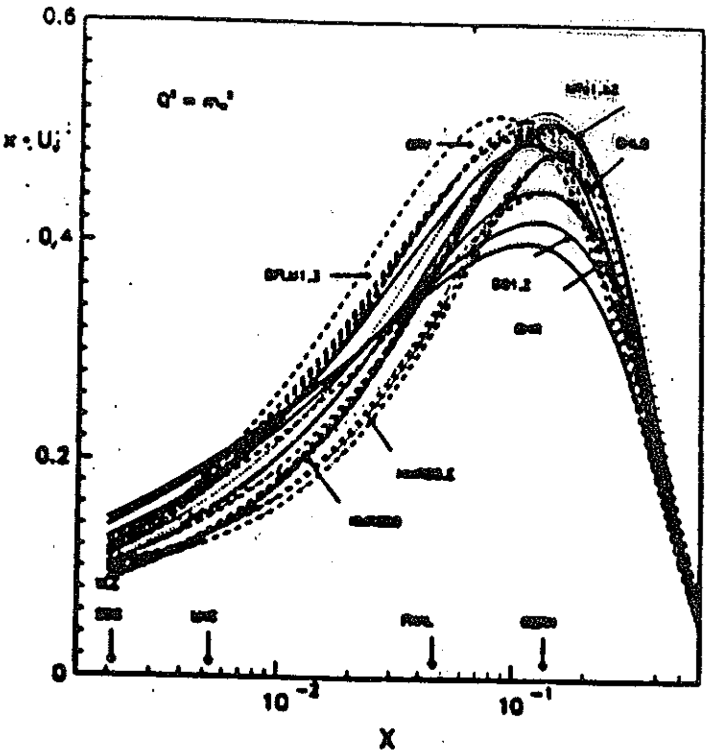

Figure 1: The valence u-quark distribution at $Q^2 = M_W^2$ [4].

F_2^{ep}

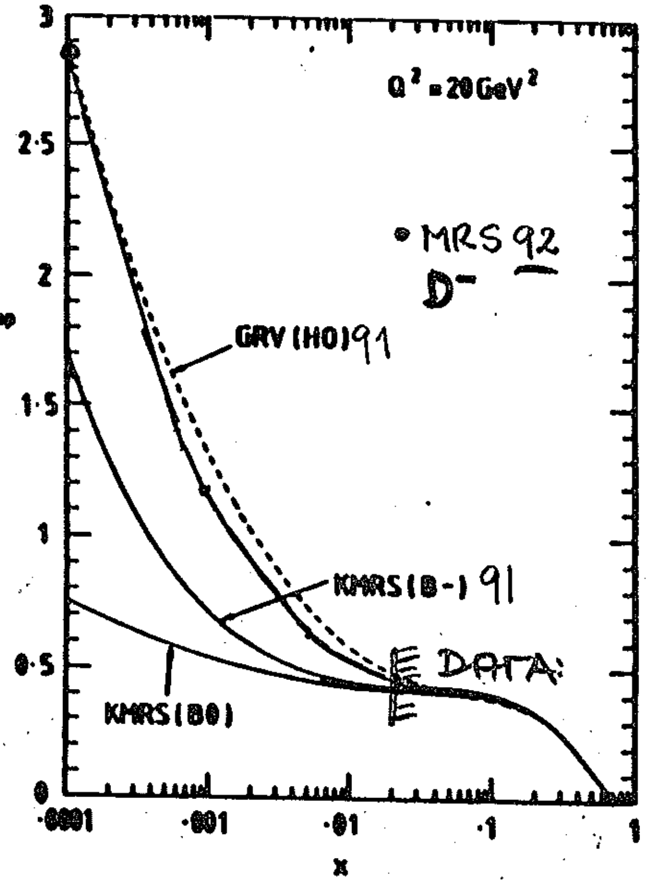

Figure 3: F_2^{ep} structure function predictions.

IDIS =1	Duke, Owens	set 1	(1984)	[12]
IDIS =2	Duke, Owens	set 2	(1984)	[12]
IDIS =3	Owens		(1991)	[13]
IDIS =4	Eichten et al.	set 1	(1984)	[14]
IDIS =5	Eichten et al.	set 2	(1984)	[14]
IDIS =6	Diemoz et al.	LO	(1988)	[15]
IDIS =7	Diemoz et al.	NTLO	(1988)	[15]
IDIS =8	Harriman et.al.	EMC	(1990)	[16]
IDIS =9	Harriman et.al.	BCDMS	(1990)	[16]
IDIS =10	Morfin,Tung	LO BCDMS+EMC SU(3) symm.sea	(1991)	[17]
IDIS =11	Morfin,Tung	DIS,BCDMS+EMC SU(3) symm.sea	(1991)	[17]
IDIS =12	Morfin,Tung	DIS,BCDMS+EMC SU(3) non-symm.sea	(1991)	[17]
IDIS =13	Morfin,Tung	DIS,BCDMS1,SU(3) symm.sea	(1991)	[17]
IDIS =14	Morfin,Tung	DIS,BCDMS2,SU(3) symm.sea	(1991)	[17]
IDIS =15	Morfin,Tung	DIS,EMC,SU(3) symm.sea	(1991)	[17]
IDIS =16	Morfin,Tung	MS,BCDMS+EMC SU(3) symm.sea	(1991)	[17]
IDIS =17	Morfin,Tung	MS,BCDMS+EMC SU(3) non-symm.sea	(1991)	[17]
IDIS =18	Morfin,Tung	MS,BCDMS1,SU(3) symm.sea	(1991)	[17]
IDIS =19	Morfin,Tung	MS,BCDMS2,SU(3) symm.sea	(1991)	[17]
IDIS =20	Morfin,Tung	MS,EMC,SU(3) symm.sea	(1991)	[17]
IDIS =21	Kwiecinski et al.	set B0	(1990)	[18]
IDIS =22	Kwiecinski et al.	set B-	(1990)	[18]
IDIS =23	Kwiecinski et al.	set B-, weak shadowing	(1990)	[18]
IDIS =24	Kwiecinski et al.	set B-, strong shadowing	(1990)	[18]
IDIS =25	Glück et al.	LO	(1991)	[19]
IDIS =26	Glück et al.	NTLO	(1991)	[19]

(1992)

etc.

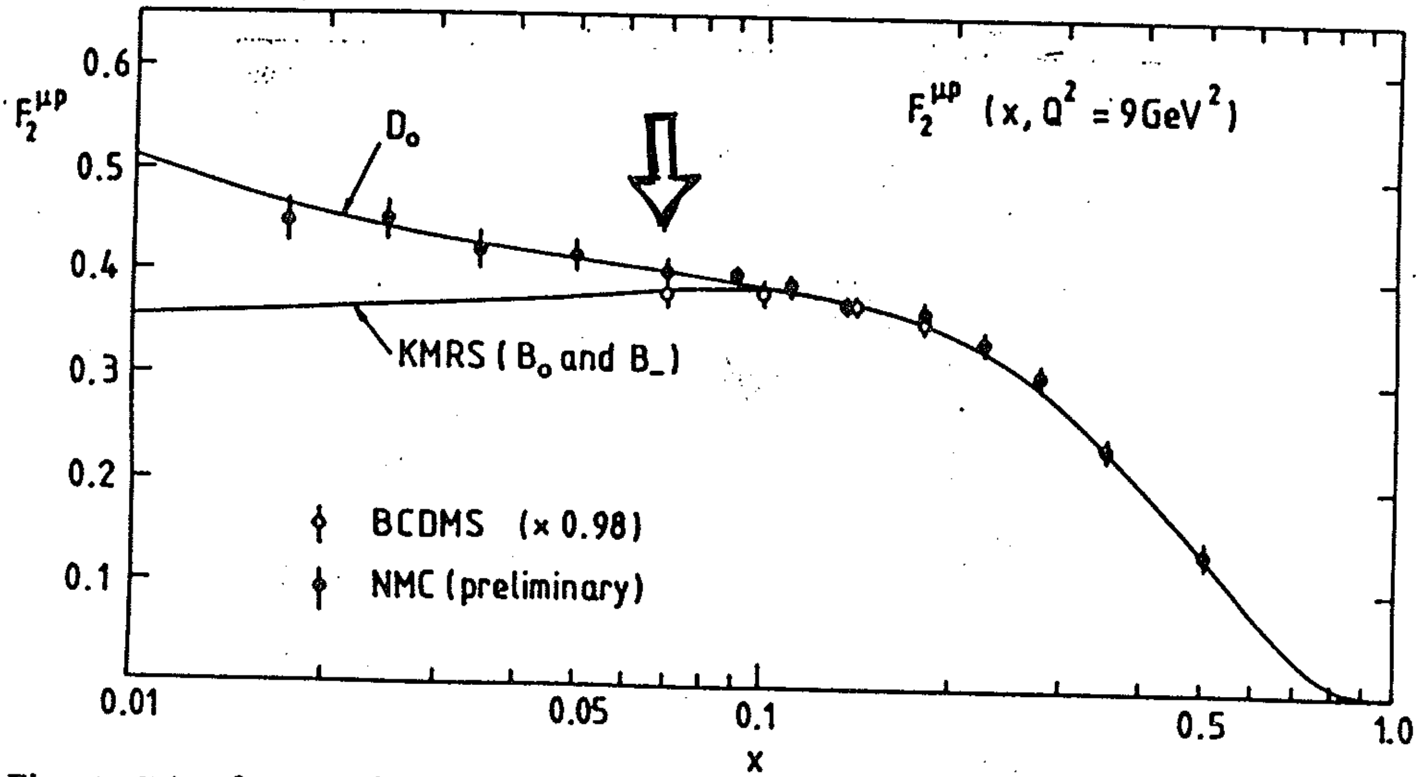

Fig. 4. $F_2(x, Q^2 = 9\mathrm{GeV}^2)$ as measured from NMC and BCDMS, compared with the extrapolation of the earlier KMRS and with the new MRS (labelled D_0) parametrization of parton densities.

1ST & 2nd ORDER EVOLUTION

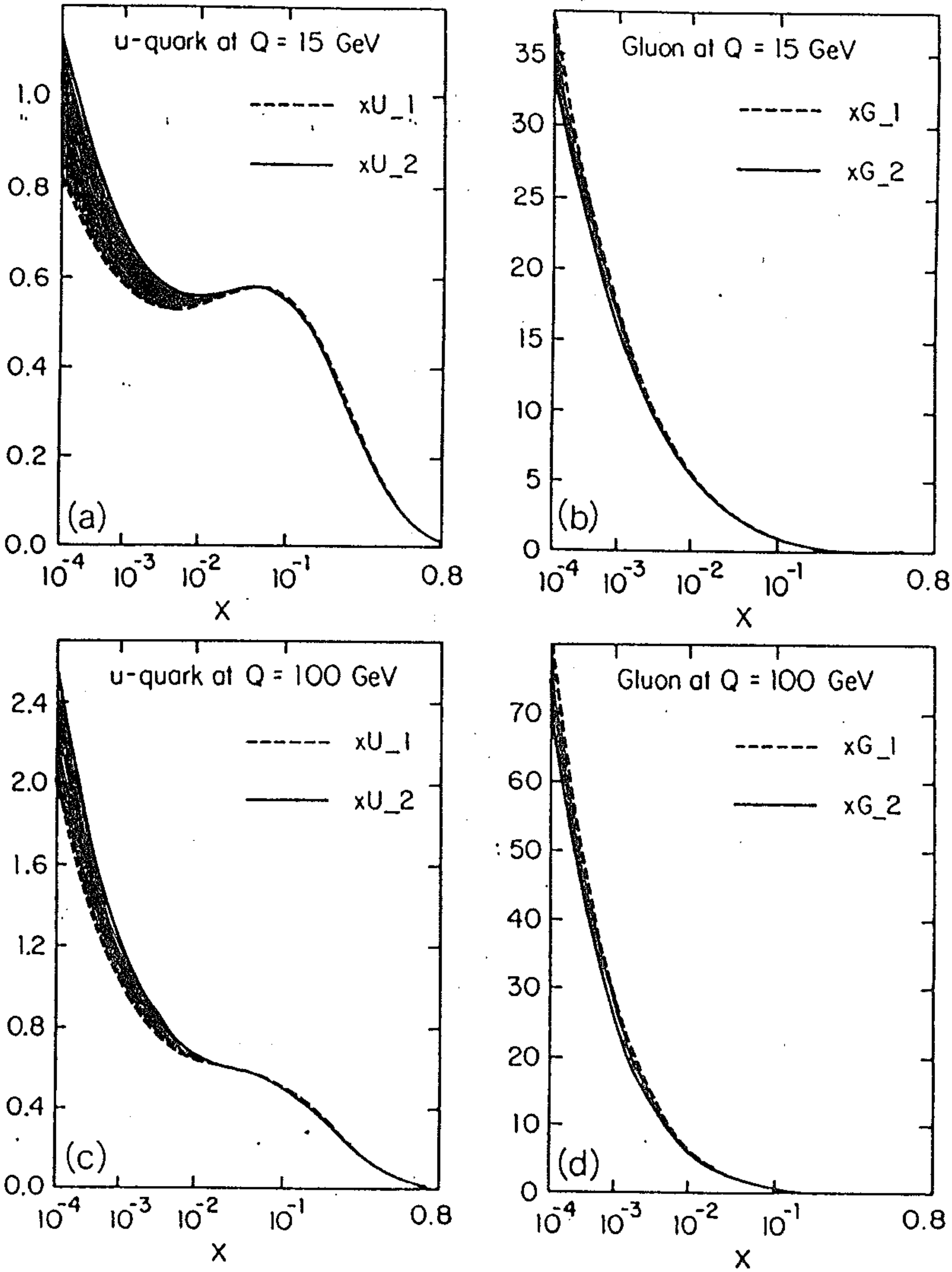

Fig. 1. Comparison of first- and second-order evolved parton distributions. Plotted are x times the probability distributions. Parton species and Q-values are as labeled. Initial distributions at $Q = 4.0$ GeV are taken from EHLQ set 1.

SCHEME DEPENDENCE

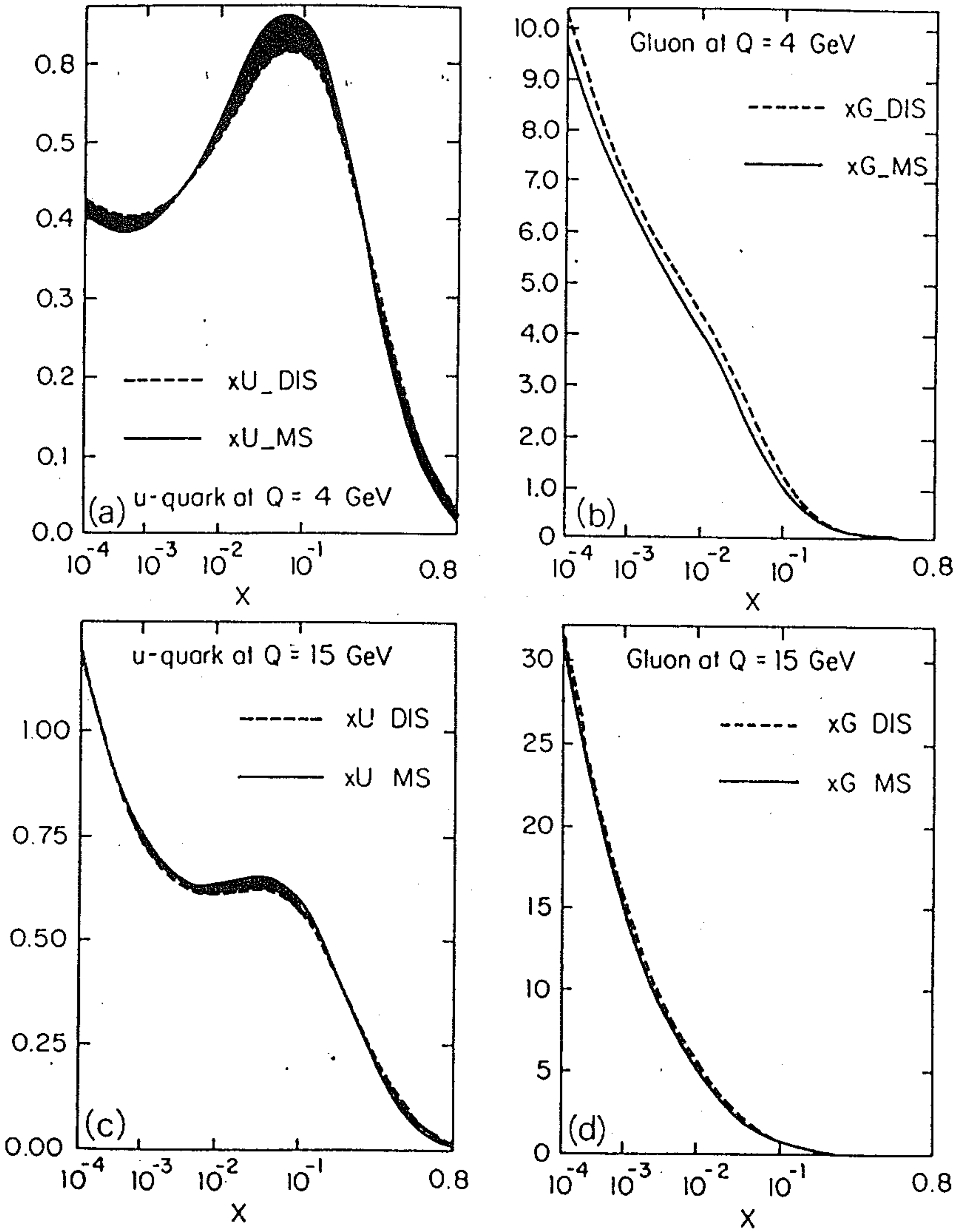

Fig. 3. Comparison of DIS-scheme and MS-bar scheme parton distributions. Plotted are x times the probability distributions. Parton species and Q-values are as labeled. Initial distributions at $Q = 4.0$ GeV are taken from EHLQ set 1.

ACCESS TO THE GLUON: F_L, $\sigma_{J/\psi}$, $\sigma_{c\bar{c}}$ ...

SO FAR: ACCESS TO QUARKS ONLY.

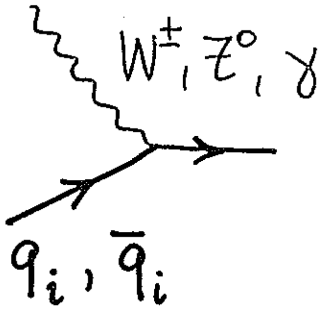

GLUONS

1) 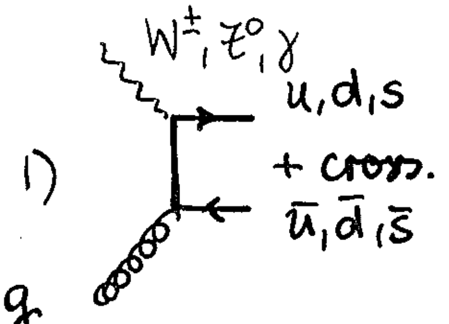

F_L^g

2) 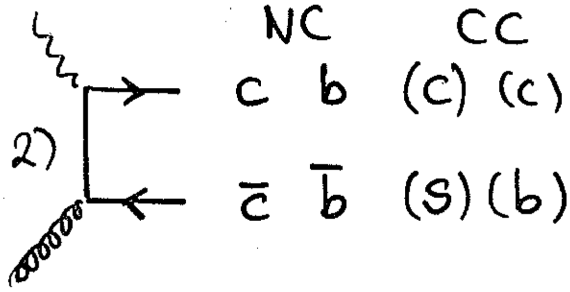

heavy flavour cross sections

3) 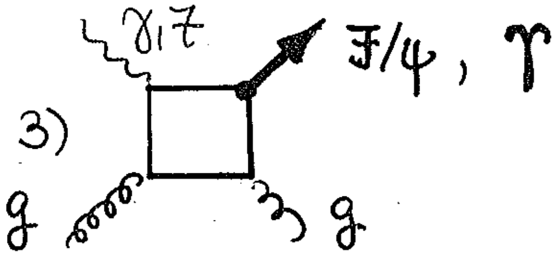

4) SCALING VIOLATIONS: next paragraph.

MARTIN, ROBERTS, STIRLING

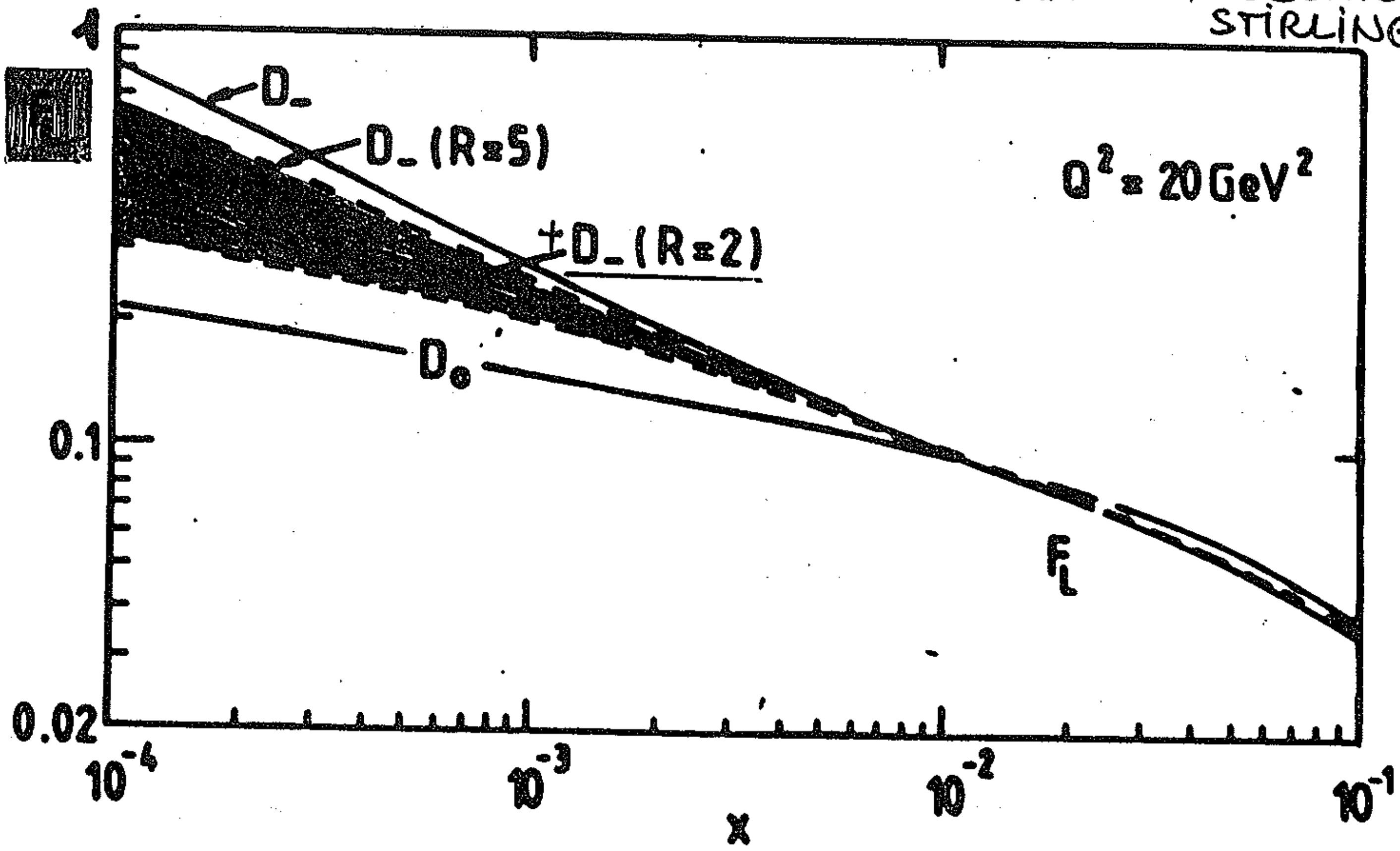

$O(\alpha_s)$:

$$F_L(x,Q^2) = \frac{\alpha_s}{2\pi}\left\{ \frac{8}{3}\int_x^1 \frac{dy}{y}\left(\frac{x}{y}\right)^2 F_2(y,Q^2) + 2\sum_{q,\bar{q}} e_q^2 \int_x^1 \frac{dy}{y}\left(\frac{x}{y}\right)^2\left(1-\frac{x}{y}\right) y\,\underline{G(y,Q^2)}\right\}$$

ROBERTS:

$$xG(x,Q^2) \simeq \frac{3}{5}\times 5.85 \left\{ \frac{3\pi}{4\alpha_s} F_L(0.4x,Q^2) - \frac{1}{2} F_2(0.8x,Q^2) \right\}$$

LO QCD

HERA

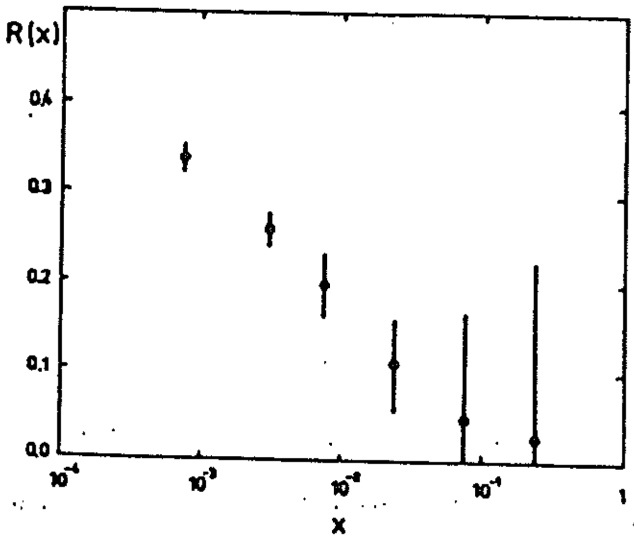

UNK

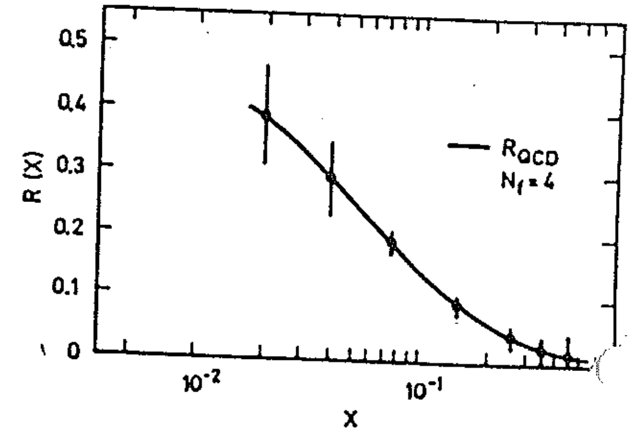

Fig. 11. Possible measurement of $R(x)$ using Eq. (6.1)

'y'- DEPENDENCE (INVARIANCE)

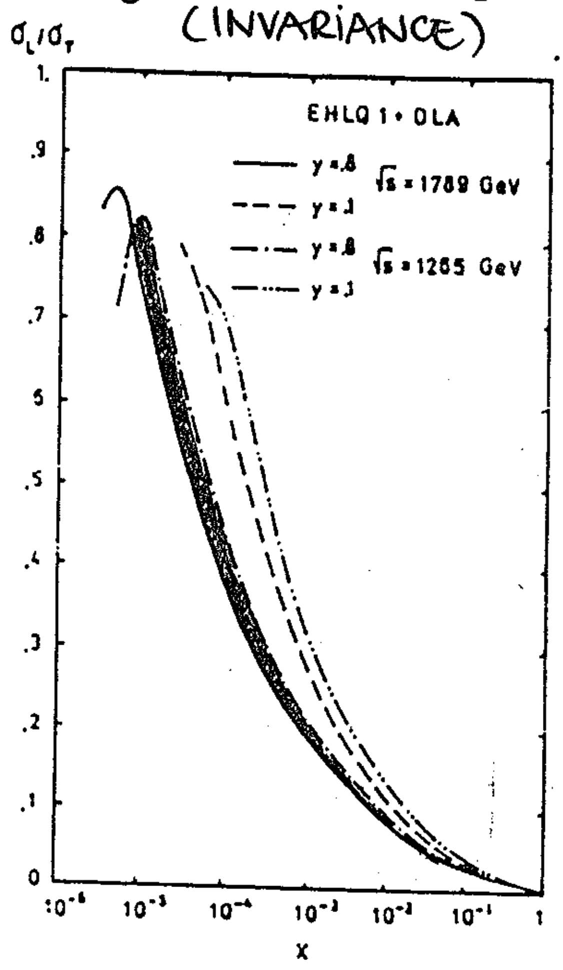

LEP × LHC

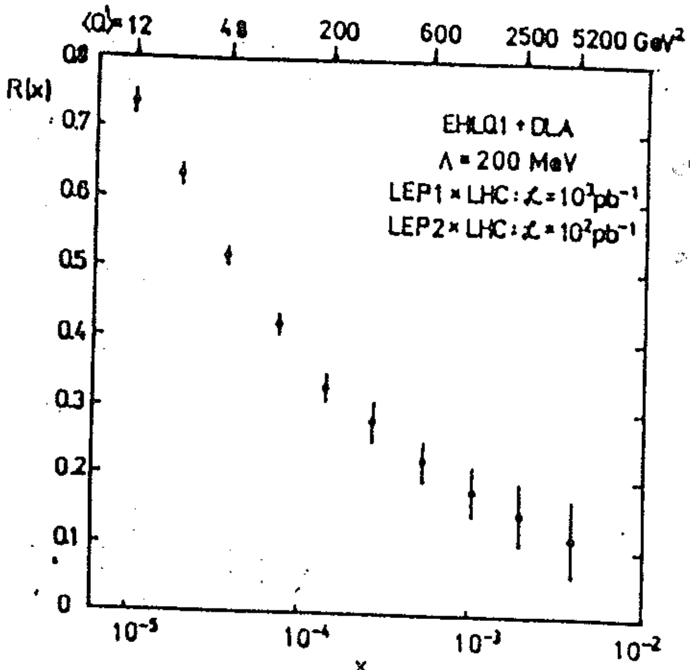

$$xG(x,Q^2) \simeq 1.77 \frac{3\pi}{2\alpha_s(Q^2)} F_L(0.4x, Q^2)$$

HERA

OXFORD GROUP

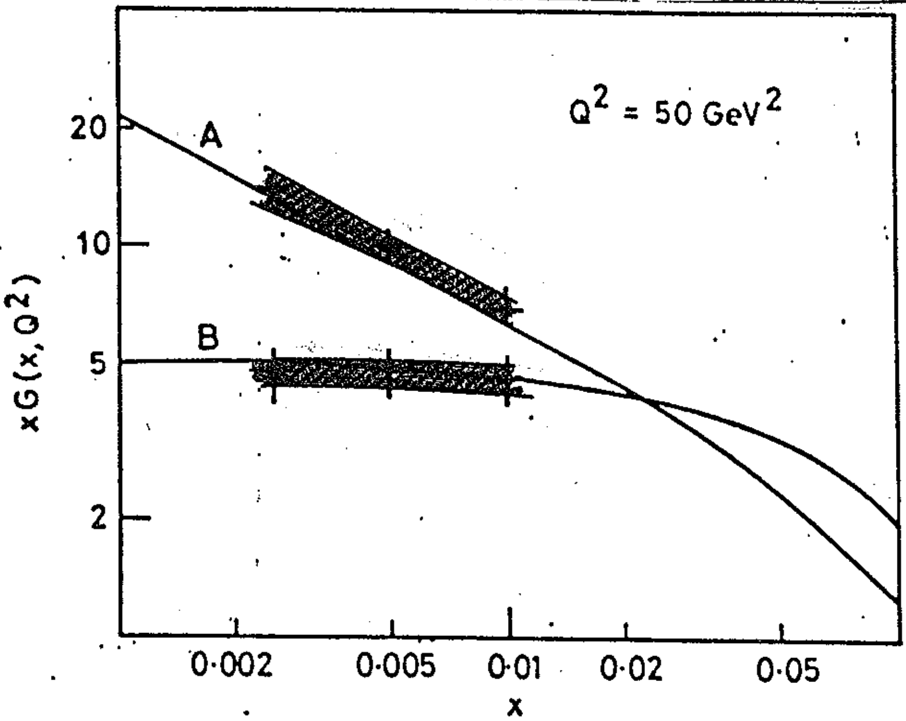

FIG. 8a

JB

LEP / LHC

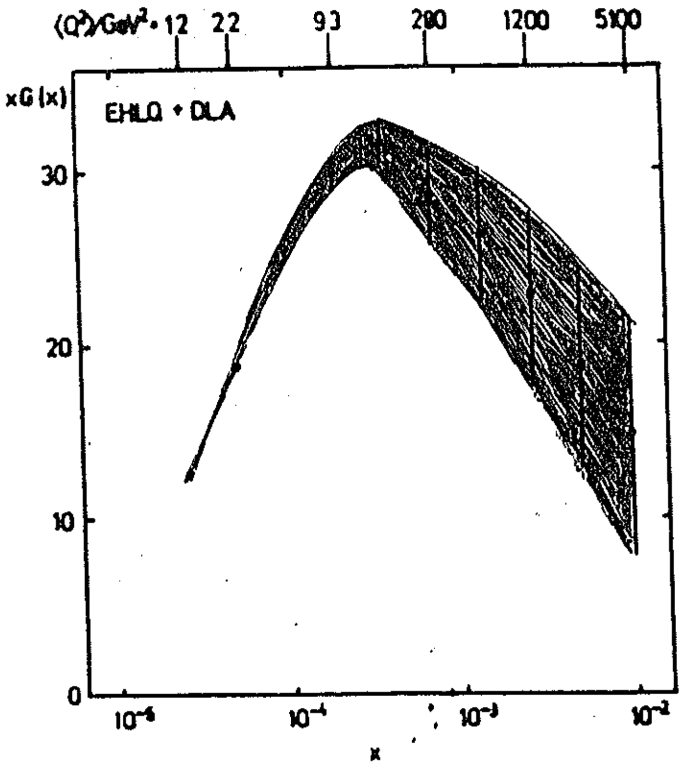

Figure 4: Statistical precision of a possible measurement of $xG(x)$

$$R^{(2)}(x,Q^2) = \frac{F_L^{(2)}(x,Q^2)}{\left(1+\frac{4M_p^2x^2}{Q^2}\right)F_2^{(1)}(x,Q^2) - F_L^{(2)}(x,Q^2)}$$

$O(\alpha_s^2)$

ZIJLSTRA, VAN NEERVEN

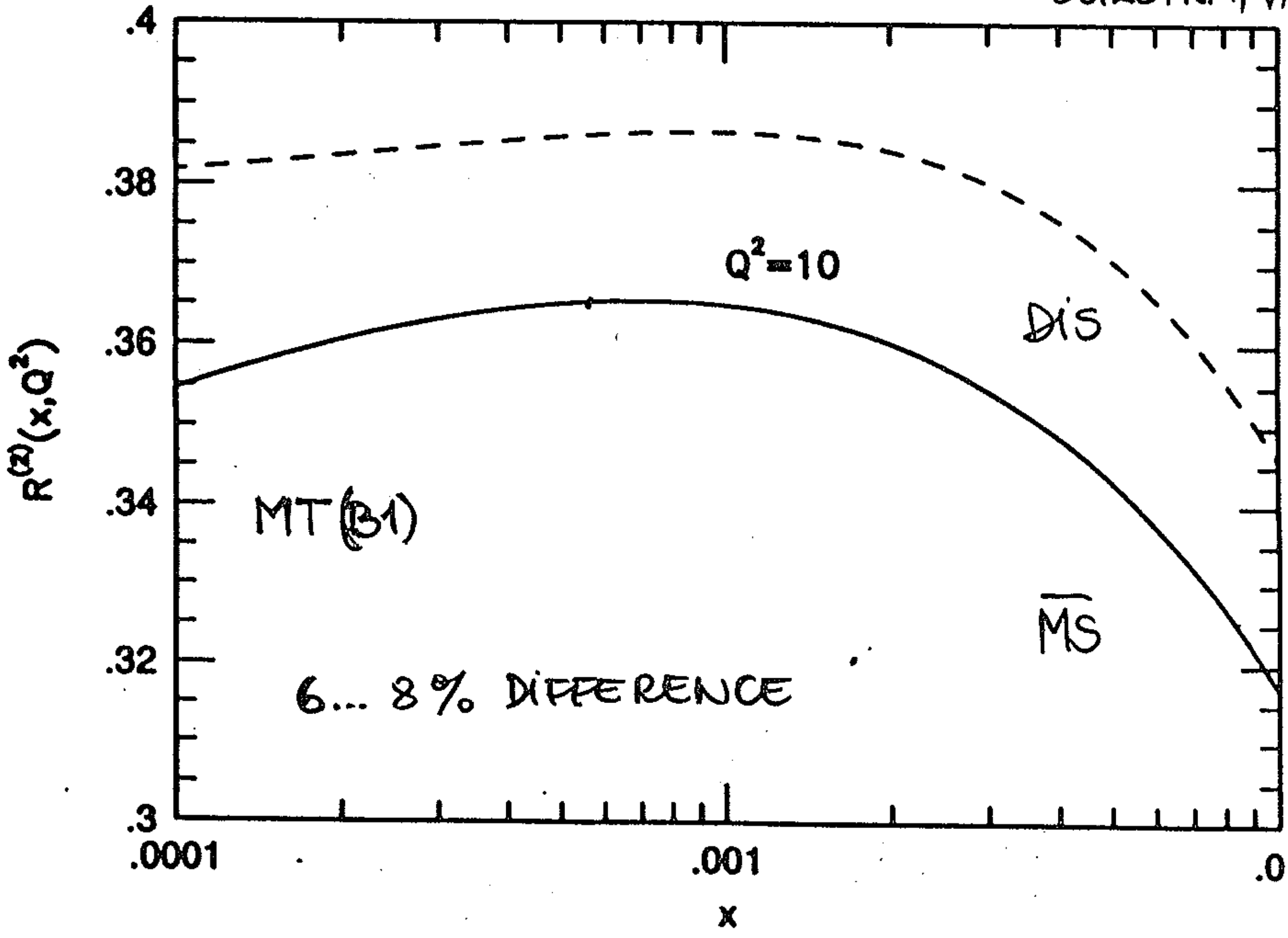

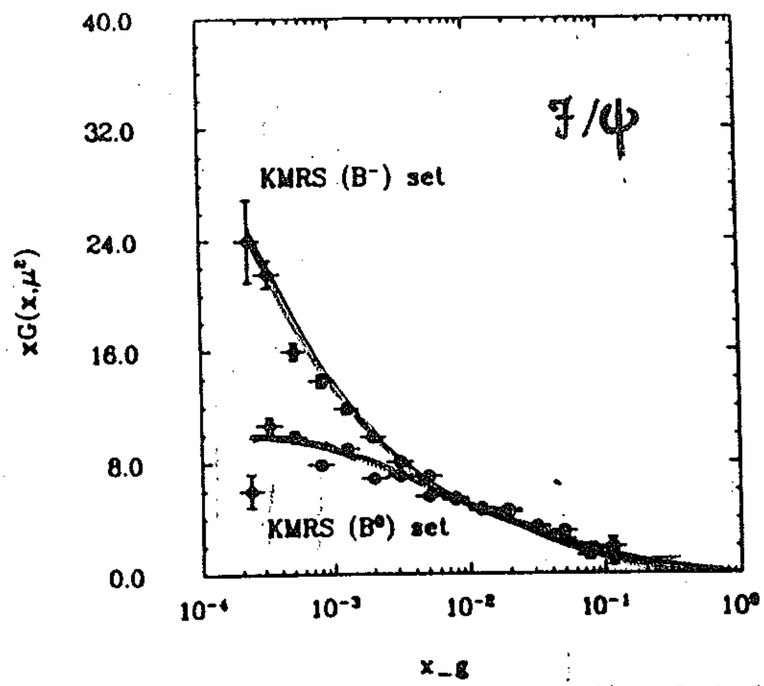

JUNG et al.

$Q^2 \approx M^2_{J/\psi}$

Figure 16: The gluon density reconstructed from inelastic J/ψ production for the input function of KMRS. The statistical error bars correspond to an integrated luminosity of 100 pb^{-1} The curves show the input gluon density.

PROBLEMS: • WF'S
• K-factors

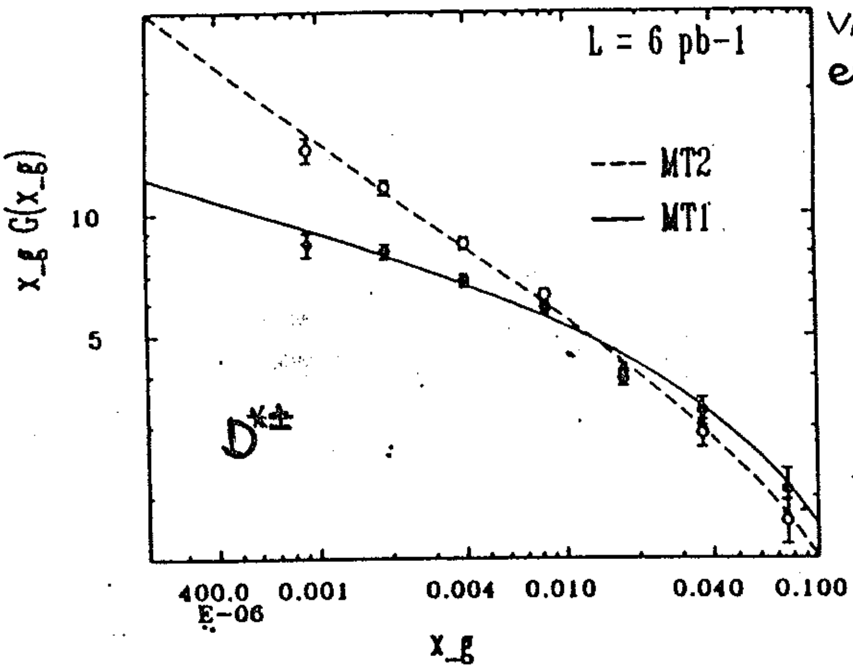

VAN WOUDENBERG et al.

PROBLEMS:
→ DECAY BG.
→ FRAGMENTAT
→ SCALE !

Figure 18

Reconstructed gluon densities from inclusive $D^{*\pm}$ production. The curves show the input gluon functions taken from Morfin and Tung [36]. The error bars include statistical errors for an integrated luminosity of 6 pb^{-1}.

QCD TESTS : α_s, Λ & THE GLUON DENSITY

EVOLUTION EQUATIONS : GLAP

NON - SINGLET DENSITIES :

$$\Delta_{ij}^{NS} = q_i(x,Q^2) - q_j(x,Q^2) \; ; \quad i,j \text{ arbitrary}$$

SINGLET - DENSITIES :

$$\Sigma = \sum_i \left[q_i(x,Q^2) + \bar{q}_i(x,Q^2) \right]$$

or flavour by flavour :

$$\Sigma_f = q_f(x,Q^2) + \bar{q}_f(x,Q^2)$$

$$G(x,Q^2) \quad \text{or} \quad \frac{1}{N_f}\, G(x,Q^2)$$

LO DIAGRAMS COLLINEAR POLES

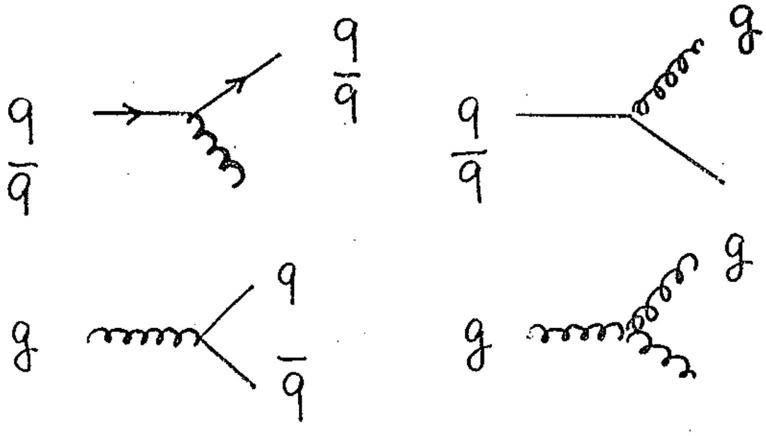

STRONG ORDERING IN $k_\perp$:

$$Q^2 \gg k_{\perp 1}^2 \gg \dots \gg k_{\perp n}^2 \gg \Lambda^2,\ p^2 = m_q^2$$

1) A SINGLE GLUON EMISSION: $q \to q$

$$\int \partial q(x,Q^2) = \int_{m^2}^{Q^2} \frac{1}{2}\, g^2(k^2)\, P(x)\, \frac{dk^2}{k^2} \otimes q(x,Q^2)$$

$$P(x) \otimes R(x) = \int_0^1 dx_1 \int_0^1 dx_2\, \delta(x - x_1 x_2)\, P(x_1)\, R(x_2)$$

$$P(x) = \frac{1}{3\pi^2}\, \frac{1+x^2}{1-x} = P_{qq} \cdot \frac{1}{3\pi^2},\ \text{NS for } q \to q.$$

$$\frac{\partial q(x,Q^2)}{\partial \log Q^2} = \frac{1}{6\pi^2}\, \alpha_s(Q^2)\, 4\pi\, P_{qq}(x) \otimes q(x,Q^2)$$

$$C_F \cdot \frac{1}{2\pi} \qquad \text{QCD}: \underline{C_F = \tfrac{4}{3}}$$

$$\boxed{\frac{d q_{NS}(x,Q^2)}{\partial \log Q^2} = \frac{\alpha_s(Q^2)}{2\pi}\, C_F\, P_{qq}(x) \otimes q_{NS}(x,Q^2)}$$

EVOLUTION OPERATORS:

$$\boxed{q_{NS}(x,Q^2) = \underline{\underline{E_{NS}(x, Q^2, \underset{Q_0^2}{\Lambda^2})}} \otimes q_{NS}(x, Q_0^2)}$$

$$\boxed{\frac{\partial E_{NS}(x,Q^2)}{\partial \log Q^2} = \frac{\alpha_s(Q^2)}{2\pi} C_F \; P_{qq}(x) \otimes E_{NS}(x,Q^2)}$$

NS

LO SPLITTING FUNCTIONS:

$$P_{qq}(x) = C_F\left[\frac{1+x^2}{(1-x)_+} + \frac{3}{2}\,\delta(1-x)\right]$$

$$P_{gq}(x) = C_F\,\frac{1+(1-x)^2}{x}$$

$$P_{qg}(x) = T_R\left[x^2+(1-x)^2\right]$$

$$P_{gg}(x) = 2N_c\left[x(1-x) + \frac{1-x}{x} + \frac{x}{(1-x)_+}\right] + \delta(1-x)\cdot\frac{1}{2}\beta_0$$

$C_F = 4/3$, $T_R = 1/2$, $N_c = 3$, $\beta_0 = 11/3 \cdot N_c - 4/3\, N_F T_R$.

$$\frac{\partial}{\partial \log Q^2}\begin{pmatrix} E_{FF} & E_{FG} \\ E_{GF} & E_{GG}\end{pmatrix} = \begin{pmatrix} P_{qq} & N_f\, P_{qG} \\ P_{Gq} & P_{GG}\end{pmatrix} \otimes \begin{pmatrix} E_{FF} & E_{FG} \\ E_{GF} & E_{GG}\end{pmatrix}$$

SINGLET

SIMILAR STRUCTURE IN NTLO:

$$P_{ij}(x,Q^2) = P_{ij}^{(0)}(x) + \frac{\alpha_s}{2\pi}\,P_{ij}^{(1)}(x) + \dots$$

AP EQUATIONS:

$$\frac{d f^a(x, Q^2)}{d \ln Q^2} = P\left(x, \frac{\alpha_s(Q^2)}{2\pi}\right)_{ab} \otimes f_b(x, Q^2)$$

$$P\left(x, \frac{\alpha_s}{2\pi}\right)_{ab} = \frac{\alpha_s}{2\pi}\left\{ P^0_{ab}(x) + \frac{\alpha_s}{2\pi} P^1_{ab}(x) + \dots \right\}$$

$$x \ll 1$$

	1 ST ORDER	2nd ORDER
FF	$C_F \frac{1+x^2}{1-x}$	$\frac{1}{x} 2N_f T_R C_F \frac{20}{9}$
FG	$2N_f T_R \left[x^2 + (1-x)^2\right]$	$\frac{1}{x} 2N_f T_R C_G \frac{20}{9}$
GF	$C_F \frac{1}{x}\left[1 + (1-x)^2\right]$	$\frac{1}{x} 2N_f T_R \left(-\frac{20}{9}\right) + C_F C_G$
GG	$2 C_G \left[\frac{1}{x} + \frac{1}{1-x} - 2 + x - x^2\right]$	$\frac{1}{x} 2N_f T_R \left(-\frac{23}{9} C_G + \frac{2}{3} C_F\right)$

$e^{\pm}p$ (d)

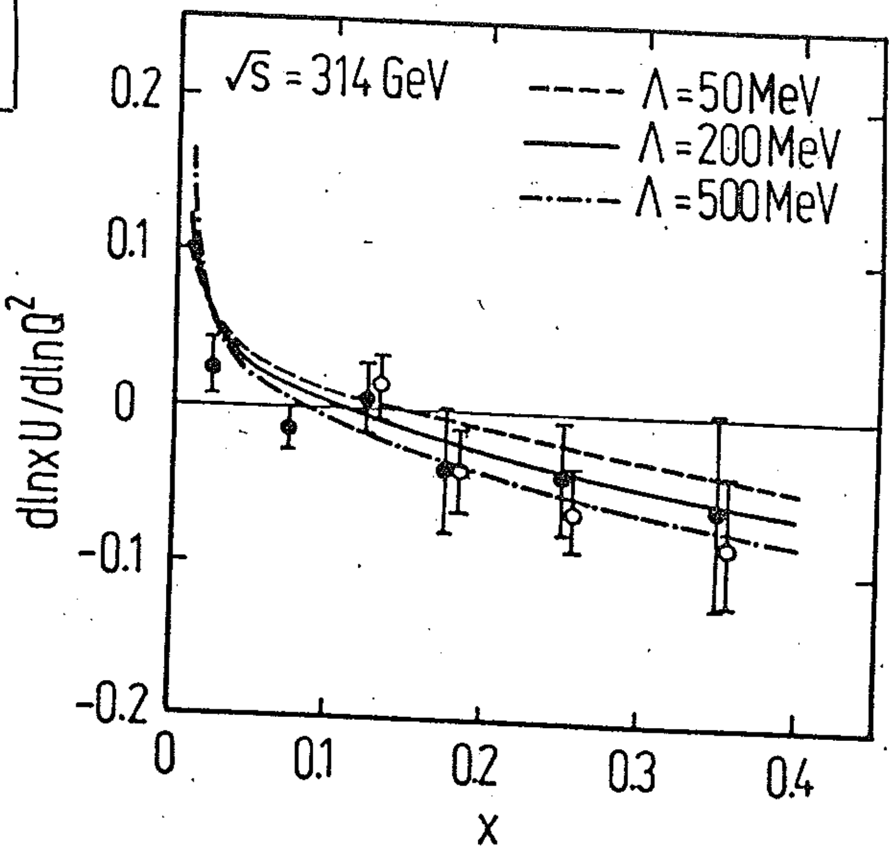

TOO LARGE ERRORS TO ALLOW A QCD ANALYSIS

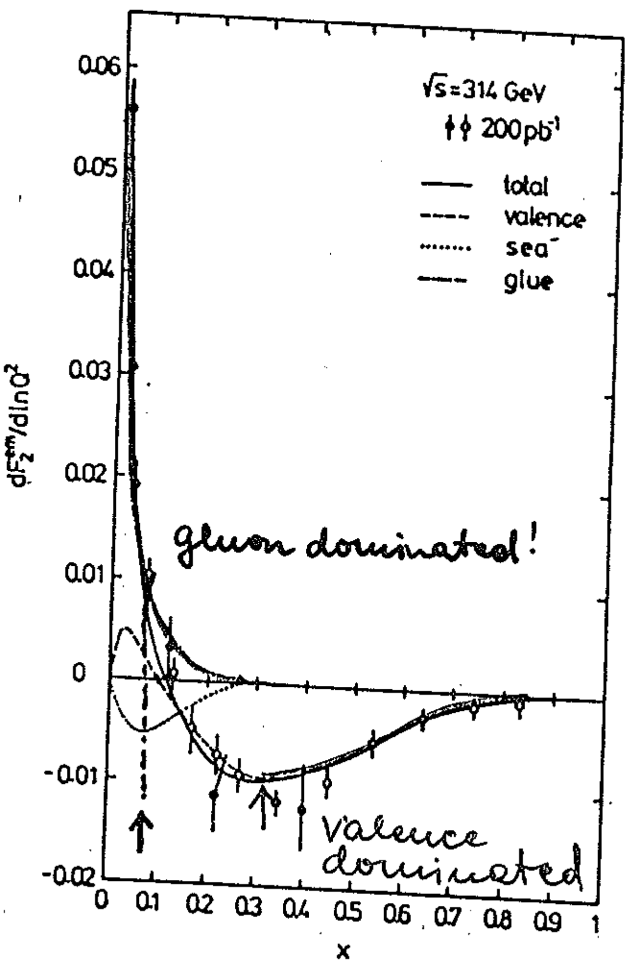

F_2^{em} !

$e^{\pm}p$: GENERAL SITUATION

$$
\boxed{\begin{aligned}
B_+(x,Q^2) &= C_\Sigma(Q^2)\,\Sigma(x,Q^2) + C_\Delta(Q^2)\,\Delta(x,Q^2) \\
&= C_\Sigma(Q^2)\Big[E_{qq}(x,Q^2)\otimes\Sigma(x,Q_0^2) \\
&\qquad + E_{gq}(x,Q^2)\otimes G(x,Q_0^2)\Big] \\
&\quad + C_\Delta(Q^2)\,E_{NS}(x,Q^2)\otimes\Delta(x,Q^2)
\end{aligned}}
$$

$$Q^2/M_Z^2 \to 0 \ : \quad C_\Sigma \to \frac{5}{18}\ , \quad C_\Delta \to \frac{1}{6}$$

VALENCE RANGE :

$$
\begin{aligned}
B_+^{VAL}(x,Q^2) &= C_\Sigma(Q^2)\otimes E_{qq}(x,Q^2)\otimes\Sigma^{val}(x,Q_0^2) \\
&\quad + C_\Delta(Q^2)\otimes E_{NS}(x,Q^2)\otimes\Delta^{val}(x,Q_0^2)
\end{aligned}
$$

for $C_\Sigma \simeq 5/18$, $C_\Delta \simeq 1/6$ & LO : $E_{qq} \equiv E_{NS}$

$$\boxed{B_+^{VAL}(x,Q^2) = E_{NS}(x,Q^2)\otimes\left[\frac{5}{18}\Sigma^{val}(x,Q_0^2) + \frac{1}{6}\Delta^{val}(x,Q_0^2)\right]}$$

QCD – ANALYSIS:

νN-SCATTERING

ONLY $\overset{(-)}{\nu}_{e,\mu} N \to e^{\pm}(\mu^{\pm}) X$ REACTIONS MAY BE MEASURED TO THE REQUIRED PRECISION FOR A QCD TEST.

1) NON-SINGLET ANALYSIS:

OBSERVABLE : $xW_3^d(x,Q^2) = \frac{1}{2}\left[xW_3^{\nu d}(x,Q^2) + xW_3^{\bar{\nu} d}(x,Q^2)\right].$

$$\boxed{\frac{\partial\, xW_3^d(x,Q^2)}{\partial \ln Q^2} = \frac{\alpha_s(Q^2)}{2\pi}\, P_{NS}(x) \otimes xW_3^d(x,Q^2)}$$

$$\chi^2 \underset{\mathrm{MIN}}{:=} \sum_{\mathrm{bins}} \left[\frac{xW_3^{exp}(x,Q^2) - E_{NS}(\Lambda, x, Q^2, Q_0^2) \otimes xW_3(x,Q_0^2)}{\delta xW_3^{exp}(x,Q^2)}\right]^2$$

with:

$$xW_3(x,Q^2) = E_{NS}(x,Q^2) \otimes xW_3(x,Q_0^2)$$

$\Lambda_{QCD}^{NS} = \Lambda_{QCD}$, NO CORREL. TO $xG(x,Q^2)$.

2) COMBINED SINGLET & NON-SINGLET ANALYSIS:

OBSERVABLES: xW_3^d

$W_2^d \equiv \Sigma$

$\bar{Q} = \sum_i x\bar{q}_i$

$$\boxed{\begin{aligned}
xW_3(x,Q^2) &= E_{NS}(x,Q^2) \otimes V \\
W_2(x,Q^2) &= E_{FF}(x,Q^2) \otimes (V+S) + E_{FG}(x,Q^2) \otimes G \\
\bar{Q}(x,Q^2) &= (E_{FF} - E_{NS})(x,Q^2) \otimes V \\
&\quad + E_{FF}(x,Q^2) \otimes S + E_{FG}(x,Q^2) \otimes G \\
V,(S,G) &= V(x,Q_0^2)\ (S(x,Q_0^2), G(x,Q_0^2))
\end{aligned}}$$

Q9/1

$e^{\pm}p$

HERA

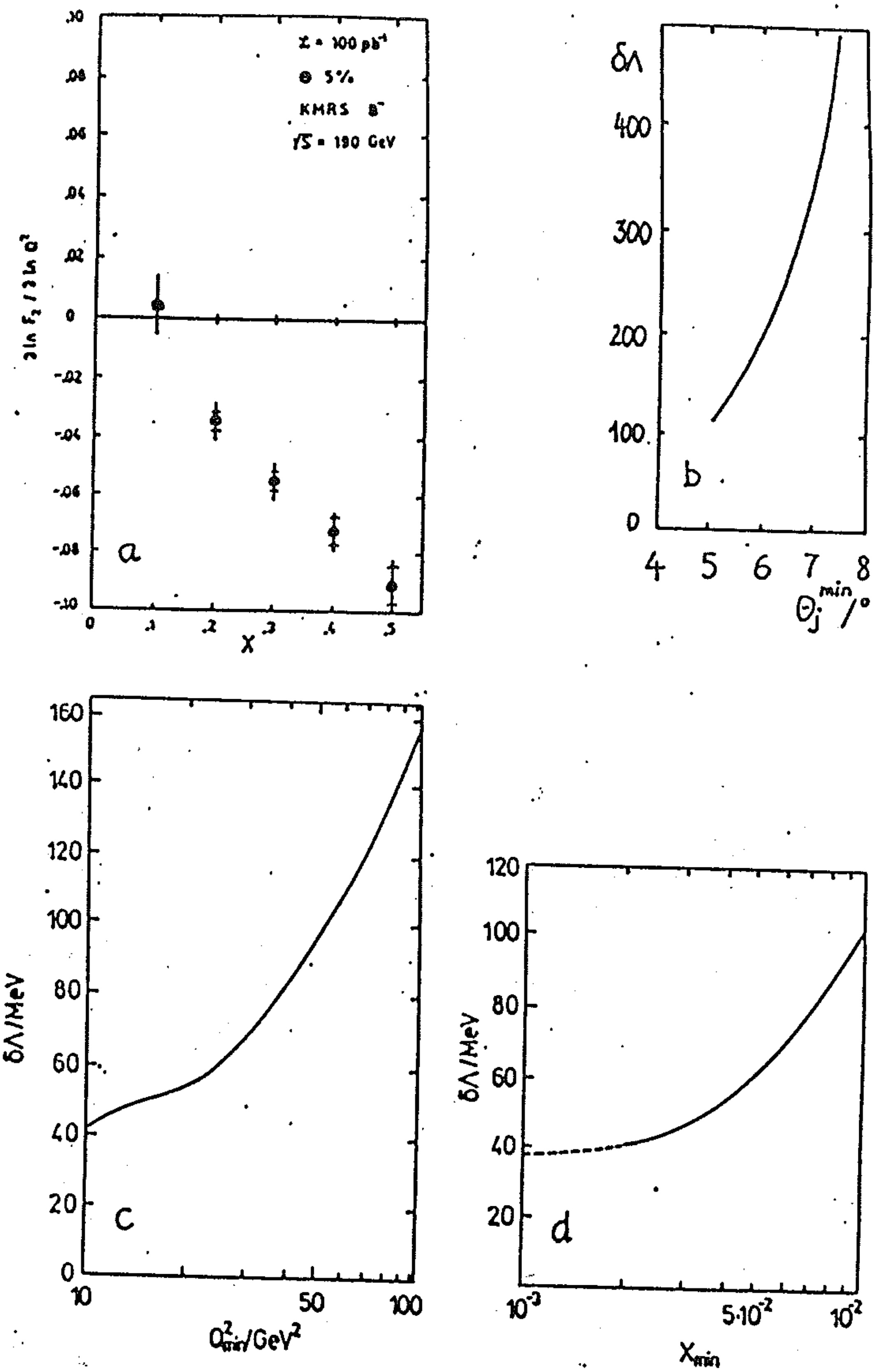

Figure 6: (a) Average slope $(\partial F_2/\partial \ln Q^2)$ *versus* x using the KMRS distribution B^- in the valence range. The inner error bars represent the statistical error for 100 pb^{-1} with a systematical error of 5% superimposed. (b) Dependence of $\delta\Lambda_{stat}$ for $x \geq 0.25$ 100 pb^{-1} and $\sqrt{s} = 110$ GeV on the minimum jet angle. Dependence of $\delta\Lambda_{stat}$ on the minimum Q^2 (c) and x (d) used in the QCD fit for the combined data sets at $\sqrt{s} = 110$ and 314 GeV for $\mathcal{L} = 100$ pb^{-1} each.

NECESSITY OF CROSS CALIBRATION OF CALORIMETERS

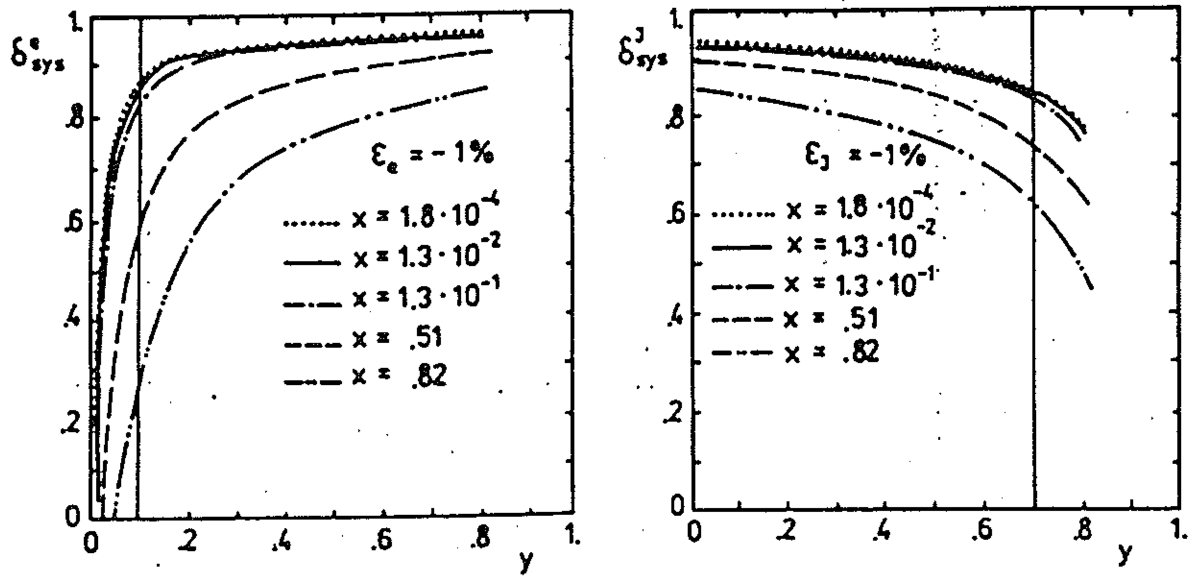

Figure 1: $\delta_{sys} = (d^2\tilde{\sigma}_{nc}/dxdy)/(d^2\sigma_{nc}/dxdy)$ for displacements of $\varepsilon_{e,J} = -1\%$ with $\frac{d^2\tilde{\sigma}}{dxdy}(\varepsilon) = \frac{d^2\sigma}{dxdy}(1+\varepsilon)$.

electromagnetic calorimeter	hadronic calorimeter	$\mathcal{L}$ in pb^{-1}	$\sqrt{s} = 314$ GeV $\delta\varepsilon_e$	$\sqrt{s} = 314$ GeV $\delta\varepsilon_J$	$\sqrt{s} = 190$ GeV $\delta\varepsilon_e$	$\sqrt{s} = 190$ GeV $\delta\varepsilon_J$
BEMC	CB	10	0.0049	0.0075	0.0050	0.0070
BBE	CB	10	0.0173	0.0220	0.0186	0.0199
CB	CB	10	0.0128	0.0097	0.0130	0.0098
CB	FB/OF	100	0.0158	0.0386	–	–
BEMC	all	10	0.0025	0.0033	0.0026	0.0033
BBE	all	10	0.0073	0.0067	0.0085	0.0068
CB	all	10	0.0031	0.0025	0.0028	0.0025
OF and IF	all	100	0.0258	0.0122	0.0762	0.0324

Table 2: Accuracies of ε_e and ε_J using $d^2\sigma_{nc}/dxdy$.

$\delta\varepsilon_e$ & $\delta\varepsilon_h$ COULD HAVE A SYSTEMATIC IMPACT ON $\Delta\Lambda = \pm$ 50 … 150 MeV !

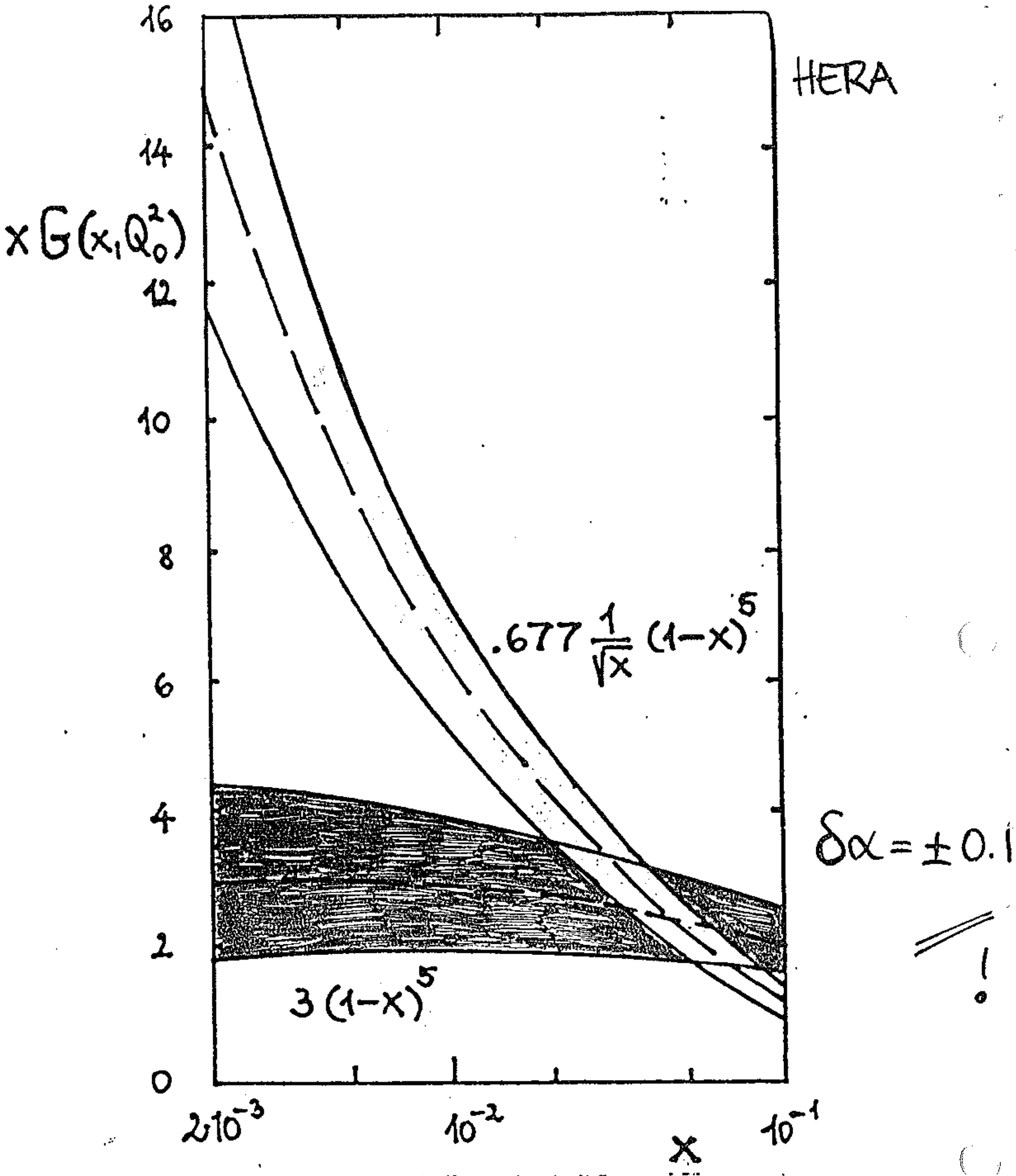

Figure 8: Possible determination of $xG(x, Q_0^2)$ in a QCD fit for $x < 0.1$, see text. The upper error band corresponds to the choice $\alpha = -0.5$ and the lower band to $\alpha = 0$, see eq. 15. The inner error denotes the statistical error for $\mathcal{L} = 100\ pb^{-1}$ for both the low and high s option.

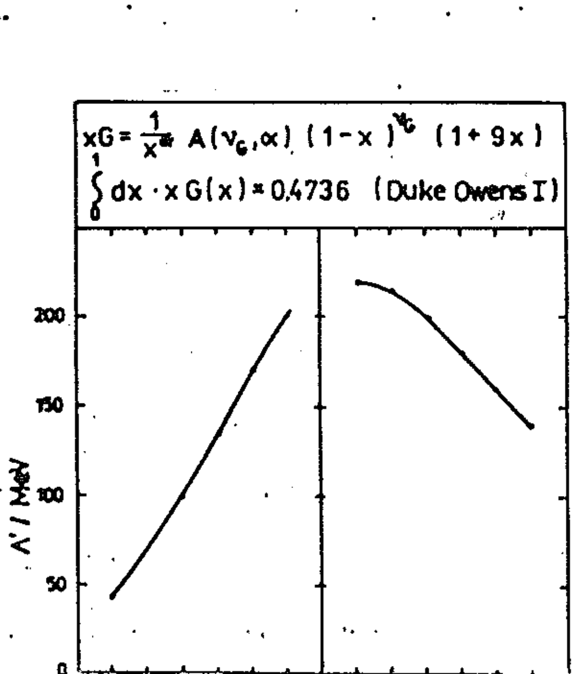

$\Lambda \leftrightarrow xG(x, Q_0^2)$

Q11

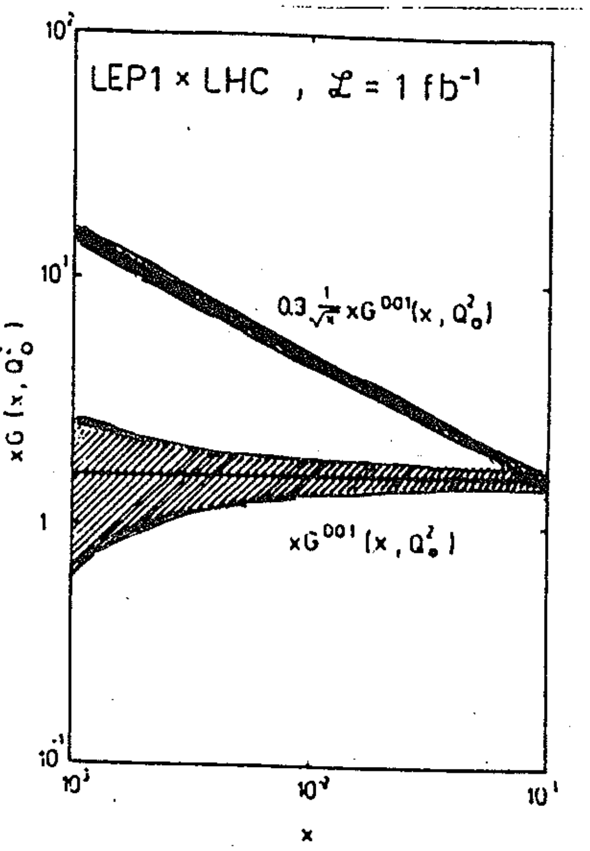

LEP × LHC

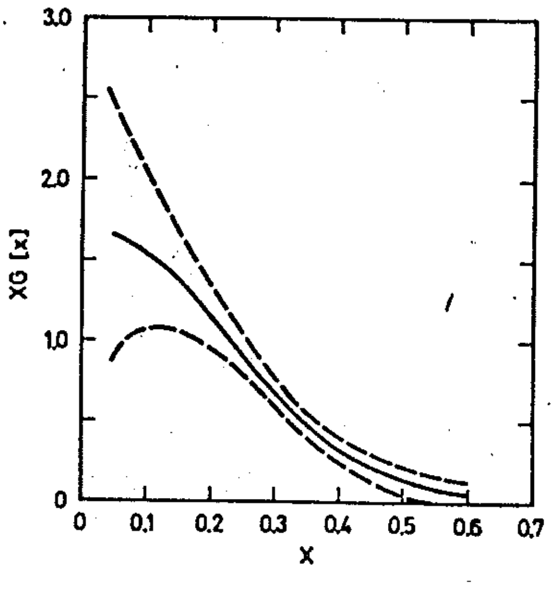

ν, UNK

Q12

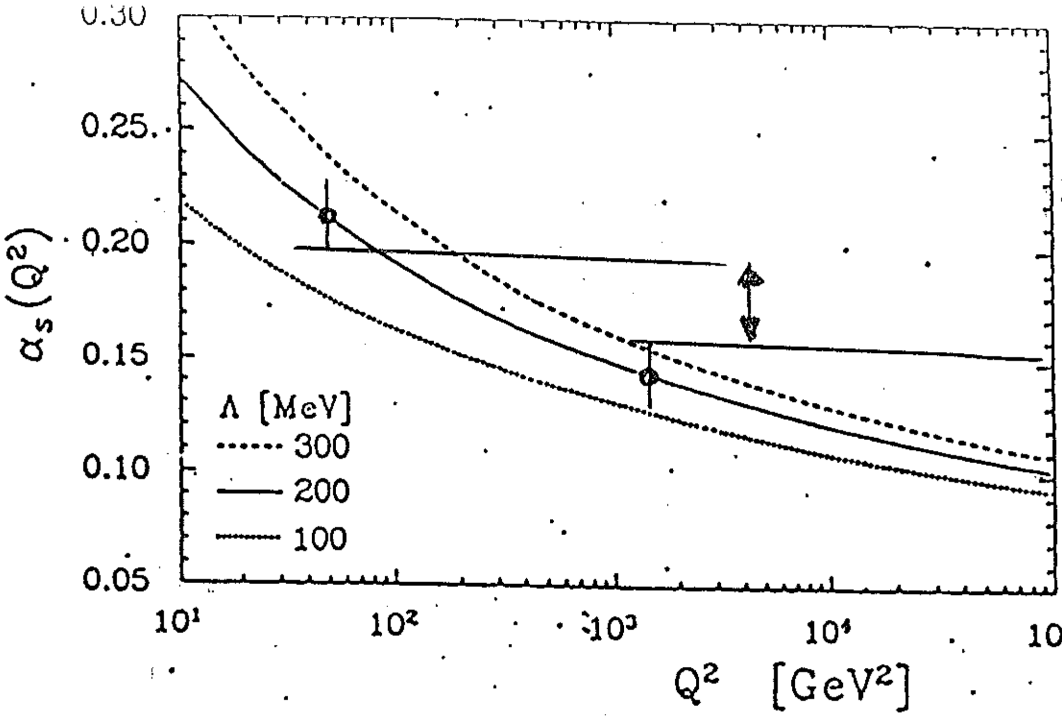

HERA

Figure 7: Dependence of α_s on Q^2 from a combined fit using two samples of $\sqrt{s} = 314$ GeV and $\sqrt{s} = 110$ GeV with $\mathcal{L} = 100\ pb^{-1}$ each. The upper point corresponds to a nonsinglet fit for $\theta_J > 5°$ and $x > 0.25$. The lower point at $Q^2 \sim 50$ GeV^2 corresponds to a fit in the range $x < 0.25$.

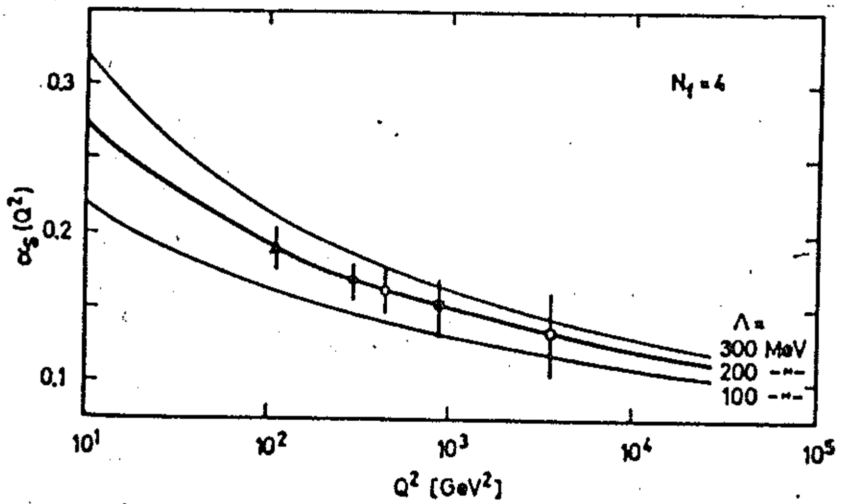

ν, UNK

Fig. 16. **The dependence of the strong coupling constant α_s on Q^2 for measurements at UNK and HERA. UNK: ▲ xW_3, HERA: (cf. [6]) xG fixed**

• $x > 0.01$ $s = 12000$ GeV

∘ $x > 0.25$ $s = 12000$ GeV

■ $x > 0.01$ $s = 98400$ GeV

□ $x > 0.25$ $s = 98400$ GeV

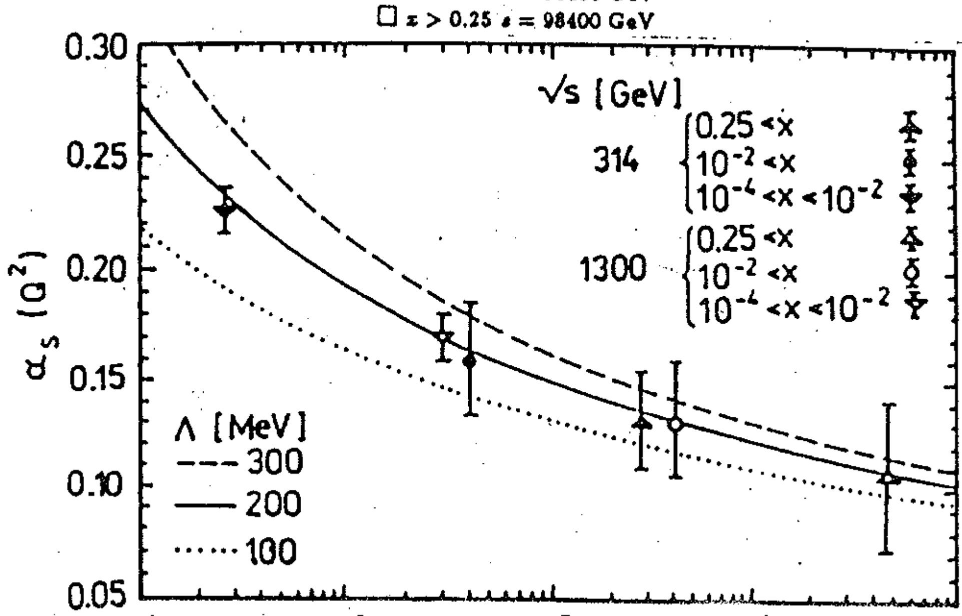

LEP x LHC

OTHER OBSERVABLES

S. BETHKE

Table 4. Processes and Observables from which significant determinations of α_s are derived.

Process	Observable	Theory	Caveats
e^+e^-	hadronic event shapes, jet production rates, energy correlations	NLO and re-summed NLO	hadronization corrections
	$R_Z = \frac{\Gamma(Z^0 \to \text{hadrons})}{\Gamma(Z^0 \to \text{leptons})}$	NNLO	small QCD corrections
	$R_\tau = \frac{Br(\tau \to \text{hadrons})}{Br(\tau \to e\nu)}$	NNLO	nonperturbative corrections
	scaling violations in $\frac{d\sigma}{dx}$ spectra	NLO	only through MC models
	$\frac{\Gamma(\Upsilon \to ggg)}{\Gamma(\Upsilon \to \mu^+\mu^-)}$; .... ; J/Ψ; ...	NLO	relativistic corrections
DIS	$\frac{d \ln F_2(x,Q^2)}{d \ln Q^2}$	NLO	higher twist; $g(x,Q^2)$
	$\frac{d \ln F_3(x,Q^2)}{d \ln Q^2}$	NLO	higher twist
$p\bar{p}$	$p\bar{p} \to W$ + jets	NLO	statistics; k-factors
	$p\bar{p} \to b\bar{b}X$	NLO	statistics; exp. systematics
$c\bar{c}$ states	mass difference of 1s and 1p charmonium states	lattice gauge theory	quenched approximation

Q14

pre HERA

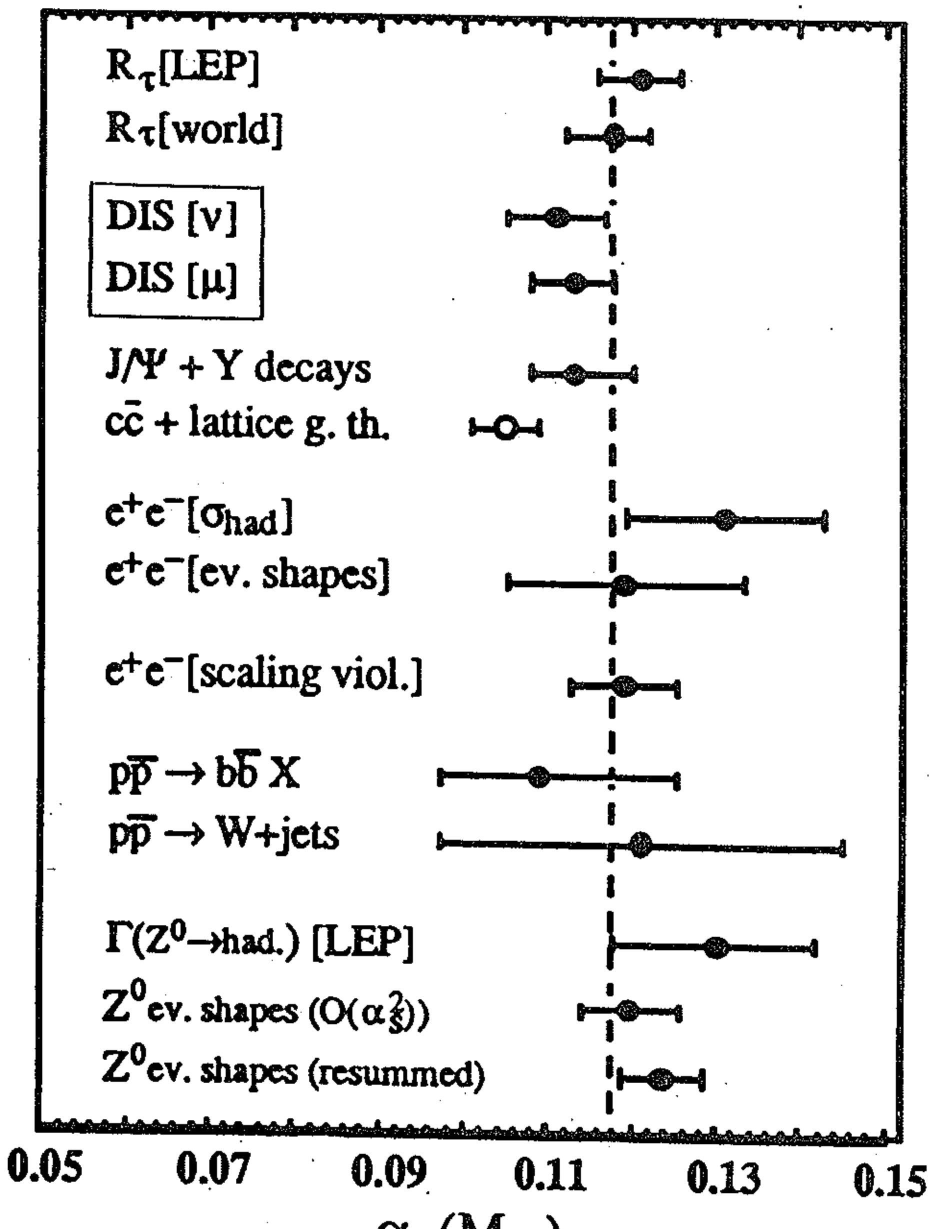

Fig. 31. Summary of measurements of $\alpha_s(M_{Z^0})$.

Q15

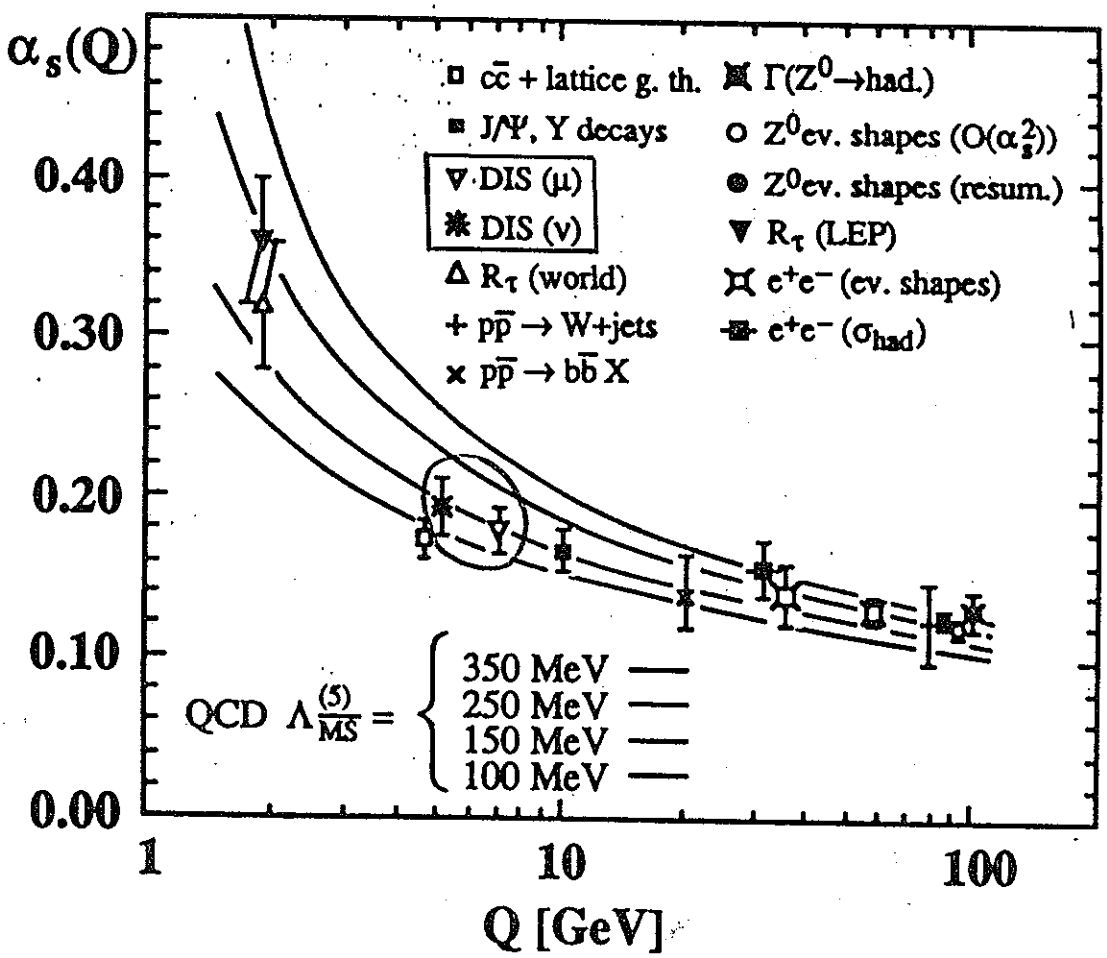

$\alpha_s(Q)$
0.40
0.30
0.20
0.10
0.00
1
10
100
Q [GeV]
$c\bar{c}$ + lattice g. th.
J/Ψ, Υ decays
DIS (μ)
DIS (ν)
R_τ (world)
$p\bar{p} \to$ W+jets
$p\bar{p} \to b\bar{b}$ X
$\Gamma(Z^0 \to$ had.)
Z^0ev. shapes $(O(\alpha_s^2))$
Z^0ev. shapes (resum.)
R_τ (LEP)
e^+e^- (ev. shapes)
e^+e^- (σ_{had})
QCD $\Lambda^{(5)}_{\overline{MS}}$ =
350 MeV
250 MeV
150 MeV
100 MeV

the
HERA

THE ONSET OF SHADOWING AT SMALL X

– SCREENING : RESTORING UNITARITY
'PARTON RECOMBINATION'
GLR
& SUBSEQUENT WORK

⟹ QUANTIFICATION.

⟹ STRATEGY TO SEE THESE EFFECTS
IN $F_2^{em}(x, Q^2)$ $\Longleftrightarrow$ Λ, $xG(x, Q_0^2)$!

AP + FAN-DIAGRAMS (xG)

MUELLER, QIU

$$\frac{d\, x q_s(x,Q^2)}{d \ln Q^2} = \frac{\alpha_s}{2\pi}\left[P_{qg} \otimes xG \quad P_{qq} \otimes x q_s\right]$$

$$- \frac{27\,\alpha_s^2}{160\, R^2 Q^2}\left(x G(x,Q^2)\right)^2$$

$$+ \frac{\alpha_s}{\pi Q^2}\,\theta(x_0 - x)\int_x^{x_0} \frac{dx'}{x'}\, \gamma\left(\frac{x}{x'}\right) x G_H \; x', Q^2)$$

$$\gamma(y) = -2y + 15y^2 - 30y^3 + 18y^4$$

$$\frac{d\, x G_H(x,Q^2)}{d \ln Q^2} = -\frac{81\,\alpha_s^2}{16\, R^2}\,\theta(x_0 - x)\int_x^{x_0} \frac{dx'}{x'}\left[x' G(x', Q^2)\right|^2$$

$$\frac{d\, x G(x,Q^2)}{d \ln Q^2} = \frac{\alpha_s}{2\pi}\left[P_{gg} \otimes xG + P_{gq} \otimes xq\right|$$

$$- \frac{81\,\alpha_s}{16\, R^2 Q^2}\,\theta(x_0 - x)\int_x^{x_0} \frac{dx'}{x'}\left[x' G(\,', Q^2)\right]^2$$

USED IN: KMRS

$\longrightarrow$ MODIFICATIONS CURRENTLY WORKED OUT!

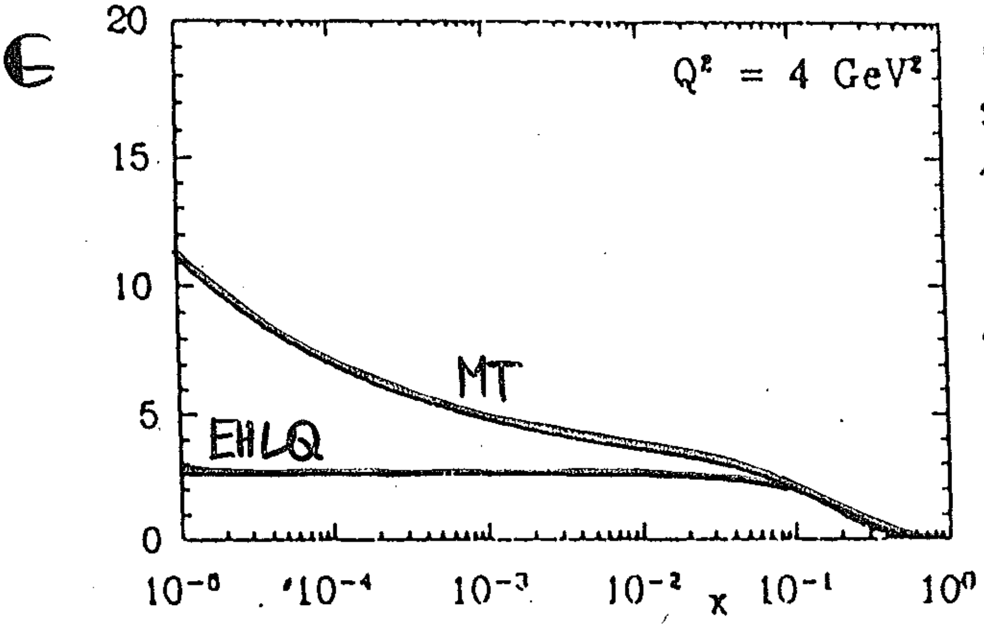

BA TELS, JB, SCH LER 199

(cf. COLLINS, KWI ZINSKI 199); ALT MANN, GL CK, RE A, 1992 FO SIMILAR INVESTIG.)

a

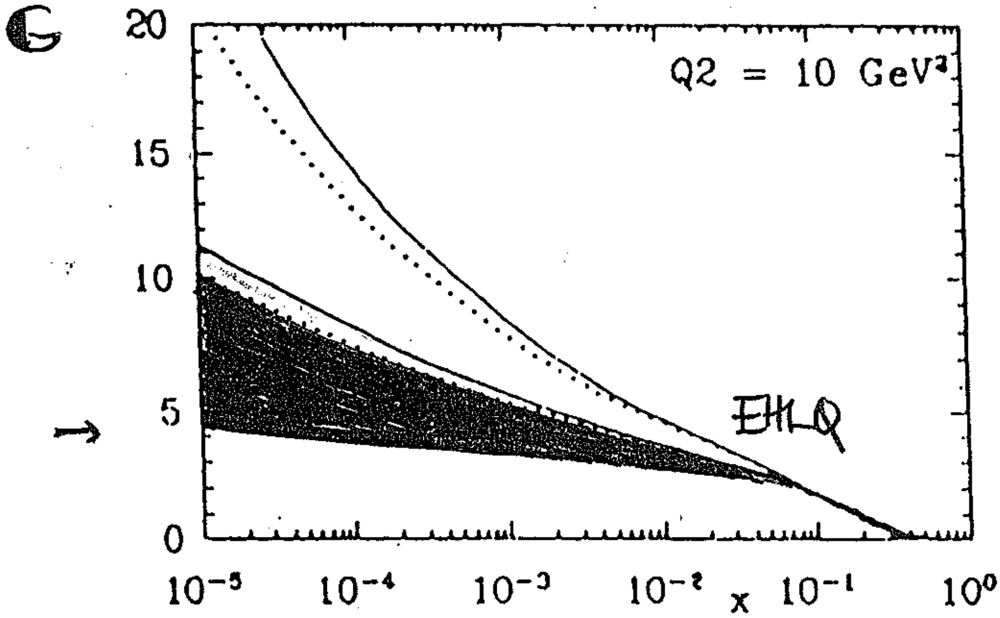

C →

$C = C(\hat{Q}_0^2)$

$Q_0 = \hat{Q}_0 (R_{sc}$

b

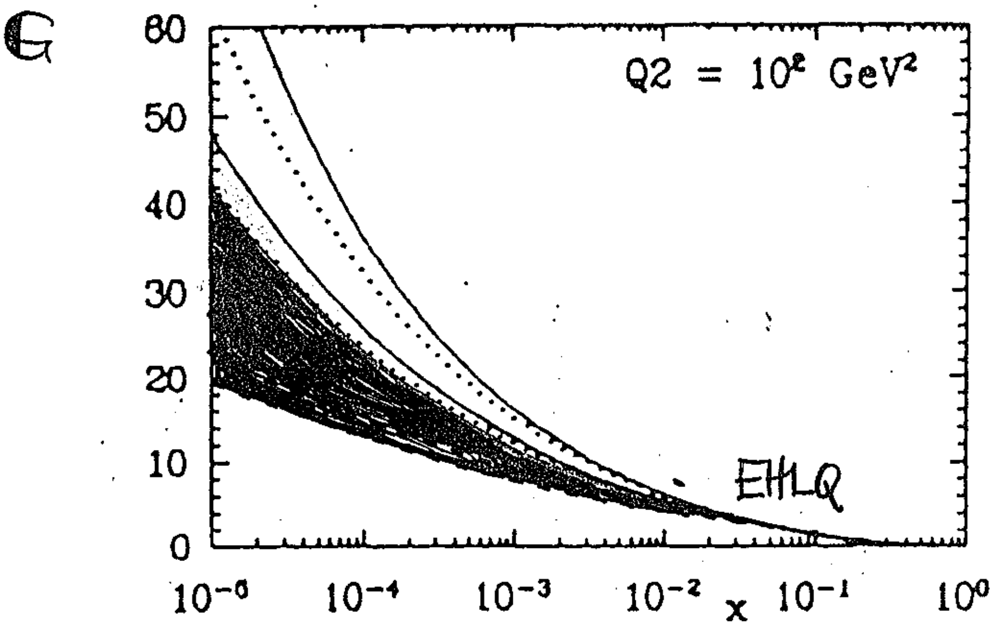

X4

BARTELS, JB, SCHULER

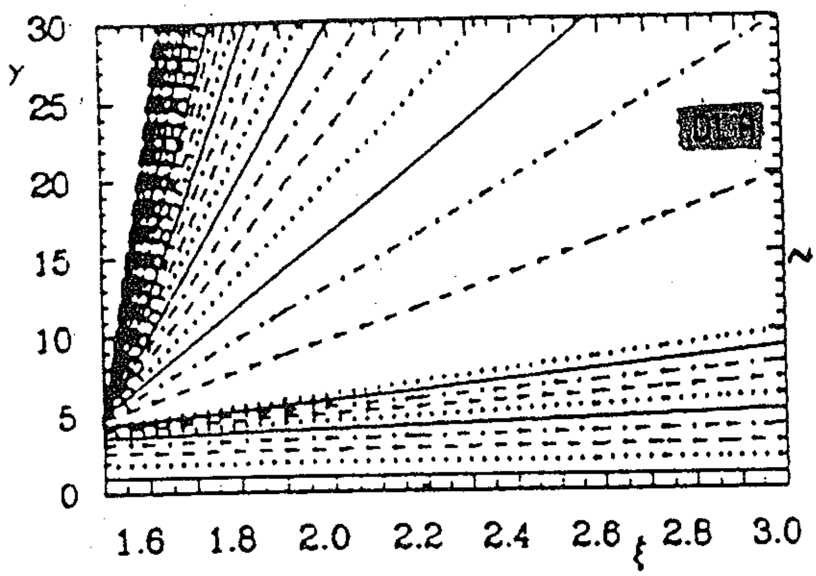

~AP

a

TRAJECTORIES STARTING BELOW

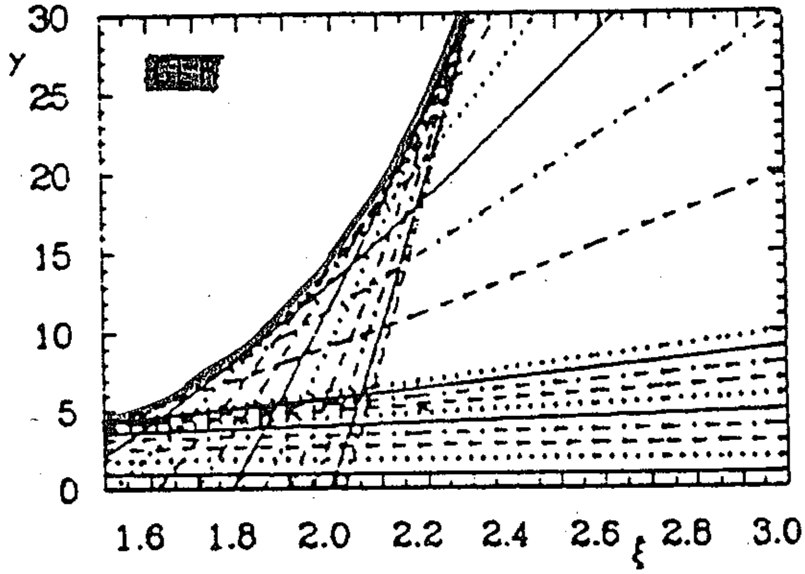

b

ABOVE THE 'CRITICAL' LINE

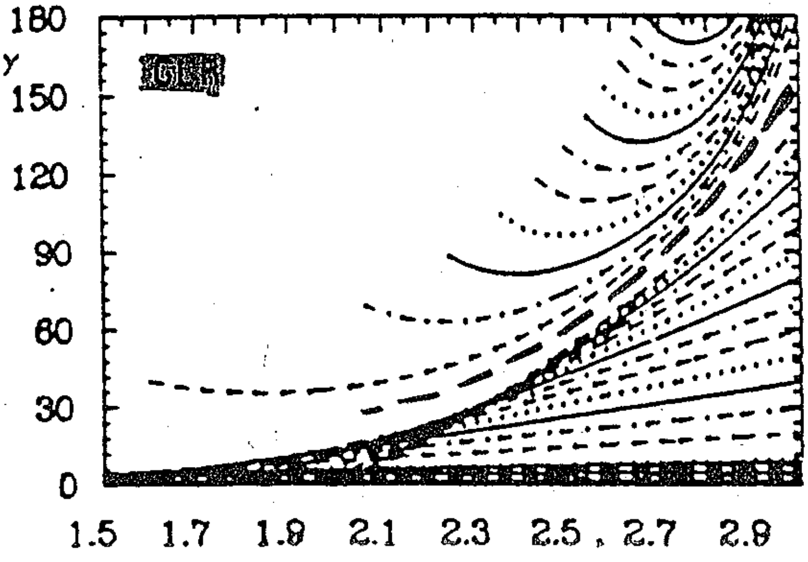

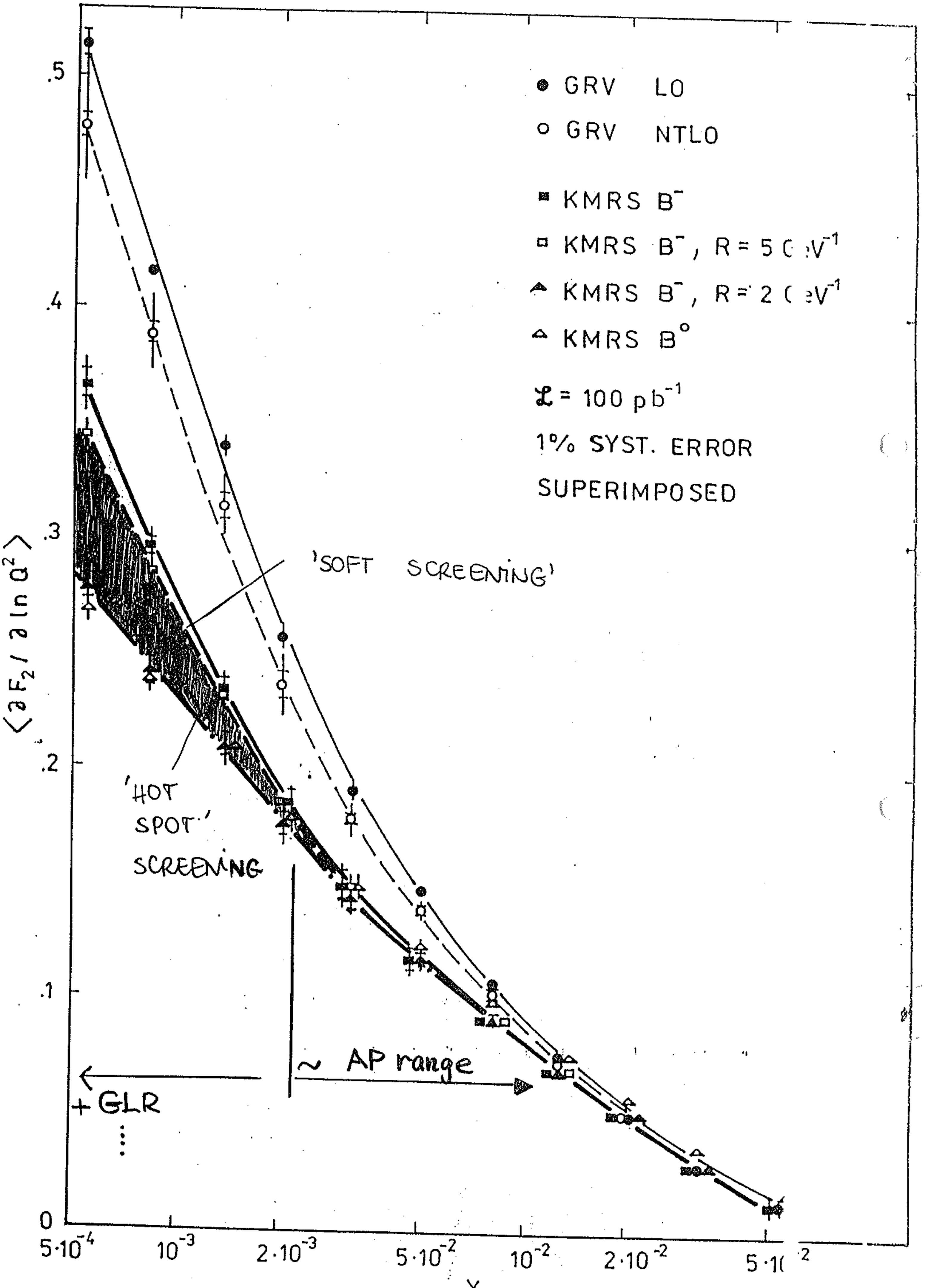

GRV LO
GRV NTLO
KMRS B⁻
KMRS B⁻, R = 5 GeV⁻¹
KMRS B⁻, R = 2 GeV⁻¹
KMRS B°
$\mathcal{L}$ = 100 pb⁻¹
1% SYST. ERROR
SUPERIMPOSED
'SOFT SCREENING'
'HOT SPOT' SCREENING
~ AP range
+ GLR
$\langle \partial F_2 / \partial \ln Q^2 \rangle$
.5
.4
.3
.2
.1
0
$5\cdot10^{-4}$
10^{-3}
$2\cdot10^{-3}$
$5\cdot10^{-2}$
10^{-2}
$2\cdot10^{-2}$
x

FIRST RESULTS FROM HERA:
DIS AT ZEUS & H1

	ZEUS	H1
LUMINOSITIES:	$\mathcal{L} = 2{,}1\ nb^{-1}$	$1{,}3\ nb^{-1}$

NEW DATA $\longrightarrow$ $* 10$

$E_e = 26.7$ GeV

$E_p = 820$ GeV

$5 \lesssim Q^2 \lesssim 50$ GeV^2 dominantly, $Q^2_{max} \sim 800$ GeV^2

$10^{-4} \lesssim x \lesssim 10^{-2}$

27. 11. 92, H1: $Q^2 = 2600$ GeV^2

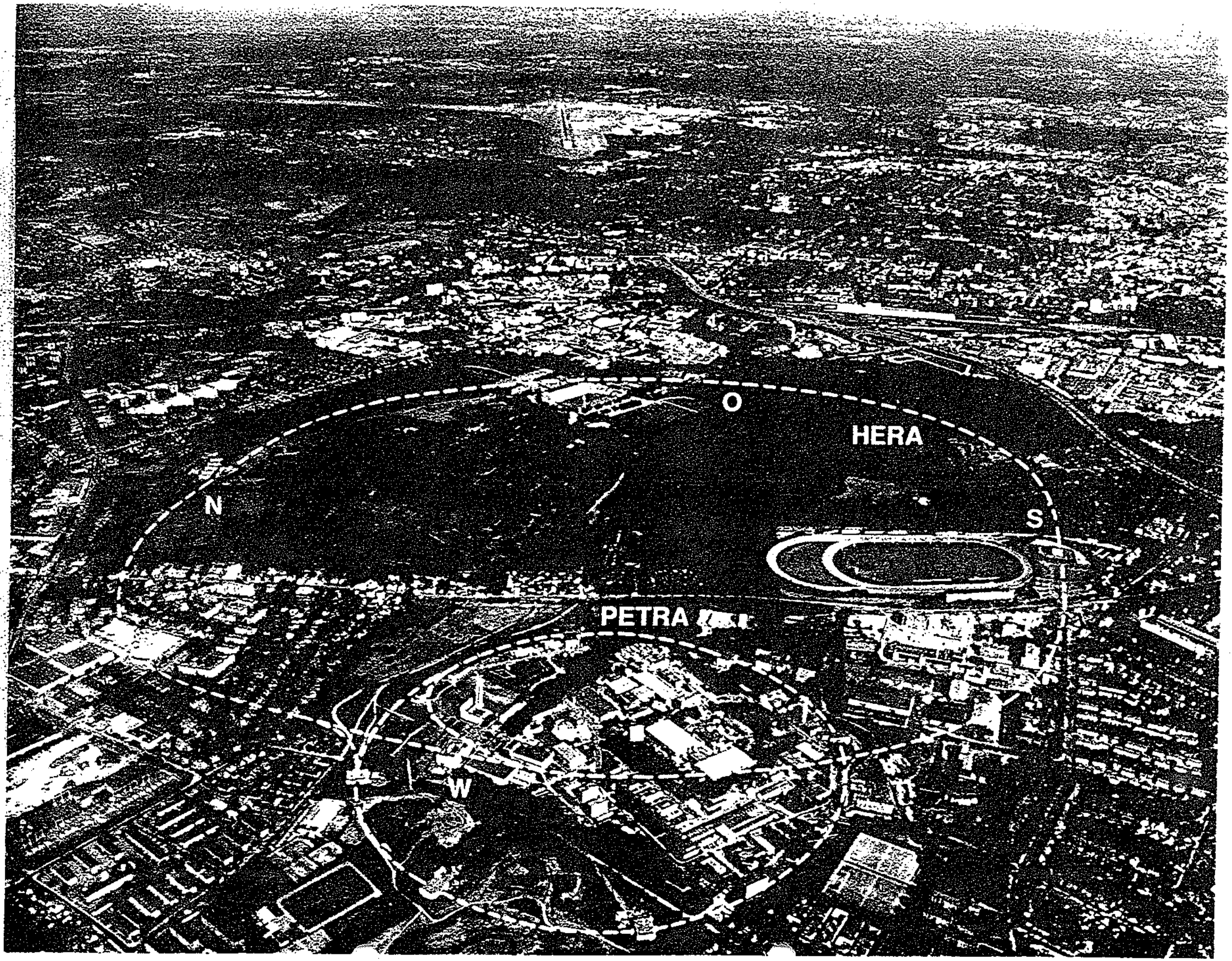
O
HERA
N
S
PETRA
W

UP SUPERIEURE OBEN おもて

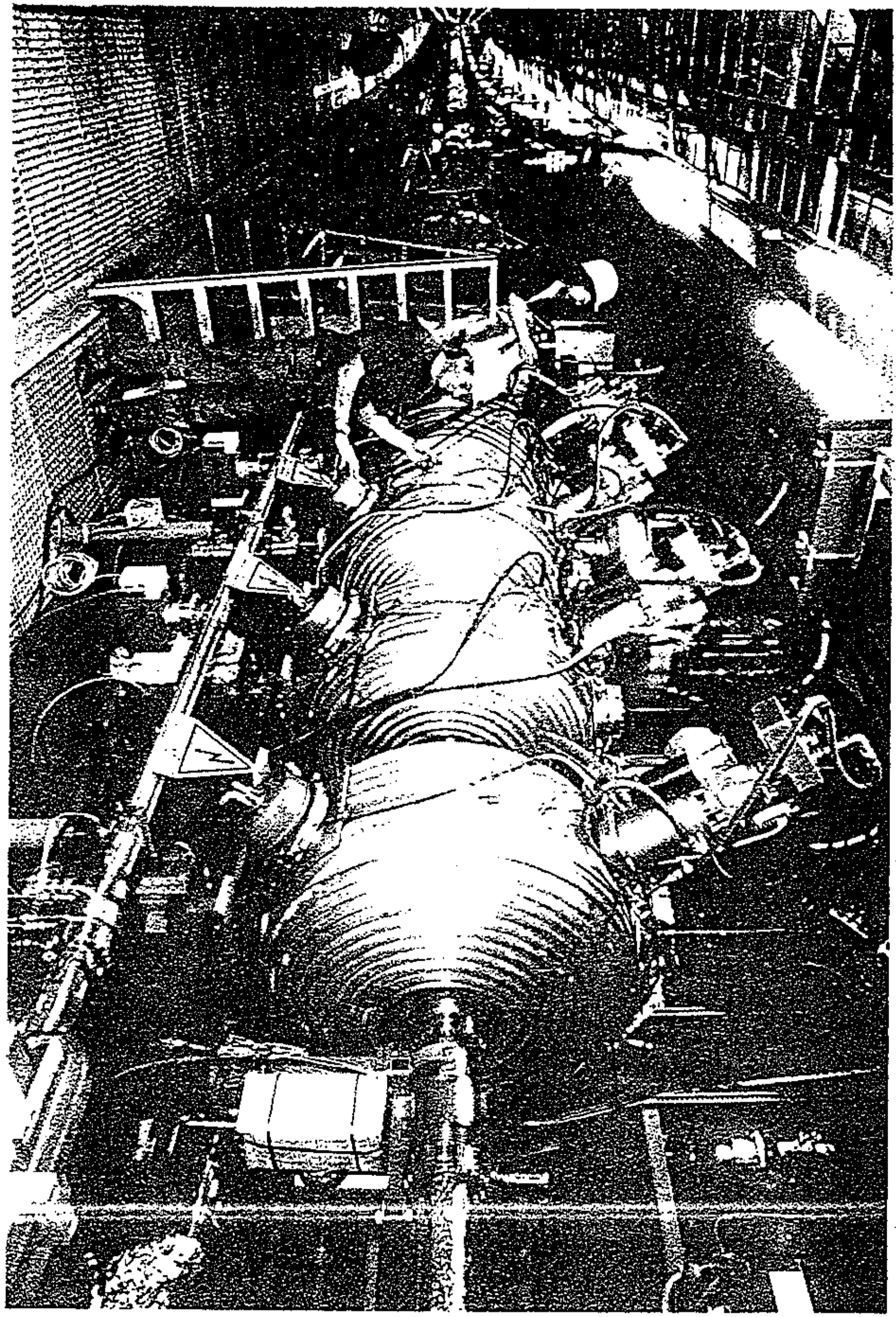

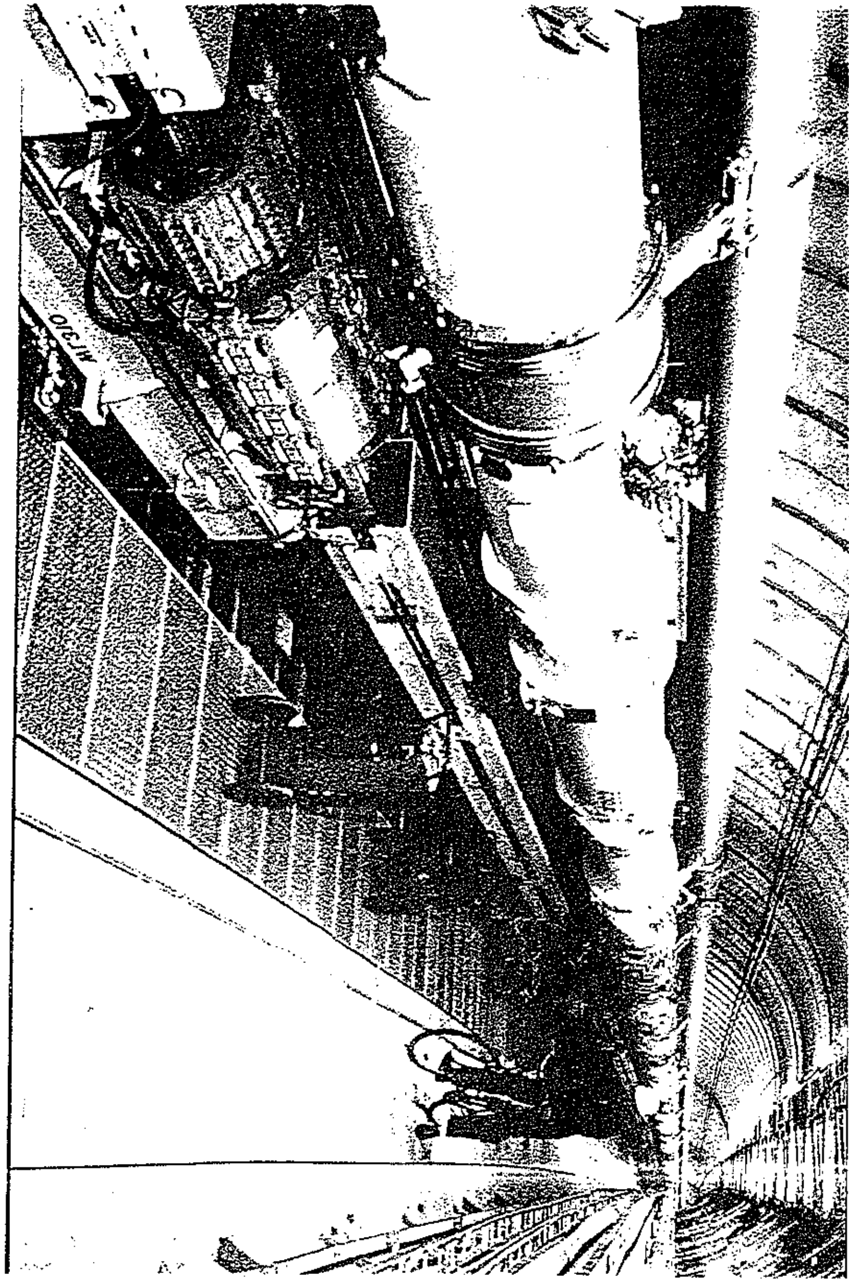

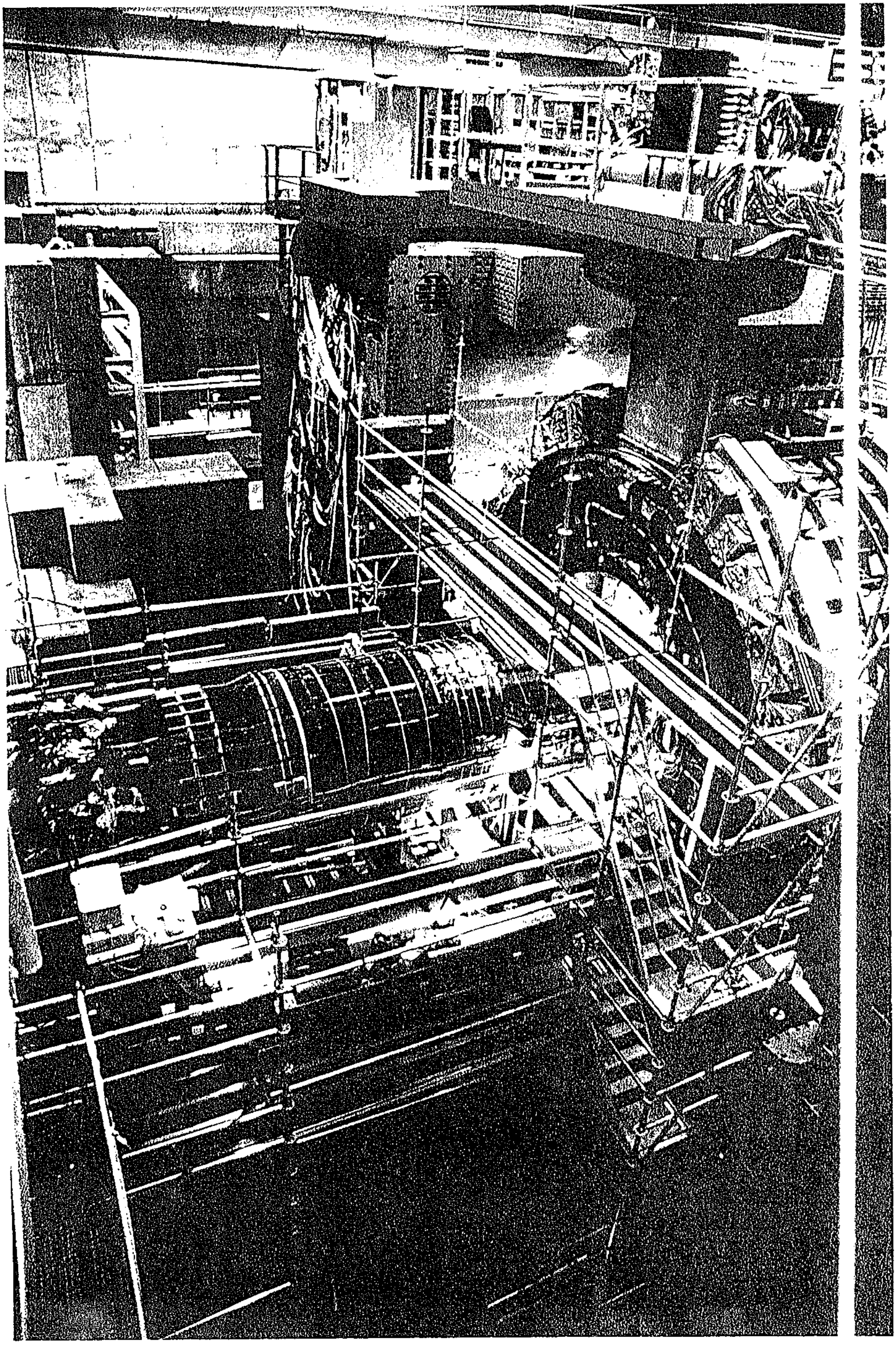

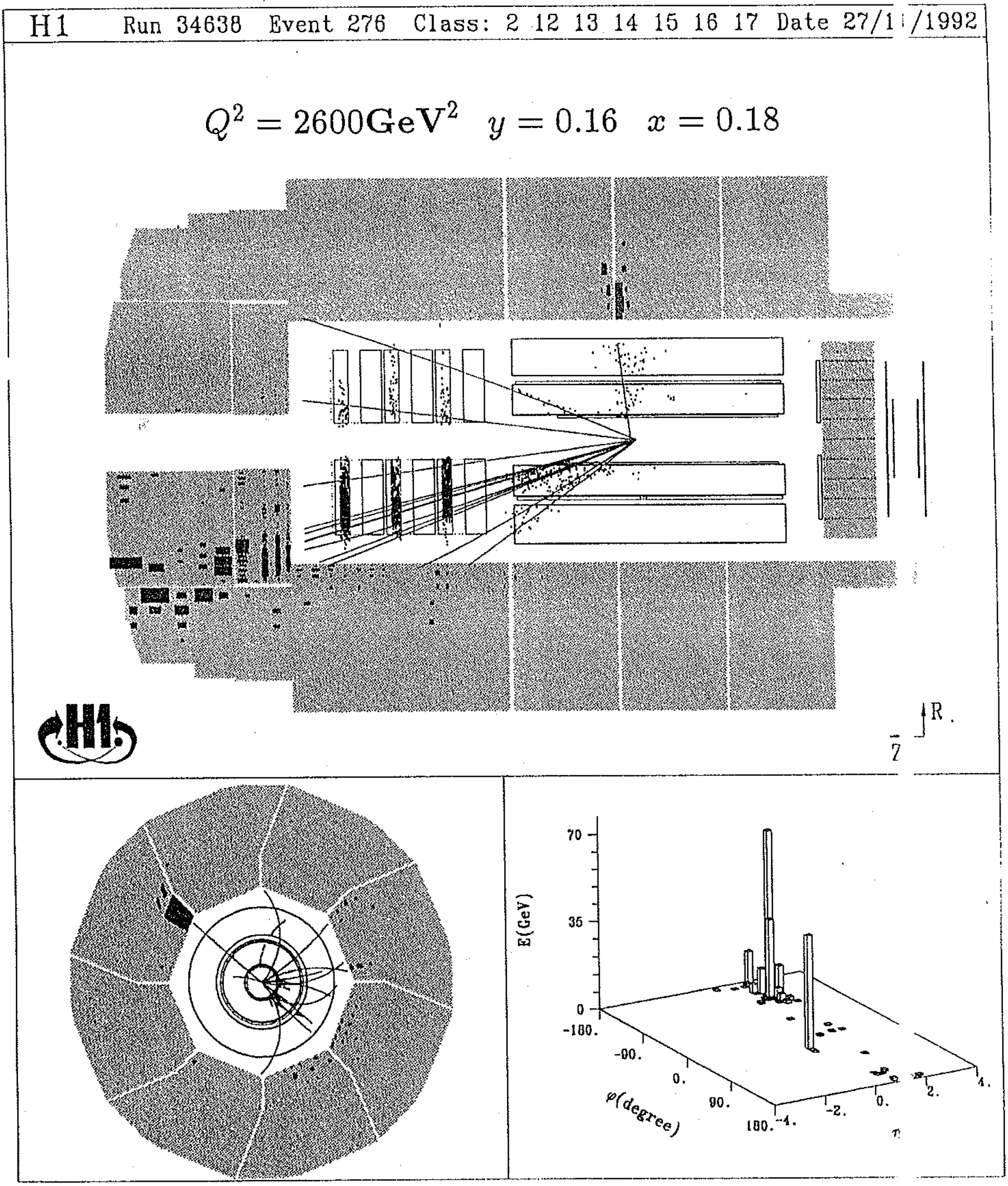
H1 Run 34638 Event 276 Class: 2 12 13 14 15 16 17 Date 27/1 /1992
$Q^2 = 2600\mathbf{GeV}^2 \quad y = 0.16 \quad x = 0.18$
R
Z
E(GeV)
70
35
0
-180.
-90.
0.
90.
180.
φ(degree)
-4.
-2.
0.
2.
4.
η

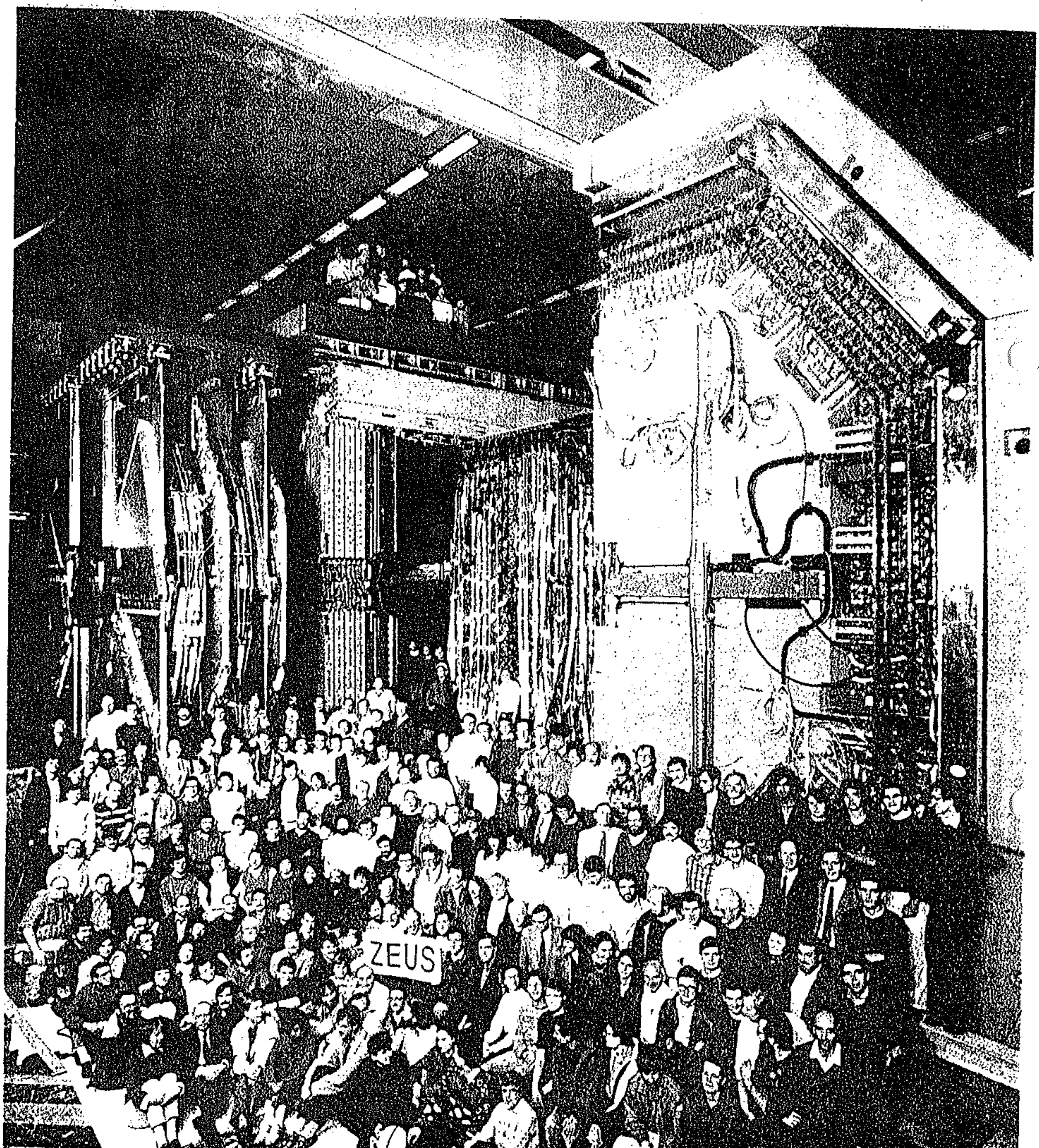
ZEUS

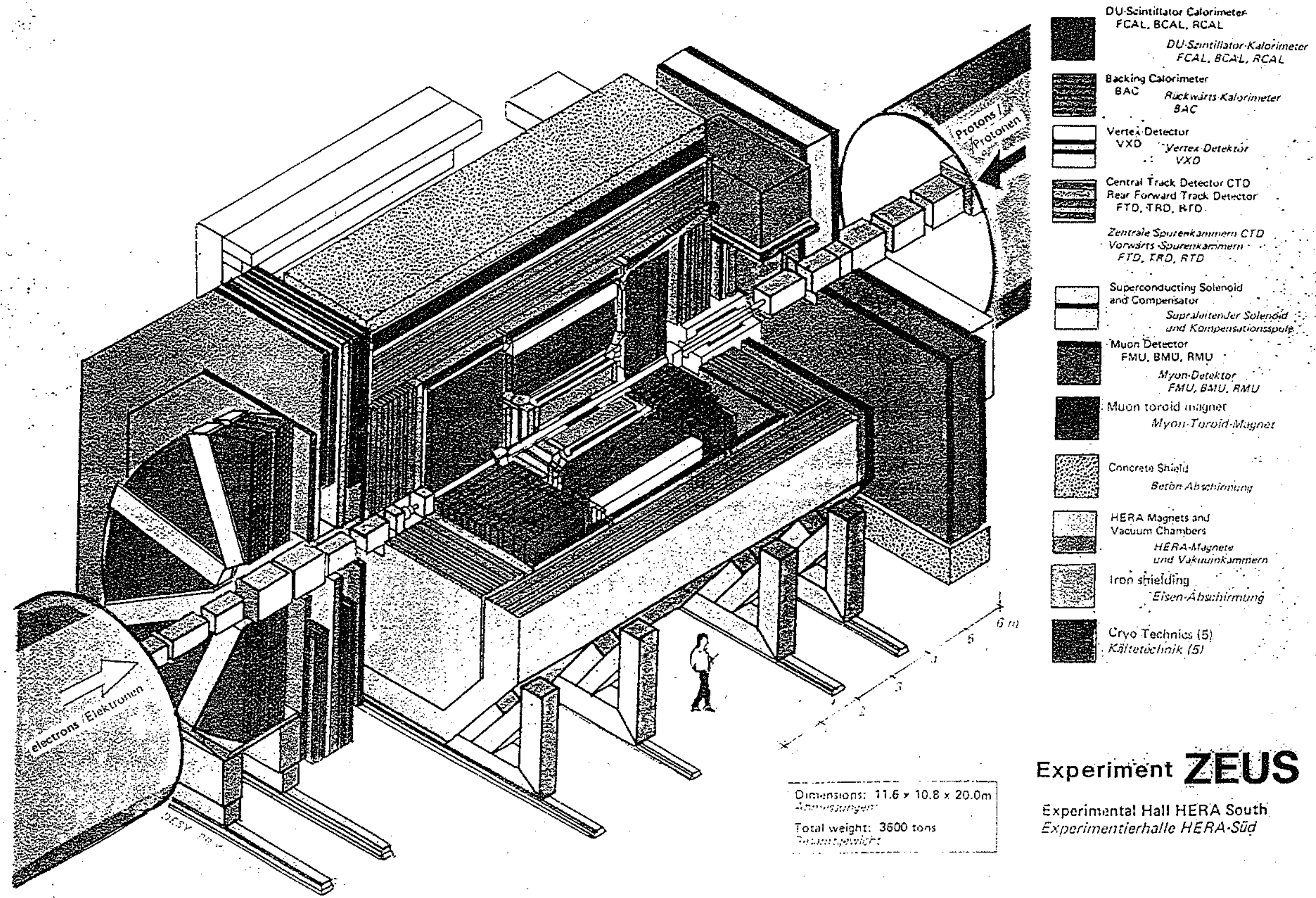

Dimensions: 11.6 × 10.8 × 20.0m

Total weight: 3600 tons

Experiment ZEUS

Experimental Hall HERA South
Experimentierhalle HERA-Süd

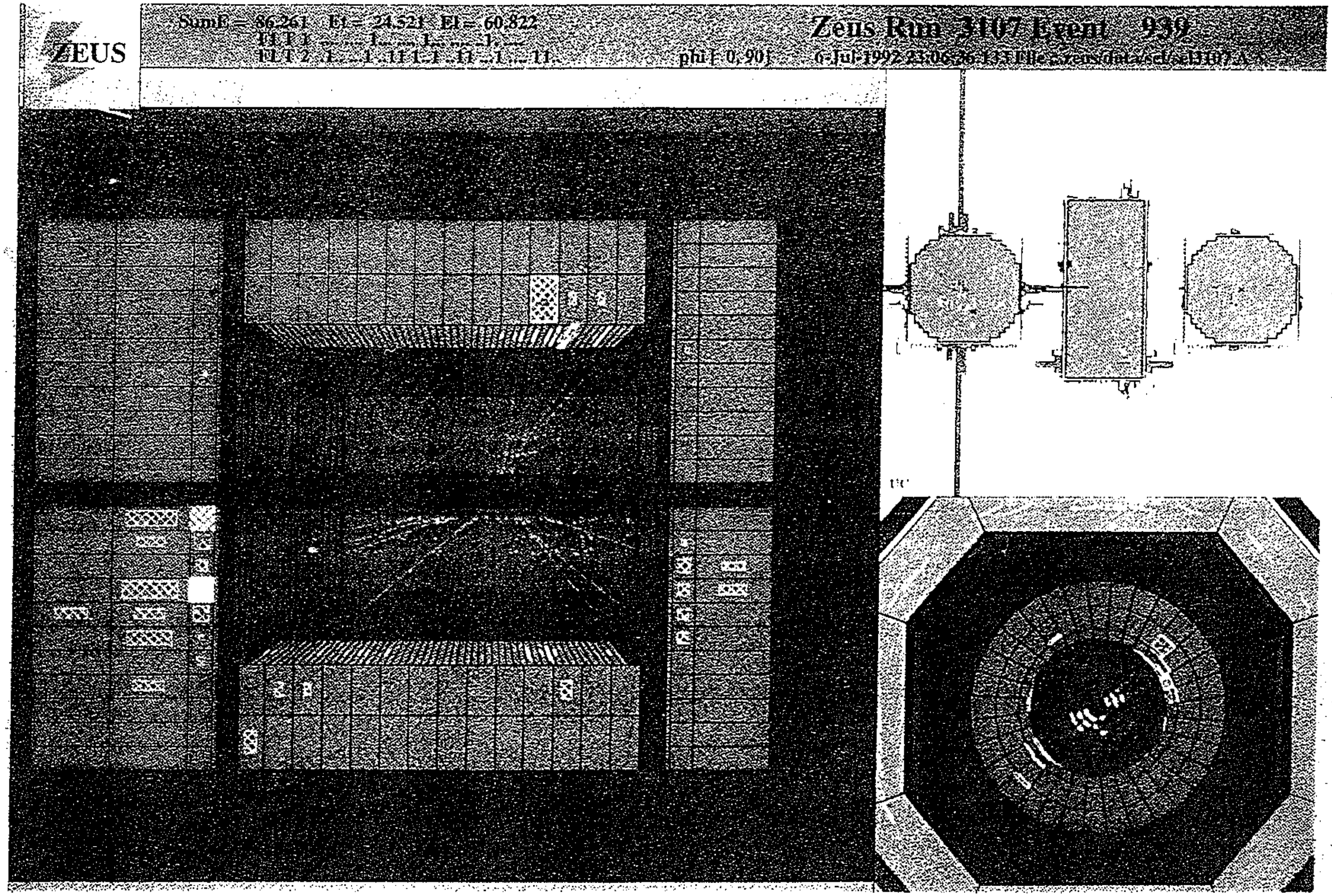
ZEUS
SumE = 86.261 Et = 24.521 El = 60.822
Zeus Run 3107 Event 939
phi [0, 90]
6-Jul-1992 23:06:26

H1

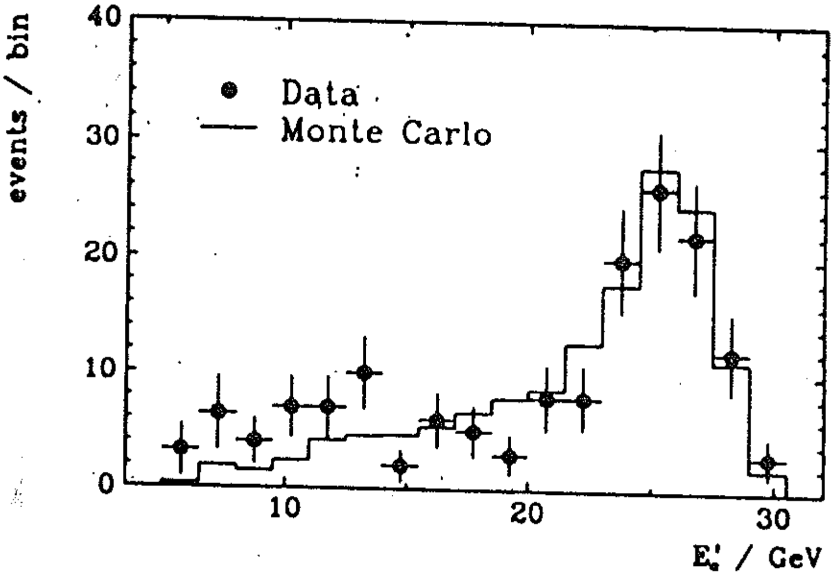

Figure 3: Electron energy spectrum of the DIS events compared with a Monte Carlo simulation [13,14] of the H1 detector using the parametrization MRSD0 [15]. The simulated spectrum is normalized to the measured integrated luminosity of 1.3 nb^{-1}.

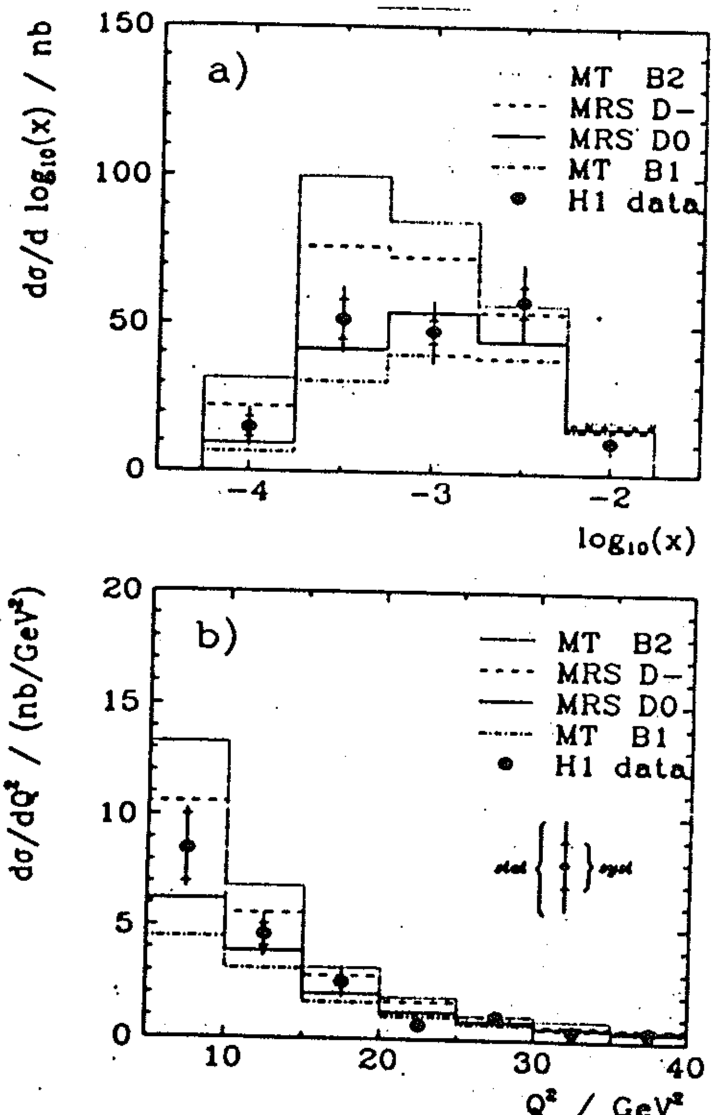

E3

ZEUS

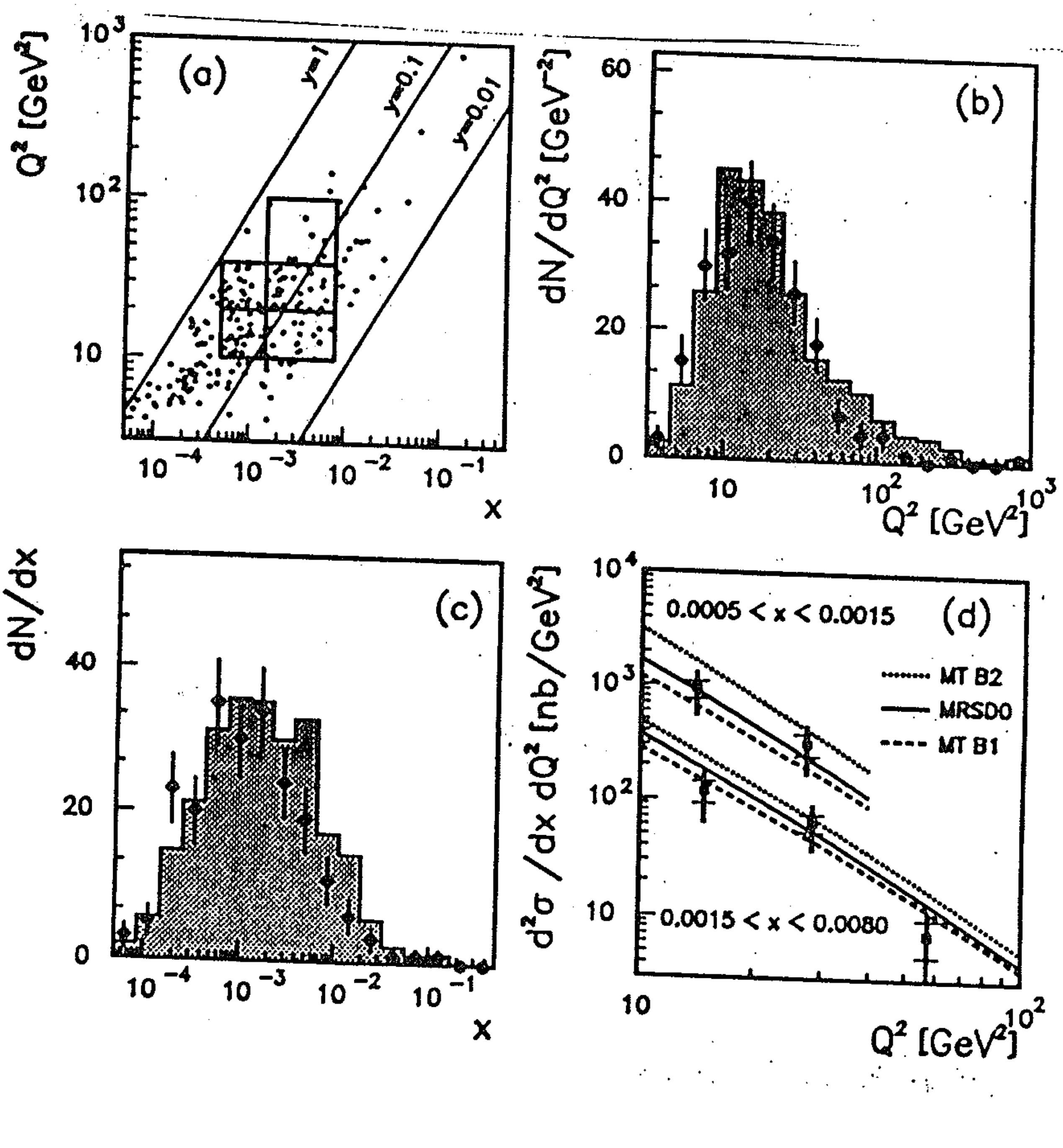

(a)
y=1
y=0.1
y=0.01
Q² [GeV²]
x
(b)
dN/dQ² [GeV⁻²]
Q² [GeV²]
(c)
dN/dx
x
(d)
0.0005 < x < 0.0015
0.0015 < x < 0.0080
MT B2
MRSD0
MT B1
d²σ /dx dQ² [nb/GeV²]
Q² [GeV²]

SUMMARY

1) DIS EXPERIMENTS IN THE FUTURE WILL EXTEND OUR INSIGHT IN THE PROTON / NUCLEON STRUCTURE GOING TO:
   - SMALLER x
   - HIGHER Q^2
   - USING THE WHOLE FLAVOUR VARIETY

2) CURRENT STUDY: HERA: $x \gtrsim 10^{-4}$, $Q^2 \lesssim 10^4\ \mathrm{GeV}^2$

   FUTURE POSSIBILITIES:
   - LEP1,2 $\times$ LHC
   - ν BEAMS IN THE TEV FIXED TARGET RANGE

3) QED & EW RADIATIVE CORRECTIONS ARE UNDER FULL CONTROL.

4) HO QCD CORRECTIONS ARE STILL TO BE WORKED OUT.

   LOW X: YET A STATUS NASCENDI FOR THEORY $(\mathrm{QCD})^{?!}$

5) VARIOUS SF CAN BE MEASURED, ALLOWING TO UNFOLD QUARK DENSITIES

6) $xG(x,Q^2)$ MAY BE DERIVED (WITH SOME ASSUMPTIONS: J/ψ, $Q\bar{Q}$)

   FROM: SCALING VIOLATIONS, F_L, $\sigma_{J/\psi}$, $\sigma_{Q\bar{Q}}$, σ_γ.

7) $\alpha_s(Q^2)$ & Λ may be measured.
RUNNING OF α_s MAY BE ESTABLISHED AT THE STATISTICAL LEVEL IN LONG TERM.

8) SHADOWING MAY BE INFERRED IN F_2^{em} COMBINED WITH A CAREFUL QCD ANALYSIS.

Further Reading

1 Reports and Textbooks

1. G. Altarelli, *Partons in Quantum Chromodynamics*, Phys. Rep. **81**, 1 (1982).
2. G. Altarelli, *Experimental tests of perturbative QCD*, Ann. Rev. Nucl. Part. Sci. **39**, 357 (1989).
3. V. I. Andreev, *Chromodynamics and hard processes at high energies*, Nauka, Moscow, 1981 (in Russian).
4. A. Bassetto, M. Ciafaloni and G. Marchesini, *Jet structure and infrared sensitive quantities in perturbative QCD*, Phys. Rep. **100**, 201 (1983).
5. P. Becher, M. Böhm and H. Joos, *Gauge Theories of Strong and Electroweak Interactions*, Teubner Studienbücherei, B. G. Teubner, Stuttgart, 1983, 2nd edition, (in German); Wiley, Chichester, UK, 1984 (in English).
6. S. Bethke and J.E. Pilcher, *Tests of Perturbative QCD at LEP*, HD-PY 92/06 and Annual Review of Nuclear and Particle Science, **42**, 1992.
7. A.J. Buras, *Asymptotic freedom in deep inelastic processes in the leading order and beyond*, Rev. Mod. Phys. **52**, 199 (1980).
8. Ta-Pei Cheng and Ling-Fong, Li, *Gauge Theory of Elementary Particle Physics*, Calendron Press, Oxford, 1984.
9. J. Collins, *Renormalization*, Cambridge University Press, 1984.
10. J. Collins, *The Theorems of Perturbative QCD*, Ann. Rev. Nucl. Part. Sci., **37** (1987) 383.
11. F.E, Close, *An Introduction to Quarks and Partons*, Wiley, London, New York, 1979.
12. M. Diemoz, F. Ferroni and E. Longo, *Nucleon structure functions from neutrino scattering*, Phys. Rep. **130**, 293 (1986).
13. Yu.L. Dokshitser, R. I. Dyakonov and S. I. Troyan, *Hard processes in Quantum Chromodynamics*, Phys. Rep. **58**, 269 (1980).
14. Yu.L. Dokshitser, A.V. Khoze, A.H. Mueller and S. I. Troyan, *Basics of Perturbative QCD*, Edition Frontiers, Paris, 1991.
15. J. Dorfan, *Experimental Tests of Quantum Chromodynamics*, SLAC-PUB-4287.
16. D.W. Duke and R.G. Roberts, *Determination of the QCD strong coupling α_s*, Phys. Rep., **120**, 275 (1985).
17. F. Eisele, *High energy neutrino interactions*, Rep. Progr. Phys. **49**, 233 (1986).
18. R. P. Feynman, *Photon-Hadron Interactions*, Benjamin Press, Reading, MA, 1972.
19. R.D. Field, *Application of Perturbative QCD*, Addison-Wesley Publ. Comp., Redwood City, 1989.
20. J.I. Friedman, *Deep inelastic scattering: comparisons with the quark model*, Rev. Mod. Phys. **63**, 573 (1991).

21. B. Geyer, D. Robaschik and E. Wieczorek, *Theory of deep inelastic lepton–hadron scattering*, Fortschr. Physik **27**, 75 (1979).

22. L.V. Gribov, E.M. Levin and M.G. Ryskin, *Semihard processes in QCD*, Phys. Rep. **100**, 1 (1983).

23. H.W. Kendall, *Deep inelastic scattering: experiments on the proton and observation of scaling*, Rev. Mod. Phys. **63**, 597 (1991).

24. E. M. Levin, *Orsay Lectures on Low x Deep Inelastic Scattering*, LPTHE Orsay 91/02.

25. E. M. Levin, *Nucleon Structure at Small x*, DESY 91-110.

26. E. M. Levin, *Parton Density at small x_B*, DESY 92-122.

27. E.M. Levin and M.G. Ryskin, *High energy hadronic collisions in QCD*, Phys. Rep. **189**, 267 (1990).

28. W. Marciano and H. Pagels, *Quantum Chromodynamics*, Phys. Rep. **36**, 137 (1978).

29. G. Martinelli, *Status of QCD*, Rome preprint, n. 842 (December 1991).

30. A.H. Mueller, *Perturbative QCD at high energies*, Phys. Rep. **73**, 283 (1981).

31. A.H. Mueller, ed., *Perturbative Quantum Chromodynamics*, Advanced Series on Directions in High Energy Physics, Vol. **5**, World, Scientific, Singapore, 1989.

32. A.H. Mueller, *QCD at High Energie*, CU–TP-489 (1990), PANIC XII, MIT, June 1990.

33. A.H. Mueller, *Lectures on High Energy QCD*, CU–TP-536 (1991).

34. T. Muta, *Foundations of Quantum Chromodynamics: an Introduction to Perturbative Methods in Gauge Theories*, World Scientific, Singapore, 1987.

35. O. Nachtmann, *Elementary Particle Physics: Concepts and Phenomena*, Texts and Monographs in Physics, Springer, Berlin, 1990.

36. J. F. Owens, *Large–momentum–transfer production of direct photons, jets, and particles*, Rev. Mod. Phys. **59**, (1987) 465.

37. R. Petronzio, *QCD*, CERN–TH. 4165/85, (1984 CERN School, Lofthus, Norway).

38. H. D. Politzer, *Asymptotic freedom: an approach to strong interactions*, Phys. Rep. **14**, 129 (1974).

39. C. Quigg, *Gauge Theories of the Strong, Weak, and Electromagnetic Interactions*, The Benjamin/Cummings Publ. Comp., Menlo Park, 1983.

40. E. Reya, *Perturbative QCD*, Phys. Rep. **69**, 3 (1980).

41. R. G. Roberts, *The structure of the proton*, Cambridge Monographs on Mathematical Physics, 1990.

42. T. Sloan, G. Smadja and R. Voss, *The quark structure of the nucleon from the CERN muon experiments*, Phys. Rep. **162**, 45 (1988).

43. G. Sterman, *Introduction to Perturbative QCD*, ITP–SB–91–55, based on lectures at the Theoretical Advanced Study Institute in Elementary Particle Physics, University of Colorado, Boulder, CO, June 1991.

44. R.E. Taylor, *Deep inelastic scattering: the early years*, Rev. Mod. Phys. **63**, 573 (1991).

45. B. R. Webber, *Monte Carlo Simulation of Hard Hadronic Processes*, Ann. Rev. Nucl. Part. Sci., Vol. . **36** (1986) 253.

46. Y. F. Ynduráin, *Quantum Chromodynamics: an introduction to the theory of quarks and gluons*, Texts and Monographs in Physics, Springer, Berlin, New York, 1983.

2 Recent Conference Proceedings

1. Proceedings of the 1987 HERA Workshop, DESY, Hamburg, October 12–14, ed. R.D. Peccei, Vol. **1,2**, DESY, Hamburg, 1988.

2. *Hadron Structure Functions and Parton Distributions*, Proceedings of the Workshop held at FNAL, 26–28 April 1990, eds. D.F. Geesaman, J. Morfin, C. Sazama and W.K. Tung, World Scientific, Singapore, 1990.

3. *Small-x behaviour of Structure Functions in QCD*, Proceedings of the 1990 Workshop, Hamburg, 14–16 May, 1990, eds. A. Ali and J. Bartels, Nucl. Phys. **B**, Proc. Suppl. **18C**, North Holland, Amsterdam, 1991.

4. *Research Directions for the Decade*, Proceedings of the Snowmass Workshop June 25 – July 13, 1990, Snowmass, CO, ed. E.L.Berger, World Scientific, Singapore, 1992.

5. Proceedings of the ECFA Large Hadron Collider Workshop, Vol. **1–3**, Aachen, Germany, 4–9 October 1990, eds. G. Jarlskog and D. Rein, CERN 90–10, ECFA 90–133, Geneva, Switzerland, 1990.

6. *Physics at HERA*, Vol. **1–3**, Proceedings of the 1991 HERA Workshop, DESY, Hamburg, October 1991, eds. W. Buchmüller and G. Ingelman, DESY, Hamburg, 1992.

7. *Deep Inelastic Scattering*, Proceedings of the 1992 Zeuthen Workshop on Elementary Particle Theory, Teupitz/Brandenburg, Germany, 6–10 April, 1992, eds. J. Blümlein and T. Riemann, Nucl. Phys. **B**, Proc. Suppl. **29A**, North Holland, Amsterdam, 1992.

8. *QCD – 20 Years Later*, Proc. of the International Workshop ~~Conference~~, Aachen, Germany, June 1992, ed. P.M. Zerwas~~, in press~~.

H.A. Kastrup, World 1993.